

## CHAPTER 3

### WATER PROPERTIES AND DISTRIBUTION OF HOT SPRING DIATOMS IN NORTHERN THAILAND

#### 3.1 Introduction

Hot springs provide researchers with a good opportunity to examine the progression of a moderately basic ecosystem that has been subjected to a limited variety of organisms. A limited number of species can grow and reproduce at high temperatures and the vibrancy of the environment, consequently, is severely reduced (Stockner 1968). Diatoms are relatively plenteous in hot springs, but they are less imperative than cyanobacteria because they do not form an official colony in the area. They are constantly scattered among other algae and are frequently attached to stones or aquatic plants, except in the furrow or close to the spring source where we regularly find pure colonies that appear yellowish–brown in shading. Diatoms are considered highly suitable bioindicators because their length of tolerance to variable factors can limit diatom distribution and this may eventually result in succession. A key issue in understanding diatom distribution is the extent to which they are constrained by geographical factors that limit species dispersal and the extent to which they are restricted only by the capability of the species to grow under a specific combination of environmental factors. Distribution is influenced by many factors, including physical barriers, the distance between suitable habitats, transportability of cells, type and importance of transport mechanism, the size and dispersal of primary populations and also whether it is a suitable habitat for colonization (Kristiansen, 1996).

In the hot spring ecosystems examined in this study, diatoms that grow at high temperatures were collected and classified. An attached algal community consists primarily of microscopic species, which are particularly found in small streams and on

rocky substrata. Diatom species can utilize a broad range of temperatures for growth from 10°C to 55°C in extreme habitats (Round *et al.*, 1990) than other species of green algae (Nurul *et al.*, 2013). Moreover, the distribution of the diatom species is confirmed and allocated within the range of the low and high limits of conductivity tolerances (Hamed, 2008). The seasonal changes were studied regarding the relevant physical, chemical and biological factors (Kochasany, 1993). The seasonal variations impact the activities of the living organisms and such is the case with algae. The diatom community might also shift due to seasonal cycles, especially in tropical regions. The diatoms of hot springs have received consideration in various frameworks of research around the globe. Arrangements of ordinarily occurring species or finish vegetation have been produced for springs in North America (Hobbs *et al.* 2009), South America (Cocquyt and Van De Vijver 2007) Europe (Dell'uomo 1986), Africa (Mpawenayo), Asia, Japan (Kobayashi 1957) and New Zealand (Owen *et al.* 2008).

Findings concentrating on the identification of diatoms in thermal springs and their dispersion have not already been archived in Thailand. Information of the relationship between the geography and diatom distribution could encourage the distinguishing proof of particular thermal spring niche biological communities. Alternately, some diatoms may have the capacity as indicators of topography and, in particular, heavy metals. The point of this study was to understand the seasonal variations of hot spring diatoms with regard to the diatoms composition and density, as well as their relationships with the water properties in some hot spring sampling sites in northern Thailand. The species composition is a characteristic that can provide valuable information on environmental conditions and seasonality.

### **3.2 Materials and Methods for the preliminary investigation**

The investigation of benthic diatoms and water properties measurement in hot spring sampling sites were followed by Figure 3.1

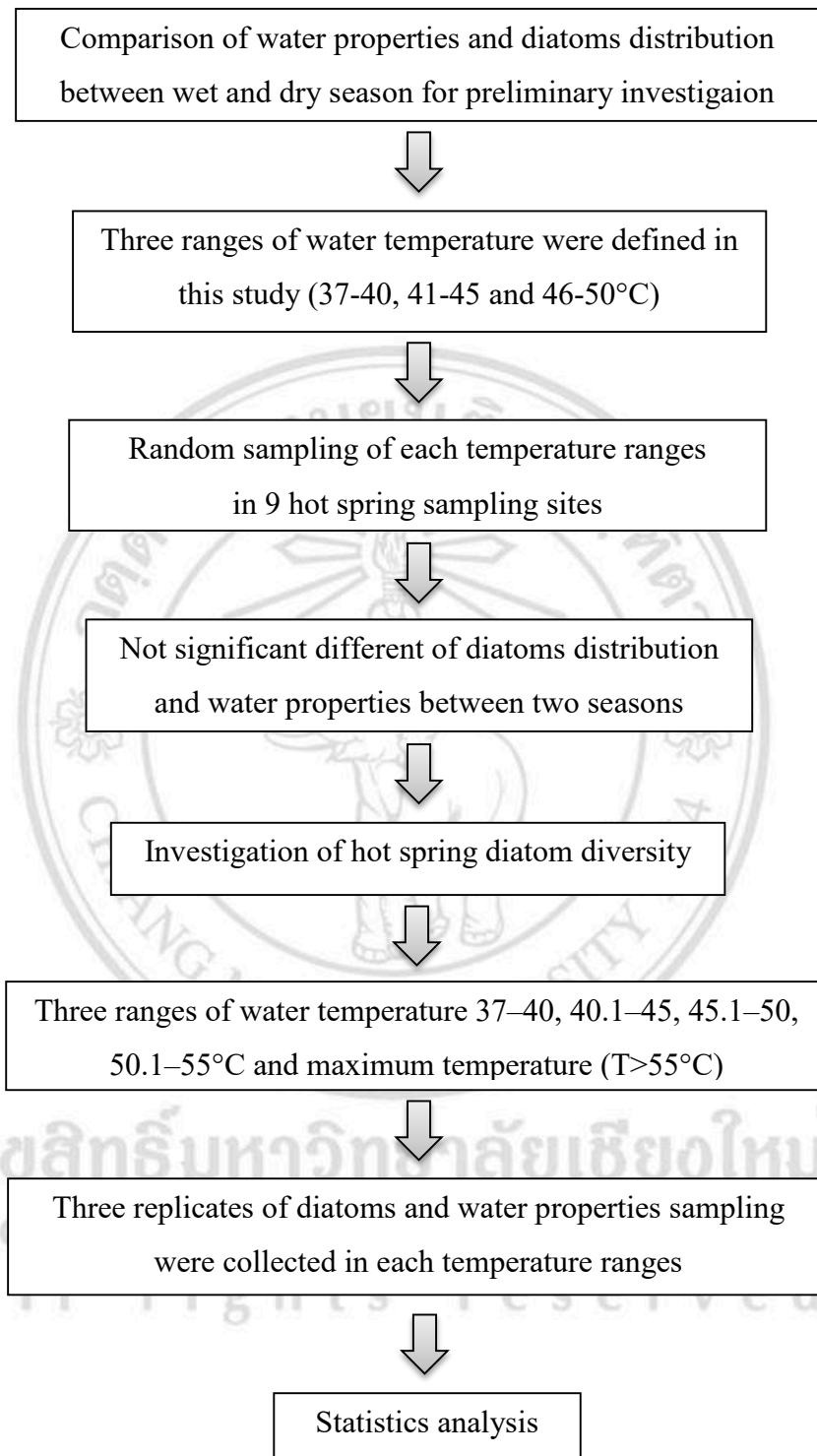


Figure 3.1 Flowchart diagram of hot spring diatoms and water properties analysis

### 3.2.1 Sampling sites

Samples of diatoms that differ in geological characteristics were collected from nine hot springs in northern Thailand (Figure 3.2) during the wet and dry seasons from October 2013 to September 2014. Ranges of water temperature were the primary consideration for community structure. Three ranges of water temperature were defined in this study (37-40, 41-45 and 46-50°C). The ecological data of each sampling site was recorded, i.e., latitude, longitude and altitude. The lists of sampling sites with some general data are given in Table 3.1.

#### 3.2.1.1 San Kamphaeng Hot Spring, Chiang Mai Province (Site 1)

Located in Mae On District, Chiang Mai Province. Before being developed into a tourist attraction, it was once a large area comprised of many individual hot springs. However, nowadays, it has been renovated and built into a cement pond and dredged to be a vacation destination. As a consequence of this development, it has caused the diversity of the algae to decrease significantly due to human disturbances. The general condition of the thermal springs revealed that the water in the ponds was transparent. The hot stream had a blanket of algae covering the surface except for the wells where water squirt ups from periodically. When the temperature is higher, the algae will flourish. Hot spring baths have a very sulfuric odor, which may be reduced by the flow of the stream (Figure 3.3).

#### 3.2.1.2 Theppanom Hot Spring, Chiang Mai Province (Site 2)

Theppanom is a natural hot spring source that is located in Op Luang National Park in Mae Cham District, Chiang Mai Province. It is currently being designated as a tourist attraction, but is not particularly popular. This means that the hot spring rarely experiences much external interference. At the entrance to the hot spring site there is a small outdoor pond that does not have the benefit of the shading of trees, and there is the clear smell of sulfur. The section in the rear area is comprised of a hot stream that flows down to the confluence with a river. The characteristics of the ground water include small stones, gravel, sand and clay-based ground waters, while shallow, clear waters contain algae (Figure 3.3).

#### 3.2.1.3 Ta Pai Hot Spring, Mae Hong Son Province (Site 3)

This hot spring is located in Pai District, Mae Hong Son Province and is a main tourist attraction. The area is not large, consisting of two hot spring ponds for which each pond brings heated water up from under the ground, and then the water flows into a number of streams below with high velocity. The surrounding area is covered with trees and forests. Rocks and gravel characterize the ground waters that contain some algae (Figure 3.3).

#### 3.2.1.4 Pong Ang Hot Spring, Chiang Mai Province (Site 4)

This hot spring is situated in Pha Daeng National Park, formerly known as Chiang Dao National Park, Chiang Dao District, Chiang Mai Province. The area consists of two ponds that are approximately 4-5 meters wide and a mild natural sulfuric odor is emitted from the groundwater. The temperature of the first pond was 58°C and the other was 51°C. Steam is created at the hot spring that increases the level of relaxation of the visiting tourists, but it is not a popular tourist attraction. The substrate includes rocks, soil, and gravel and there is very little algae found in this area (Figure 3.3).

#### 3.2.1.5 Chae Sorn Hot Spring, Lampang Province (Site 5)

This hot spring is located in Chae Sorn National Park Mueang Pan District, Lampang Province and consists of nine ponds in a greater area of approximately three acres. This place is a tourist attraction that attracts a lot of tourist attention. It is made up of fascinating topographical conditions. There is a mild odor of sulfur. The area consists of large and small rocks that are scattered throughout the area. Steam rises up from the ponds and creates a mist. The principle characteristic of the ground water is a gray sludge. The water temperature was not quite high and the water contained algae (Figure 3.3).

#### 3.2.1.6 Mae Chok Hot Spring, Phrae Province (site 6)

This small hot spring is located in the Wiang Kosai National Park Wang Chin District, Phrae Province. It is characterized by sulfur baths that have sprung

up from the ground. The water temperature in the original pond was about 80°C. The greater hot spring area is currently being developed into a tourist attraction (Figure 3.4).

#### 3.2.1.7 Wat Salaeng Hot Spring, Phrae Province (Site 7)

This hot spring is a small natural spring that is located in Long District, Phrae Province. Developers are currently creating a pond made of concrete and the location is being developed as a tourist attraction, but it is not well known; therefore, it has become somewhat of a desolate area. The hot spring is close to streams that flow through the village that still experience hot water springing up from the ground and flowing into the side creeks (Figure 3.4).

#### 3.2.1.8 Ban Su Men Hot Spring, Sukhothai Province (Site 8)

This hot spring is located in a village and is surrounded by lime and orange orchards. The ponds were built with concrete. Hot water flows into streams that are connected with the pond. This area is not open as a tourist attraction, so it remains in its natural environment (Figure 3.4).

#### 3.2.1.9 Pong Gi Hot Spring, Nan Province (Site 9)

This hot spring is situated in Nanthaburi National Park, Tha Wang Pha District, Nan Province. The hot springs occur naturally as the mineral water mixes with sulfur. The area is comprised of a tribal village and the villagers have developed it as a tourist attraction. The neighboring areas of the pond contain cold-water streams and hot water runs into the streams (Figure 3.4).

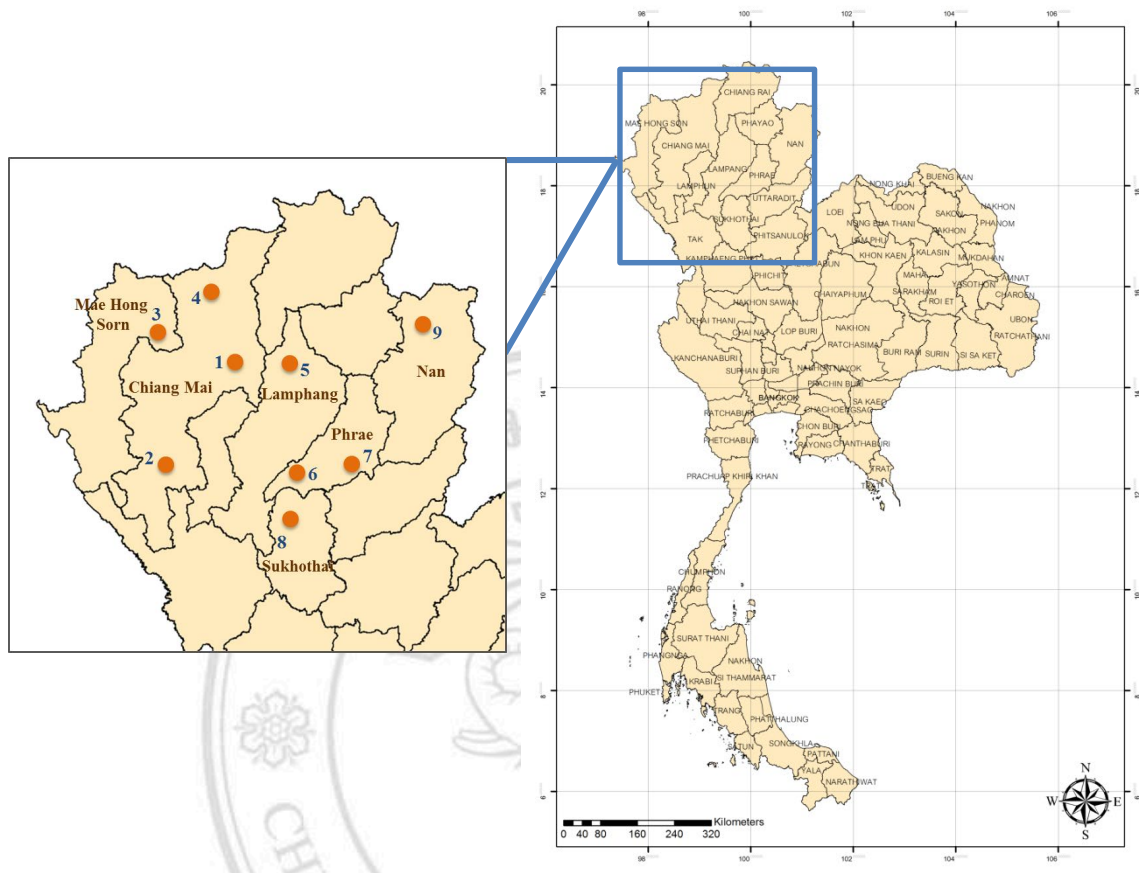


Figure 3.2 Map of Thailand giving 9 sampling sites of hot springs in northern Thailand  
 (1) San Kamphaeng hot spring, Chiang Mai province, (2) Theppanom Hot Spring, Chiang Mai province, (3) Ta Pai Hot Spring, Mae Hong Son province, (4) Pong Ang Hot Spring, Chiang Mai province, (5) Chae Sorn Hot Spring, Lamphang province, (6) Mae Chok Hot Spring, Phrae province, (7) Wat Salaeng Hot Spring, Phrae province, (8) Ban Su Men Hot Spring, Sukhothai province, (9) Pong Gi Hot Spring, Nan province



Figure 3.3 Hot Springs sampling sites in northern Thailand

1. San Kamphaeng Hot Spring, Chiang Mai province

2. Theppanom Hot Spring, Chiang Mai province

3. Ta Pai Hot Spring, Mae Hong Son province

4. Pong Ang Hot Spring, Chiang Mai province

5. Chae Sorn Hot Spring, Lampang province



Figure 3.4 Hot Springs sampling sites in northern Thailand

6. Mae Chok Hot Spring, Phrae province

7. Wat Salaeng Hot Spring, Phrae province

8. Ban Su Men Hot Spring, Sukhothai province

9. Pong Gi Hot Spring, Nan province

ลิขสิทธิ์มหาวิทยาลัยเชียงใหม่  
Copyright © by Chiang Mai University  
All rights reserved

Table 3.1 Location and description of nine hot spring sampling sites

Site	Hot spring	Code	Location	Altitude (m)
			Co-ordinates	
1	San Kamphaeng (Chiang Mai Province)	SK	18° 48' 49.33" N 99° 13' 46.11" E	381
2	Theppanom (Chiang Mai Province)	TPN	18° 16' 17.11" N 98° 23' 48.59" E	369
3	Ta Pai (Mae Hong Son Province)	TP	19° 18' 40.55" N 98° 28' 33.89" E	565
4	Pong Ang (Chiang Mai Province)	CHD	19° 35' 48.46" N 98° 56' 45.72" E	501
5	Chae Sorn (Lampang Province)	JS	18° 50' 11.03" N 99° 28' 09.82" E	472
6	Mae Chok (Phrae Province)	MJ	17° 58' 42.23" N 99° 38' 18.06" E	137
7	Wat Salaeng (Phrae Province)	SL	18° 05' 39.05" N 99° 49' 54.28" E	146
8	Ban Su Men (Sukhothai Province)	SM	17° 43' 44.01" N 99° 38' 39.06" E	95
9	Pong Gi (Nan Province)	NG	19° 13' 54.23" N 100° 41' 15.55" E	537

### 3.2.2 Water sampling analysis

One replicate of water sample was collected in each water temperature ranges from nine hot spring sampling sites. Water samples were collected in polyethylene bottles and kept in a thermal box to retain the proper temperature.

#### Physico-chemical analysis

3.2.2.1 The limnological data of each sampling site, such as details of the environment and the types of substrates, were observed.

3.2.2.2 Altitude and ordination were recorded with a GPS Receiver (Batch Meridian XL).

3.2.2.3 Water temperature were registered with the use of a thermometer.

3.2.2.4 Conductivity was measured by using a conductivity meter (electrode kit of TRANS Company).

3.2.2.5 pH measurement was done with a pH meter (electrode kit of TRANS Company).

3.2.2.6 Alkalinity was analyzed by the phenolphthalein methyl orange indicator method (Eaton *et al.*, 2005).

Nutrient analysis followed the method of Eaton *et al.* (2005)

3.2.2.7 Nitrate-nitrogen was analyzed by the cadmium reduction method.

3.2.2.8 Ammonium nitrogen analysis was conducted by the nesslerization method.

3.2.2.9 Soluble Reactive Phosphorus (SRP) analysis was carried out by the ascorbic acid method.

3.2.2.10 Silica content was analyzed by the silico-molybdate method.

3.2.2.11 Total hardness (Ca, Mg) was examined by the EDTA titrimetric method.

3.2.2.12 The dissolved sulfide concentration ( $S^{2-}$ ) was determined by the methylene blue method

### 3.2.3 Biological analysis

Investigation of benthic diatoms was performed according to the method of Rott *et al.* (1997)

#### 3.2.3.1 Collection of benthic diatoms

One replicate of benthic diatom samples were scraped from the edges of hot spring pools or from 5-10 stones per site. They were brushed and rinsed with distilled water until the surface was completely clean. Diatom mats, which are attached to soil, sand, cobble or concrete, were collected with a spatula. Each sample was collected in a small plastic container and labeled with the site name, location code, date, and replicate number, and then transferred to a foam box to maintain a high temperature.

#### 3.2.3.2 Cleaning process for benthic diatoms

The samples were cleaned via the strong acid digestion method. The fresh samples were mounted on glass slides with a mounting agent (Pleurex) and covered with coverslips on a hotplate to remove toluene. The permanent slides were used for the counting and identifying processes.

#### 3.2.3.3 Benthic diatom identification and counting

A 100x light microscope was used to identify the diatom samples. The specimens were photographed using an Olympus Normaski microscope and scanning electron microscope. The samples were identified according to relevant reference books; Foged (1974; 1979); Krammer and Lange-Bertalot (1991); Lange-Bertalot and Krammer (1989); Lange-Bertalot (2001), Krammer, Kurt (1997); Krammer and Cramer (1997); Krammer and Cramer (2000); Krammer and Lange Bertalot (2002); Krammer *et al.* (2003); Kelly and Haworth (2002) and Jüttner *et al.*, (2011).

### 3.2.4 Statistical analysis

A T-test of each water properties and diatom species was calculated to determine statistical significance between wet and dry season and data were revealed as the mean  $\pm$  standard deviation (SD) ( $p < 0.01$ ).

## 3.3 Results and discussions for the preliminary investigation

In terms of the results, the values of the physicochemical factors and the species distribution of diatoms during the wet and dry seasons have been arranged in Table 3.2, Table 3.3 and Table 3.4, respectively.

### 3.3.1 Physico-chemical analysis

There was a variation in the range of water chemicals found at each sampling site (Table 3.2). The results shown in Table 3.2 present the non-significant differences in most of the physicochemical factors during the wet and dry seasons with the exception of alkalinity ( $p < 0.01$ ). The seasonal deviations in the water temperature of each spring was less than  $3^{\circ}\text{C}$  (Figure 3.5). This because hot springs show a greater stability of physico-chemical parameters than other surface aquatic ecosystems (Van der Kamp 1995, Glazier 1998). Sompong *et al.* (2005) reported the stability of the water temperature related to the minor yearly variations in the encompassing temperatures of tropical regions. According to the sampling process, most of the sampling sites recorded pH values of a slight alkaline nature (Figure 3.6), which corresponded with Sompong *et al.* (2005). In agreement with the water type indicated by Hamed (2008), conductivity in the thermal springs of the Bahariya Oasis was measured at  $592\text{-}1028\ \mu\text{s}\cdot\text{cm}^{-1}$ , which correlated with the current level of conductivity recorded in this study that was valued at  $215\text{-}1016\ \mu\text{s}\cdot\text{cm}^{-1}$  in the dry season and  $366\text{-}968\ \mu\text{s}\cdot\text{cm}^{-1}$  in the wet season (Figure 3.7). Other important parameters included silicon dioxide and sulfide levels. Silicon dioxide levels in San Kamphaeng Hot Spring were recorded at  $108.8\text{-}110.4\ \text{mg}\cdot\text{L}^{-1}$  in the wet season and  $114\text{-}157\ \text{mg}\cdot\text{L}^{-1}$  in the dry season (Figure 3.11), which was the highest value from all thermal samplings. This was proportional to the sulfide values and the diatom variations in the same sampling sites (Figure 3.12). Furthermore, the level of nitrate-nitrogen concentrations (Figure 3.8) during both seasons did not to exceed the quality

standards for surface water ( $<5 \text{ mg}\cdot\text{L}^{-1}$ ) indicating that they could be used to promote the growth of the diatom species (Chu 1943). The concentration of ammonium-nitrogen showed almost the same ranges in both the wet and dry seasons (Figure 3.9) as it did with regard to the concentration of soluble reactive phosphorus (Figure 3.10).

Table 3.2 Physicochemical factors of nine study sites in the wet and dry seasons

Factors	wet	dry	p
Water Temperature ( $^{\circ}\text{C}$ )	$42.8 \pm 3.49$	$43.5 \pm 3.54$	0.490
pH	$8.19 \pm 0.43$	$8.04 \pm 0.58$	0.333
Conductivity ( $\mu\text{s}\cdot\text{cm}^{-1}$ )	$583.57 \pm 144.64$	$624.26 \pm 216.88$	0.458
$\text{NO}_3\text{-N}$ ( $\text{mg}\cdot\text{L}^{-1}$ )	$0.67 \pm 0.28$	$0.80 \pm 0.29$	0.135
$\text{NH}_4\text{-N}$ ( $\text{mg}\cdot\text{L}^{-1}$ )	$0.25 \pm 0.15$	$0.28 \pm 0.15$	0.491
SRP ( $\text{mg}\cdot\text{L}^{-1}$ )	$0.41 \pm 0.33$	$0.42 \pm 0.28$	0.920
$\text{SiO}_2$ ( $\text{mg}\cdot\text{L}^{-1}$ )	$65.43 \pm 30.89$	$72.69 \pm 34.97$	0.459
$\text{S}^{2-}$ ( $\text{mg}\cdot\text{L}^{-1}$ )	$0.002 \pm 0.005$	$0.005 \pm 0.008$	0.125
Alkalinity ( $\text{mg}\cdot\text{L}^{-1}$ as $\text{CaCO}_3$ )	$481.96 \pm 223.48$	$301.74 \pm 138.11$	0.002*
Total Hardness ( $\text{mg}\cdot\text{L}^{-1}$ as $\text{CaCO}_3$ )	$81.83 \pm 23.64$	$96.48 \pm 40.44$	0.141

Data are expressed as mean  $\pm$  standard deviation (SD) using t-test ( $p < 0.01$ )

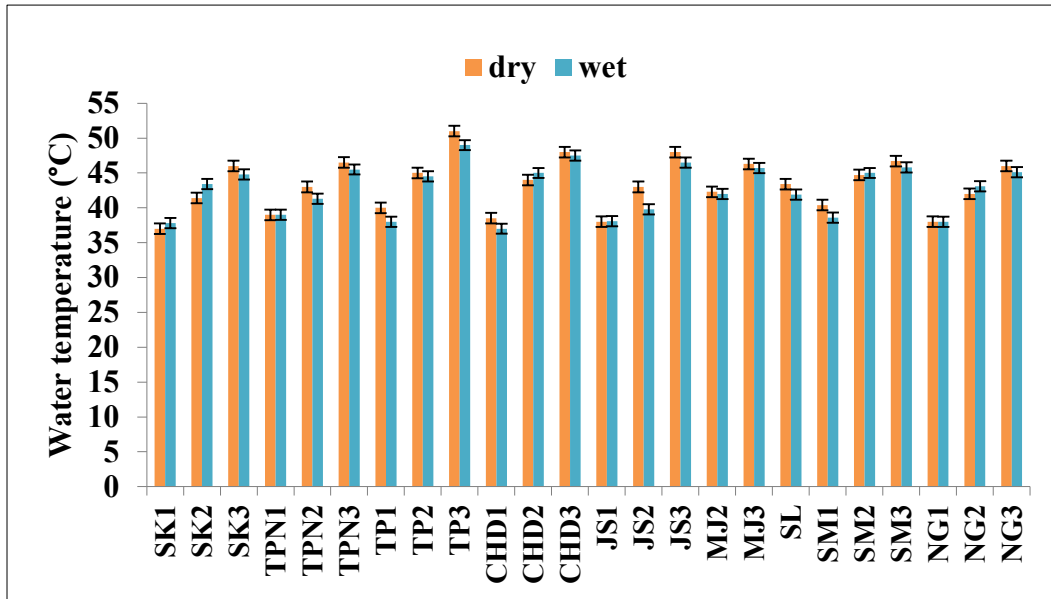


Figure 3.5 Comparison of water temperature (°C) in the investigated localities between wet and dry season. The x-axis is sampling sites and digits after the alphabet is the temperature range each sampling sites (1 = 37-40°C, 2 = 41-45°C, 3 = 46-50°C).

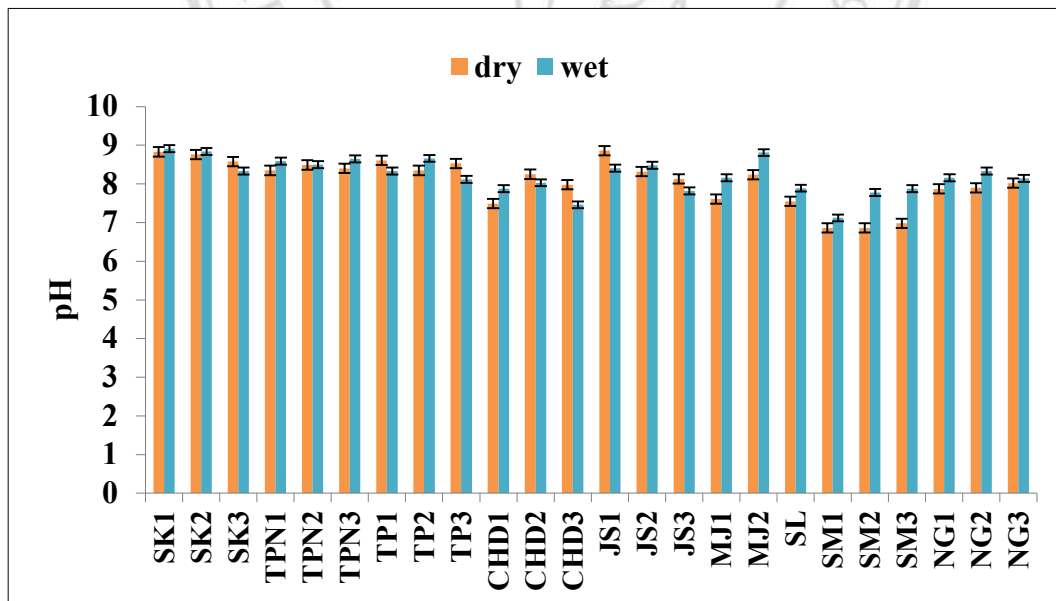


Figure 3.6 Comparison of pH in the investigated localities between wet and dry season. The x-axis is sampling sites and digits after the alphabet is the temperature range each sampling sites (1 = 37-40°C, 2 = 41-45°C, 3 = 46-50°C).

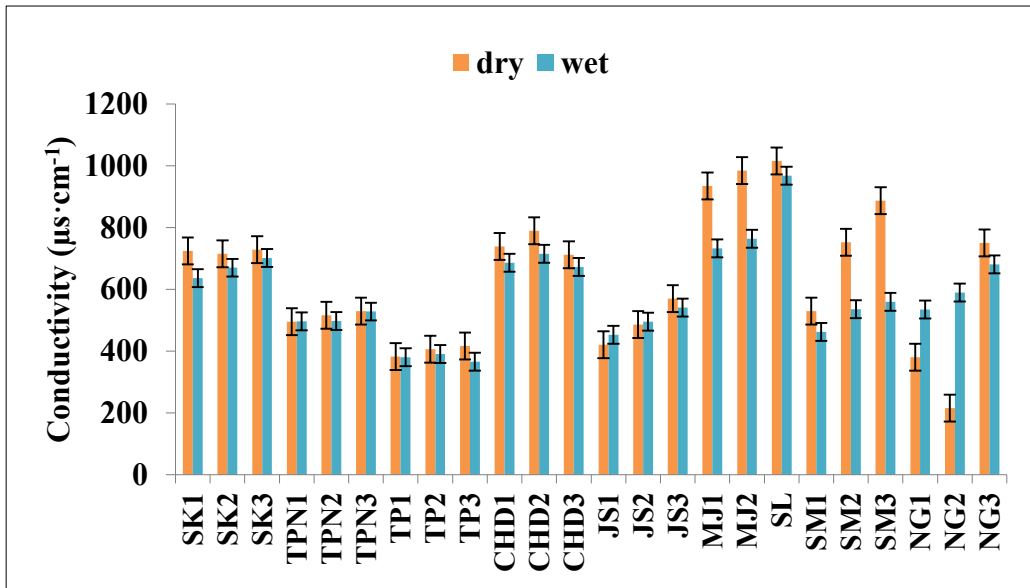


Figure 3.7 Comparison of conductivity ( $\mu\text{s}\cdot\text{cm}^{-1}$ ) in the investigated localities between wet and dry season. The x-axis is sampling sites and digits after the alphabet is the temperature range each sampling sites (1 = 37-40°C, 2 = 41-45°C, 3 = 46-50°C).

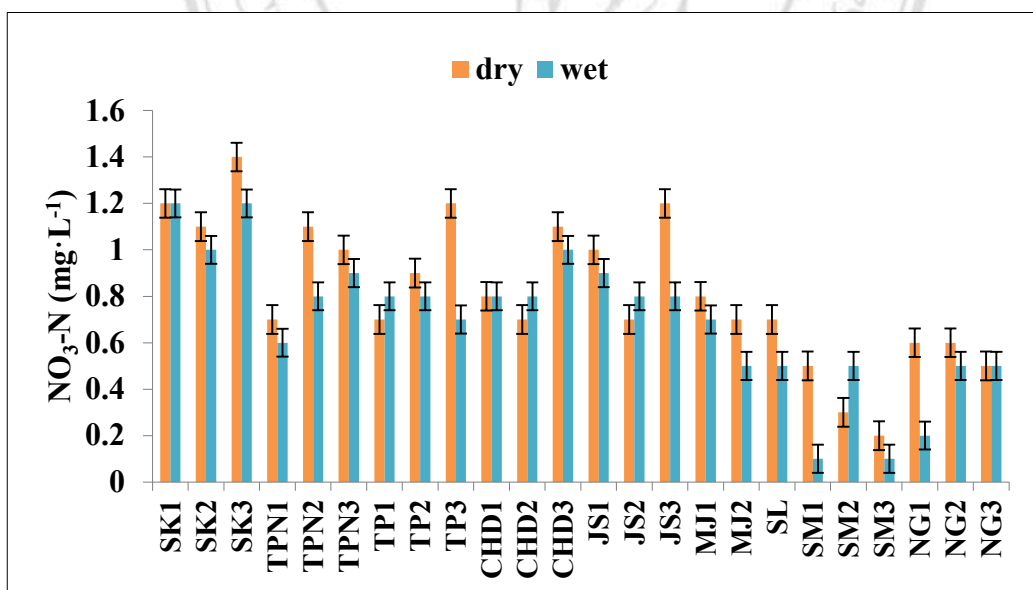


Figure 3.8 Comparison of  $\text{NO}_3\text{-N}$  ( $\text{mg}\cdot\text{L}^{-1}$ ) in the investigated localities between wet and dry season. The x-axis is sampling sites and digits after the alphabet is the temperature range each sampling sites (1 = 37-40°C, 2 = 41-45°C, 3 = 46-50°C).

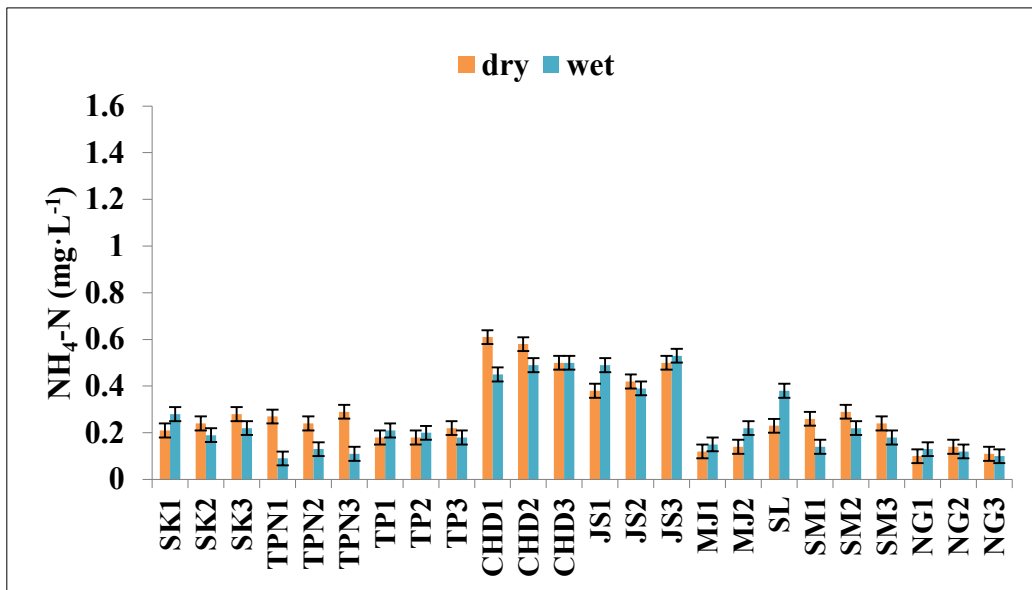


Figure 3.9 Comparison of NH<sub>4</sub>-N (mg·L<sup>-1</sup>) in the investigated localities between wet and dry season. The x-axis is sampling sites and digits after the alphabet is the temperature range each sampling sites (1 = 37-40°C, 2 = 41-45°C, 3 = 46-50°C).

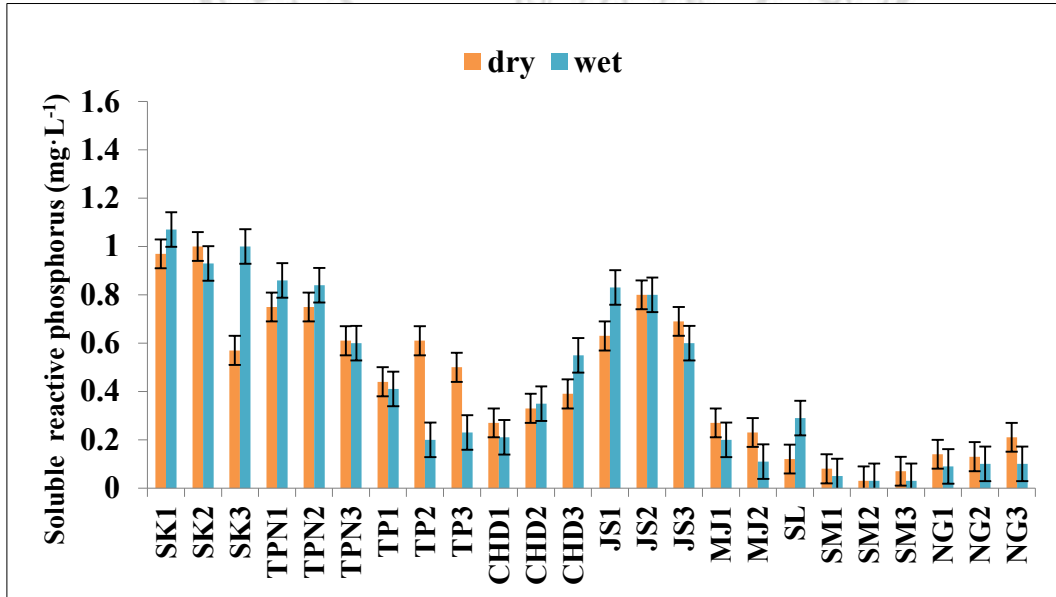


Figure 3.10 Comparison of SRP (mg·L<sup>-1</sup>) in the investigated localities between wet and dry season. The x-axis is sampling sites and digits after the alphabet is the temperature range each sampling sites (1 = 37-40°C, 2 = 41-45°C, 3 = 46-50°C).

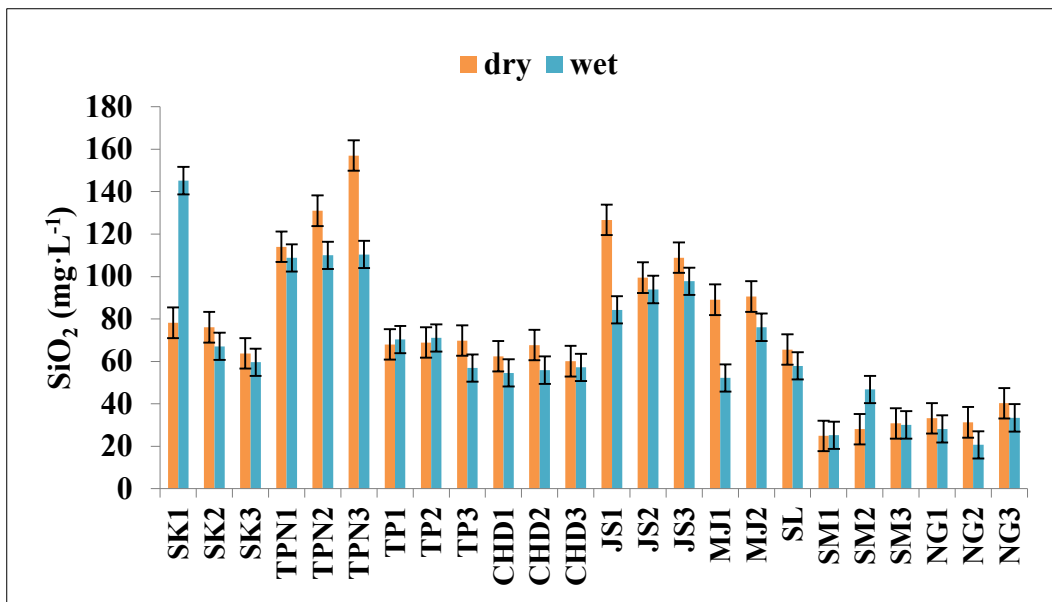


Figure 3.11 Comparison of SiO<sub>2</sub> (mg·L<sup>-1</sup>) in the investigated localities between wet and dry season. The x-axis is sampling sites and digits after the alphabet is the temperature range each sampling sites (1 = 37-40°C, 2 = 41-45°C, 3 = 46-50°C).

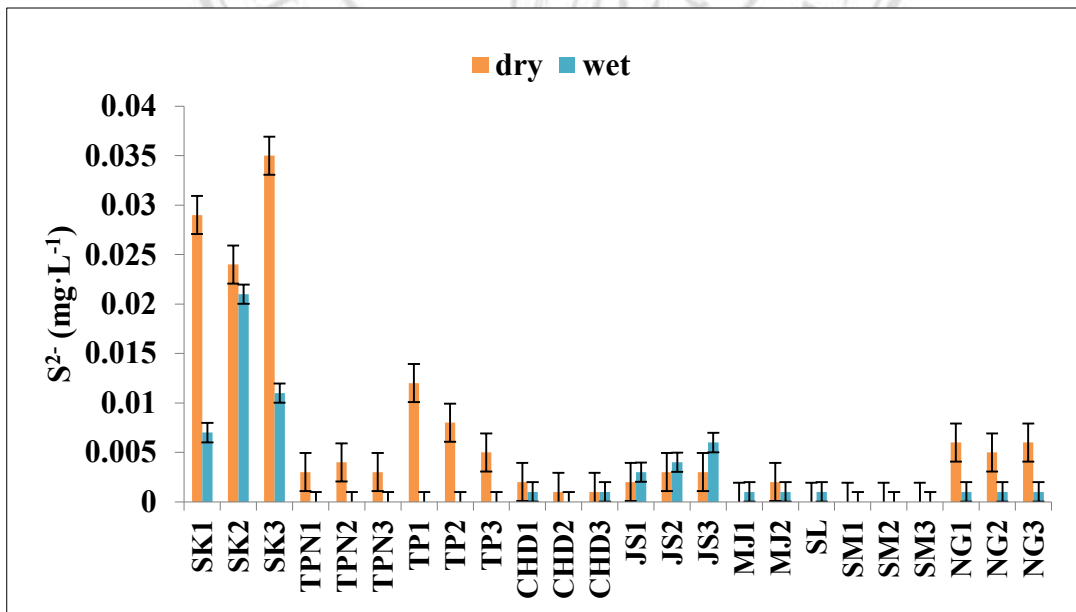


Figure 3.12 Comparison of S<sup>2-</sup> (mg·L<sup>-1</sup>) in the investigated localities between wet and dry season. The x-axis is sampling sites and digits after the alphabet is the temperature range each sampling sites (1 = 37-40°C, 2 = 41-45°C, 3 = 46-50°C).

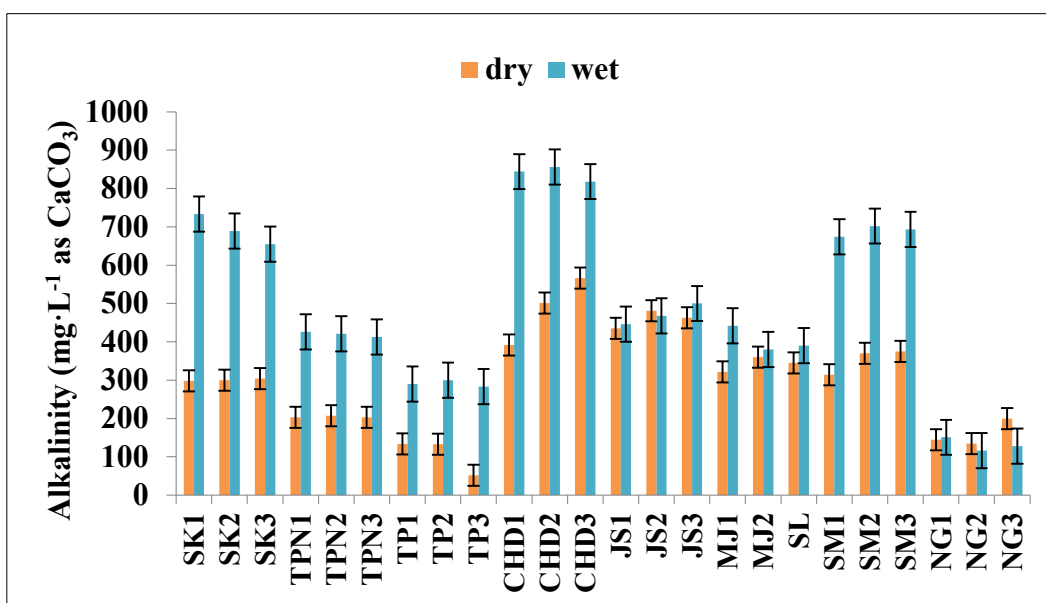


Figure 3.13 Comparison of alkalinity ( $\text{mg}\cdot\text{L}^{-1}$  as  $\text{CaCO}_3$ ) in the investigated localities between wet and dry season. The x-axis is sampling sites and digits after the alphabet is the temperature range each sampling sites (1 = 37-40°C, 2 = 41-45°C, 3 = 46-50°C).

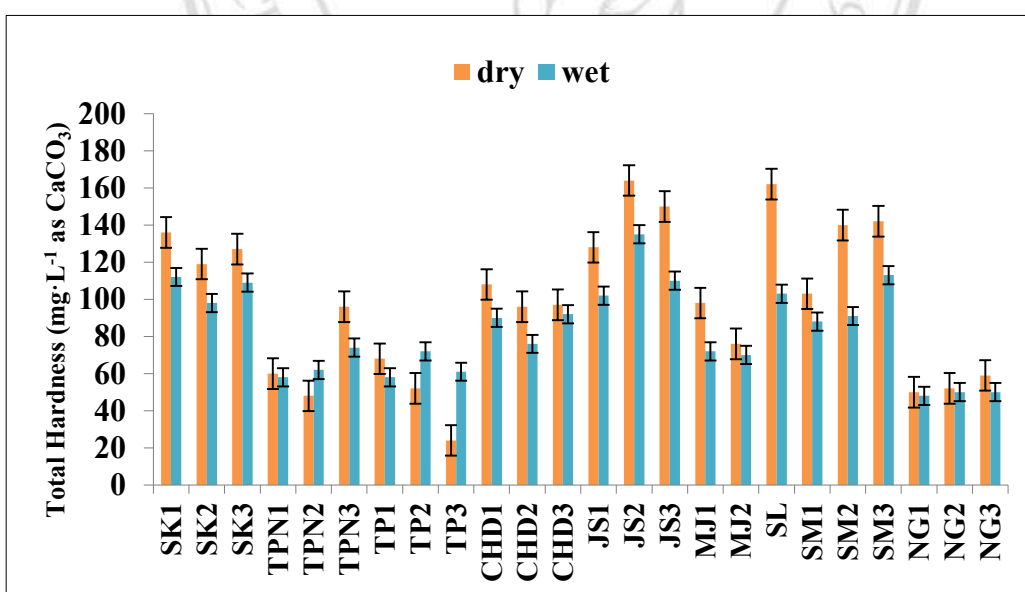


Figure 3.14 Comparison of total hardness ( $\text{mg}\cdot\text{L}^{-1}$  as  $\text{CaCO}_3$ ) in the investigated localities between wet and dry season. The x-axis is sampling sites and digits after the alphabet is the temperature range each sampling sites (1 = 37-40°C, 2 = 41-45°C, 3 = 46-50°C).

### 3.3.2 Diatoms distribution

Thirty-six diatom taxa including centric and pennate diatoms were observed in nine investigated sites. The abundant species among nine hot spring samples were *Diatomella balfouriana* Greville [Figure 3.48, plate 3(6-10)], *Rhopalodia gibberula* (Ehrenberg) O.F. Müller [Figure 3.48, plate 4(1-4)] and *Sellaphora lanceolata* D.G. Mann & S. Dropp in Mann *et al.* [Figure 3.48, plate 2(1-3)]. They have been found at a wide range of temperatures from 37°C to 51°C in the thermal samplings. Furthermore, the hot spring marshes in Kenya, which recorded temperatures ranging from 32°C to 50°C, showed a high diversity of diatoms, while *Rhopalodia gibberula* (Ehrenberg) O.F. Müller was found to be the most abundant species (Owen *et al.*, 2004). It was noticeable that these three above-mentioned diatom species could grow in a wide range of temperatures.

Along with the physical and chemical factors measured in this investigation, seasonality was a principal factor in determining the variability of species composition. The highest recorded levels of diatom density during both seasons were in San Kamphaeng Hot Spring (SK) at 21% and 20% in the dry season and wet season, respectively. This was followed by Pong Ang Hot Spring (CHD) in the dry season (20%). Theppanom Hot Spring (TPN) presented the next highest level during the wet season. The least amount of density was detected in Ban Su Men Hot Spring (SM) during both seasons (Figure 3.16, 3.17). In a comparison of the two seasons, *Achnantheidium exiguum* (Grunow) Czarnecki, *Navicula grimmei* Krasske in Hustedt and *Nitzschia palea* (Kützing) W. Smith revealed the highest density during the wet season (Table 3.3); however, this value decreased during the dry season (Table 3.4). Additionally, *Anomoeoneis* sp. in this research was believed to be a rare species or new taxa for the reason that there were differences in the morphology and some environmental conditions with regard to their growth [Figure 3.48, plate 3(3)].

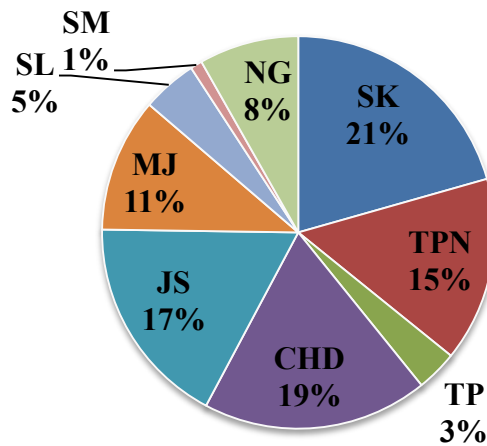


Figure 3.15 Relative abundance of diatoms at nine hot springs sampling sites during the dry season.

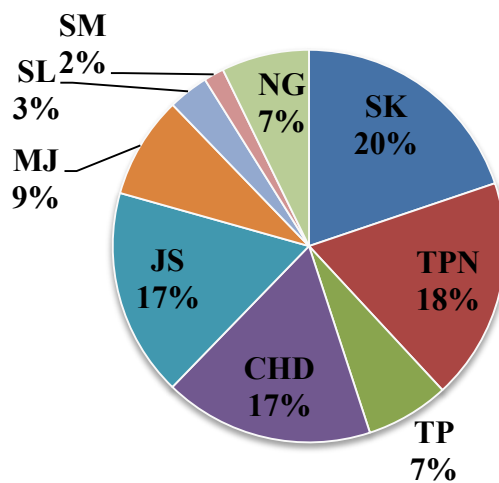


Figure 3.16 Relative abundance of diatoms at nine hot spring sampling sites during the wet season Where; SK= San Kamphaeng Hot Spring, TPN = Thepphanom Hot Spring, TP = Tha Pai Hot Spring, CHD = Pong Ang Hot Spring, JS = Chae Son Hot Spring, MJ = Mae Chok Hot Spring, SL = Salaeng Hot Spring, SM = Ban Su Men Hot Spring and NG = Pong Gi Hot Spring

Table 3.3 Distribution of diatom taxa during the wet season at nine hot spring sites

Taxon/Sites	1	2	3	4	5	6	7	8	9
<i>Aulacoseira ambigua</i> (Grunow) Simonsen									
<i>Aulacoseira granulata</i> Ehrenberg									
<i>Meloseira varians</i> Agardh			+						
<i>Achnantheidium exiguum</i> (Grunow) Czarnecki	+	+	+	+		+		+	+
<i>Achnantheidium</i> sp.	+	+	+	+	+				
<i>Amphora montana</i> Krasske		+	+	+					
<i>Amphora ovalis</i> (Kützing) Kützing	+	+		+	+				
<i>Anomoeneis</i> sp.1	+								
<i>Anomoeneis</i> sp.2							+		
<i>Anomoeneis</i> sp.3	+			+		+			
<i>Caloneis aequatorialis</i> Hustedt	+				+				
<i>Cocconeis placentula</i> Ehrenberg		+							
<i>Craticula ambigua</i> (Ehrenberg) Mann in Round, Crawford & Mann	+			+	+				
<i>Diademsis confervacea</i> Kützing									
<i>Diatomella balfouriana</i> Greville	+	+	+	+	+			+	+
<i>Diploneis ovalis</i> (Hilse) Cleve			+						
<i>Fragillaria crotonensis</i> Kitton									
<i>Gomphonema acutiusculum</i> (O. Müller) Cleve-Euler		+	+		+				
<i>Gomphonema gracile</i> Ehrenberg									
<i>Gomphonema parvulum</i> (Kützing) Van Heurck									
<i>Halamphora fontinalis</i> (Hustedt) Z. Levkov									
<i>Hantzchia amphioxys</i> (Ehrenberg) Grunow in cleve et Grunow		+							
<i>Navicula grimmei</i> Krasske in Hustedt		+	+	+		+	+		+
<i>Navicula subrhynchocephala</i> Hustedt									
<i>Nitzschia amphibia</i> Grunow									
<i>Nitzschia clausii</i> Hantzsch							+		
<i>Nitzschia palea</i> (Kützing) W. Smith	+	+	+	+	+	+			
<i>Pinnularia capitata</i> Ehrenberg		+			+	+			
<i>Pinnularia lapponica</i> Hustedt					+				
<i>Planothidium lanceolatum</i> (Breb.) Round & Bukhtiyarova									
<i>Rhopalodia gibberula</i> (Ehrenberg) O.F. Müller	+	+	+	+	+	+			+
<i>Sellaphora lanceolata</i> D.G. Mann & S. Dropp in Mann et al.	+	+	+	+	+	+	+	+	+
<i>Stausosira elliptica</i> (Schumann) D.M. Williams & Round									
<i>Surirella biseriata</i> Br&A©bisson									
<i>Surirella elegans</i> Ehrenberg				+		+			
<i>Synedra ulna</i> (Nitzsch) Ehrenberg	+			+					

+ indicated that diatoms were found in this sampling site

Table 3.4 Distribution of diatom taxa during the dry season at nine hot spring sites

Taxon/Sites	1	2	3	4	5	6	7	8	9
<i>Aulacoseira ambigua</i> (Grunow) Simonsen							+		
<i>Aulacoseira granulata</i> Ehrenberg	+						+		
<i>Meloseira varians</i> Agardh	+								
<i>Achnantheidium exiguum</i> (Grunow) Czarnecki	+					+		+	
<i>Achnantheidium</i> sp.	+	+	+	+	+				
<i>Amphora montana</i> Krasske	+	+	+	+	+				
<i>Amphora ovalis</i> (Kützing) Kützing	+	+		+	+				
<i>Anomoeneis</i> sp.1	+								
<i>Anomoeneis</i> sp.2							+		
<i>Anomoeneis</i> sp.3	+			+		+			
<i>Caloneis aequatorialis</i> Hustedt	+								
<i>Cocconeis placentula</i> Ehrenberg									+
<i>Craticula ambigua</i> (Ehrenberg) Mann in Round, Crawford & Mann	+	+		+	+				
<i>Diadsmis confervacea</i> Kützing		+				+			
<i>Diatomella balfouriana</i> Greville	+	+	+	+	+	+		+	+
<i>Diploneis ovalis</i> (Hilse) Cleve		+	+						+
<i>Fragillaria crotonensis</i> Kitton	+								+
<i>Gomphonema acutiusculum</i> (O. Müller) Cleve-Euler	+	+			+				
<i>Gomphonema gracile</i> Ehrenberg		+							
<i>Gomphonema parvulum</i> (Kützing) Van Heurck		+							
<i>Halamphora fontinalis</i> (Hustedt) Z. Levkov	+	+	+	+	+				
<i>Hantzchia amphioxys</i> (Ehrenberg) Grunow in cleve <i>et</i> Grunow		+	+	+					
<i>Navicula grimmei</i> Krasske in Hustedt						+	+		+
<i>Navicula subrhynchocephala</i> Hustedt							+		
<i>Nitzschia amphibia</i> Grunow	+				+				
<i>Nitzschia clausii</i> Hantzsch									
<i>Nitzschia palea</i> (Kützing) W. Smith	+				+	+			
<i>Pinnularia capitata</i> Ehrenberg					+	+			
<i>Pinnularia lapponica</i> Hustedt									+
<i>Planothidium lanceolatum</i> (Breb.) Round & Bukhtiyarova	+								
<i>Rhopalodia gibberula</i> (Ehrenberg) O.F. Müller	+	+		+	+	+			+
<i>Sellaphora lanceolata</i> D.G. Mann & S. Dropp in Mann <i>et al.</i>	+	+		+	+	+	+		+
<i>Stausosira elliptica</i> (Schumann) D.M. Williams & Round							+		
<i>Surirella biseriata</i> BrÄ©bison		+							
<i>Surirella elegans</i> Ehrenberg							+		
<i>Synedra ulna</i> (Nitzsch) Ehrenberg									

+ indicated that diatoms were found in this sampling site

### 3.3.3 Statistical analysis

An independent-samples t-test ( $p < 0.01$ ) was conducted to compare hot spring diatoms distribution in wet and dry seasons. The selected diatom taxa with high relative abundant ( $>5\%$ ) were distinguished based on percentage diatom data. This reduced number of species to 12. There was a non-significant different between both seasons in diatoms distribution (Table 3.5). The results showed that the seasons did not affect the distribution of hot spring diatoms. So, the collecting of diatoms in hot springs could done at any time that does not depend on the season. From this point can be traced to the next experiment.

Table 3.5 p-value for diatom taxa during wet and dry season in nine hot spring sites

Taxon	Wet	Dry	p
<i>Achnantheidium exiguum</i> (Grunow) Czarniecki	14.565 ± 30.057	40.478 ± 56.219	0.058
<i>Achnantheidium</i> sp.	24.261 ± 37.824	40.261 ± 51.491	0.236
<i>Amphora montana</i> Krasske	2.609 ± 12.295	1.522 ± 6.480	0.709
<i>Anomoeneis</i> sp.1	3.478 ± 11.774	1.304 ± 6.255	0.438
<i>Anomoeneis</i> sp.2	8.522 ± 40.869	6.261 ± 30.026	0.832
<i>Anomoeneis</i> sp.3	7.696 ± 25.501	8.348 ± 29.125	0.936
<i>Craticula ambigua</i> (Ehrenberg) Mann in Round, Crawford & Mann	7.739 ± 24.423	8.000 ± 21.132	0.969
<i>Diatomella balfouriana</i> Greville	61.739 ± 112.640	52.304 ± 97.442	0.763
<i>Navicula grimmei</i> Krasske in Hustedt	14.739 ± 54.041	12.174 ± 25.008	0.837
<i>Nitzschia palea</i> (Kützting) W. Smith	7.913 ± 34.039	7.261 ± 20.145	0.937
<i>Rhopalodia gibberula</i> (Ehrenberg) O.F. Müller	12.696 ± 29.168	14.087 ± 27.878	0.869
<i>Sellaphora lanceolata</i> D.G. Mann & S. Dropp in Mann <i>et al.</i>	18.565 ± 36.405	23.087 ± 36.897	0.678

Data are expressed as mean ± standard deviation (SD) using t-test ( $p < 0.01$ )

## 3.4 Materials and Methods for Investigation of Diatom Diversity

### 3.4.1 Sampling sites

Samples of diatoms, which differed in geological characteristics, were collected from the same hot springs as previous experiment exception Ban Su Men hot spring because the area was demolished to build up a reservoir by villagers. The period of this investigation was from December 2015 to April 2016. The ranges of water temperature were the primary consideration for community structure. Four ranges of water temperature (37–40, 40.1–45, 45.1–50, 50.1–55°C) and maximum temperature

( $T > 55^{\circ}\text{C}$ ) were defined in this study. The ecological data of each sampling site was recorded, i.e., latitude, longitude and altitude. The descriptions of the sampling sites are presented in the previous studied and the lists of the sampling sites with some general data are given in Table 3.6.

### **3.4.2 Water sampling analysis**

Three replicates of water samples in each temperature ranges were collected followed by previous experiment method exception of continuous 24-hour water temperature was monitored by a Elitech RC-5 LCD USB temperature data logger.

### **3.4.3 Biological analysis**

Investigation of benthic diatoms (Rott *et al.* 1997)

#### **3.4.3.1 Collection of benthic diatoms**

For each sampling process, the epipellic/epilithic and periphytic diatom samples were scraped from the edges of hot spring pools or stones in three replicates for each range of temperature. A plastic sheet with a  $10\text{ cm}^2$  cutout was placed on the upper surface of the selected substrates. They were brushed and rinsed with distilled water until the surface was apparent.

#### **3.4.3.2 Cleaning process, identification and counting for benthic diatoms**

The samples were cleaned, identified and counted by using the previous method in 3.2.3.2 and 3.2.3.3.

### **3.4.4 Data evaluation**

#### **3.4.4.1 Study of diversity**

The diversity of benthic diatoms was quantified with the Shannon Weiner's Diversity Index (Shannon 1948). The ensuing formula was used to calculate the values:

$$H' = - \sum_{i=1}^R p_i \ln p_i$$

where  $H'$  = Shannon Weiner's Diversity Index

$p_i$  = The ratio of individuals in the  $i$ th species

$R$  = Number of species

$$E = H' / \ln S$$

where  $E$  = Evenness

$S$  = Total number of species in the population

#### 3.4.4.2 Statistics analysis

Diatom assemblage patterns were examined utilizing several approaches including R Project for Statistical Computing version 3.4.2 supported by CRAN (the Comprehensive R Archive Network). Water properties and sampling sites were distinguished by Hierarchical Cluster Analyses (HCA) carried out with the R package NbClust. The Principal Component Analysis (PCA) was utilized for the investigation of the relationship between the sampling sites and the water quality of each sampling site. The complete option was embraced for the clustering as it includes a greater proportion of the information than other options. A non-metric multidimensional scaling technique (NMDS) with Bray–Curtis distance measure was used to evaluate variations of diatom assemblages and the water quality of each sampling site in the studied hot springs. The physico-chemical factors were correlated to the NMDS axes using the Fits an Environmental Vector (envfit function) of the Vegan library (Oksanen *et al.*, 2018). Environmental variables were transformed using square-root transformation and standardized by Wisconsin command. The fit ( $R^2$ ) of each variable to the ordination was assessed using the envfit function with a Monte-Carlo analysis of 999 permutations. The NMDS result was plotted using ggplot function of the ggplot2 library (Wickham, 2009).

Table 3.6 Location of 8 hot spring sampling sites

Site	37–40 (°C)		40.1–45 (°C)		45.1–50 (°C)		50.1–55 (°C)		Tmax (°C)	
	Location Co-ordinates	Altitude (m)	Location Co-ordinates	Altitude (m)	Location Co-ordinates	Altitude (m)	Location Co-ordinates	Altitude (m)	Location Co-ordinates	Altitude (m)
<b>SK</b>	18° 48' 59" N 99° 13' 39" E	360	18° 48' 59" N 99° 13' 39" E	360	18° 48' 59" N 99° 13' 39" E	360	18° 48' 59" N 99° 13' 39" E	360	18° 48' 59" N 99° 13' 39" E	360
<b>TPN</b>	18° 16' 16" N 98° 23' 42" E	372	18° 16' 16" N 98° 23' 42" E	320	18° 16' 13" N 98° 23' 54" E	363	18° 16' 21" N 98° 23' 44" E	369	18° 16' 21" N 98° 23' 45" E	351
<b>TP</b>	19° 18' 35" N 98° 27' 57" E	518	19° 17' 53" N 98° 28' 14" E	536	19° 17' 52" N 98° 28' 13" E	505	19° 18' 27" N 98° 28' 33" E	481	19° 18' 26" N 98° 28' 34" E	524
<b>CHD</b>	19° 35' 42" N 98° 56' 32" E	485	19° 35' 49" N 98° 56' 43" E	491	19° 35' 54" N 98° 56' 50" E	497	– –	– –	– –	– –
<b>JS</b>	18° 50' 12" N 99° 28' 19" E	424	18° 50' 12" N 99° 28' 19" E	424	18° 50' 12" N 99° 28' 19" E	424	18° 50' 12" N 99° 28' 19" E	424	18° 50' 12" N 99° 28' 20" E	430
<b>MJ</b>	– –	–	17° 58' 44" N 99° 38' 15" E	143	17° 58' 44" N 99° 38' 15" E	143	17° 58' 44" N 99° 38' 15" E	143	17° 58' 44" N 99° 38' 15" E	131
<b>SL</b>	– –	–	18° 05' 35" N 99° 49' 45" E	131	– –	– –	– –	– –	– –	– –
<b>NG</b>	19° 13' 19" N 100° 39' 12" E	408	19° 13' 19" N 100° 39' 12" E	408	19° 13' 19" N 100° 39' 12" E	408	– –	– –	– –	– –

## 3.5 Results for Investigation of Diatom Diversity

Hot spring diatoms and water quality measurements were examined at eight hot springs located in northern Thailand during the period of December 2015 – April 2016.

### 3.5.1 Physico-chemical analysis

#### 3.5.1.1 Water temperature

The ranges of water temperature in the SK, TPN, TP, CHD, JS, MJ, SL and NG sites were 38.4–98.0, 39.1–85.0, 38.5–75.2, 38.9–45.4, 40.0–73.4, 41.1–66.7, 41.8 and 39.1–46.9°C, respectively (Figure 3.17, Appendix C). The highest and lowest water temperatures were established at SK5 and SK1. Furthermore, three sampling sites, CHD, SL and NG, could not find the maximum temperature ( $T > 55^\circ\text{C}$ ).

#### 3.5.1.2 pH

The pH of the water is the acidic or basic measurement of the water on a scale of 0–14. The common range for pH in surface water is 6.5 to 8.5 and for groundwater is 6 to 8.5. All hot spring sampling sites had a range of pH values from 6.8–8.8. The ranges of pH in the SK, TPN, TP, CHD, JS, MJ, SL and NG sites were 8.7–8.8, 8.2–8.5, 6.8–7.3, 7.0–7.2, 7.3–7.7, 7.3–7.4, 7.6 and 7.0–7.2, respectively. The highest level was recorded in SK1 and the lowest was found at TP5 (Figure 3.18, Appendix C).

ลิขสิทธิ์มหาวิทยาลัยเชียงใหม่  
Copyright © by Chiang Mai University  
All rights reserved

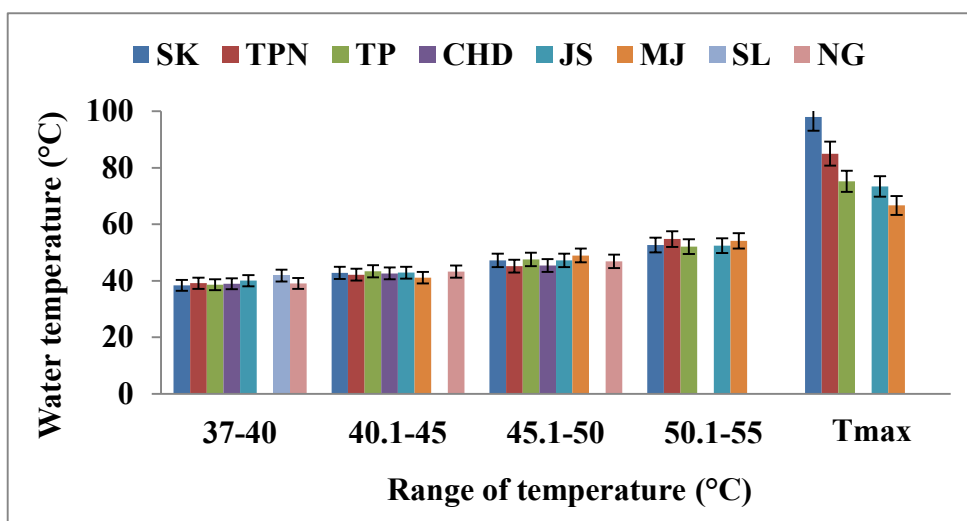


Figure 3.17 Water temperatures of 8 hot springs sampling sites in 4 temperature ranges and Tmax (T>55°C)

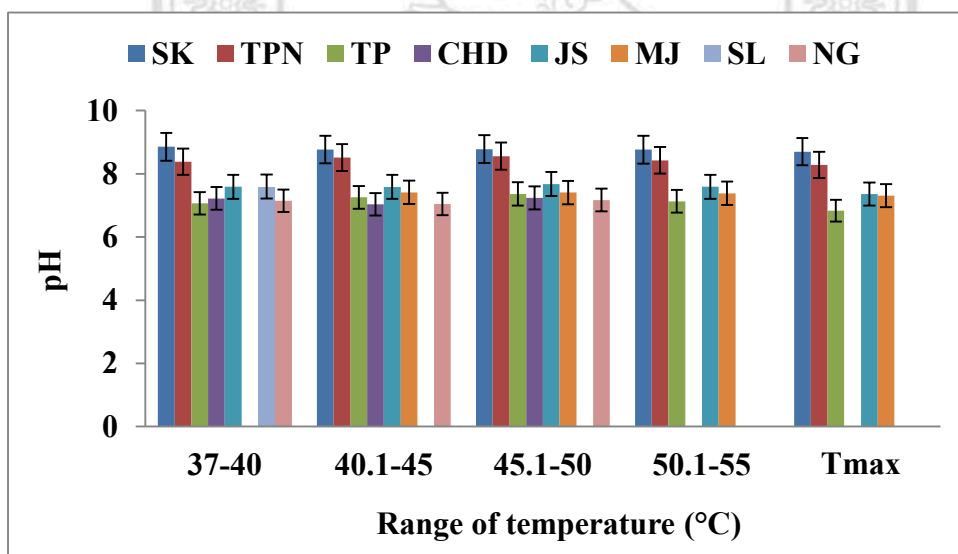


Figure 3.18 pH of 8 hot springs sampling sites in 4 temperature ranges and Tmax (T>55°C)

### 3.5.1.3 Conductivity

Conductivity is the measurement of the capacity of an aqueous solution to induce an electric current. Cations and anions carry the ion current by which a solution conducts electricity and this relies on the concentration of ions, the mobility of ions, the valence of ions and temperature. All hot spring sampling sites had a range of conductivity from 364.67-1104.3  $\mu\text{s}\cdot\text{cm}^{-1}$ . The ranges of conductivity in the SK, TPN, TP, CHD, JS, MJ, SL and NG sites were 743.7–821, 521.3–575.7, 364.7–379.3, 797.7–804.3, 524–576.3, 1014.3–1062.7, 1104.3 and 517–682  $\mu\text{s}\cdot\text{cm}^{-1}$ , respectively. The highest value was found at SL2 and the lowest at TP5 (Figure 3.19, Appendix C). The tendency of conductivity in hot springs was high because of the presence of carbonate ions in mountainous limestone areas, and also high temperatures are known to affect the ions that are present in the water.

### 3.5.1.4 Nitrate–nitrogen

The most significant contribution of nitrate in surface water occurs from decaying organic matter, sewage waste and nitrate fertilizers. The ranges of nitrate–nitrogen in the SK, TPN, TP, CHD, JS, MJ, SL and NG sites were 0.40–15.43, 0.23–0.80, 0.17–0.30, 0.20–0.33, 0.13–3.40, 0.23–0.53, 0.47 and 0.27–0.33  $\text{mg}\cdot\text{L}^{-1}$ , respectively. The range of nitrate–nitrogen content of all sampling sites was 0.13–15.43  $\text{mg}\cdot\text{L}^{-1}$ . The lowest and highest concentrations were found at JS1 and SK5 (Figure 3.20, Appendix C).

### 3.5.1.5 Ammonium–nitrogen

The ranges of ammonium–nitrogen in the SK, TPN, TP, CHD, JS, MJ, SL and NG sites were 0.53–3.52, 0.17–0.35, 0.02–0.30, 0.36–0.42, 0.24–1.58, 0.14–0.15, 0.23 and 0.06–0.1  $\text{mg}\cdot\text{L}^{-1}$ , respectively. The range of ammonium–nitrogen content of all sampling sites was 0.002–3.52  $\text{mg}\cdot\text{L}^{-1}$ . The highest and lowest concentrations of ammonium–nitrogen were found at SK5 and NG1 (Figure 3.21, Appendix C).

### 3.5.1.6 Soluble reactive phosphorus (SRP)

Concentrations of SRP are low in groundwater and do not greatly alter the distribution of major cations. The ranges of the SRP in SK, TPN, TP, CHD, JS,

MJ, SL and NG sites were 0.52–0.98, 1.12–1.29, 0.08–0.26, 0.95–1.02, 0.14–0.50, 0.36–1.15, 0.38 and 0.30–0.56 mg·L<sup>-1</sup>, respectively. The range of SRP of all sampling sites was 0.08–1.29 mg·L<sup>-1</sup>. The highest and lowest concentrations were recorded at TPN5 and TP1 (Figure 3.22, Appendix C).

#### 3.5.1.7 Silicon dioxide (SiO<sub>2</sub>)

Silica is one of the key components that are essential for diatom growth. The ranges of SiO<sub>2</sub> in all sampling sites were 35.1–218.8 mg·L<sup>-1</sup>. The ranges of the SiO<sub>2</sub> in SK, TPN, TP, CHD, JS, MJ, SL and NG sites were 130.1–218.8, 103.1–115.7, 68.–71.9, 54.8–56.8, 93.6–126.9, 79.8–84.4, 82.7 and 35.1–39.2, respectively. The highest level was recorded at SK5 and the lowest at NG1 (Figure 3.23, Appendix C).

#### 3.5.1.8 Alkalinity

All sampling sites were located in mountainous limestone areas (Land Development Department Thailand, 2011), which led to high alkalinity levels. The ranges of alkalinity in the SK, TPN, TP, CHD, JS, MJ, SL and NG sites were 323.7–349.7, 216.3–229.0, 156.7–168.0, 436.0–445.7, 226.0–254.3, 353.3–366, 448 and 155.3–197.3 mg·L<sup>-1</sup> CaCO<sub>3</sub>, respectively. The ranges of alkalinity at all sampling sites were 155.3–448 mg·L<sup>-1</sup> CaCO<sub>3</sub>. The highest level was recorded at SL1 and the lowest at NG1 (Figure 3.24, Appendix C).

#### 3.5.1.9 Total hardness

Total hardness denotes the concentration of calcium and magnesium in the water and is usually expressed as the equivalent of CaCO<sub>3</sub>. Hardness is an important criterion for determining the usability of water for domestic use and drinking, as well as for a variety of industrial supplies. Hardness is an alkalinity component (of about 10%) that made the low value showed in graph. The ranges of total hardness in the SK, TPN, TP, CHD, JS, MJ, SL and NG sites were 4–9, 11–15, 35–45, 57–59, 47–65, 64–72, 50 and 28–57, respectively. The ranges of total hardness at all sampling sites were 4–72. The highest level was recorded at MJ5 and the lowest at SK2. (Figure 3.25, Appendix C).

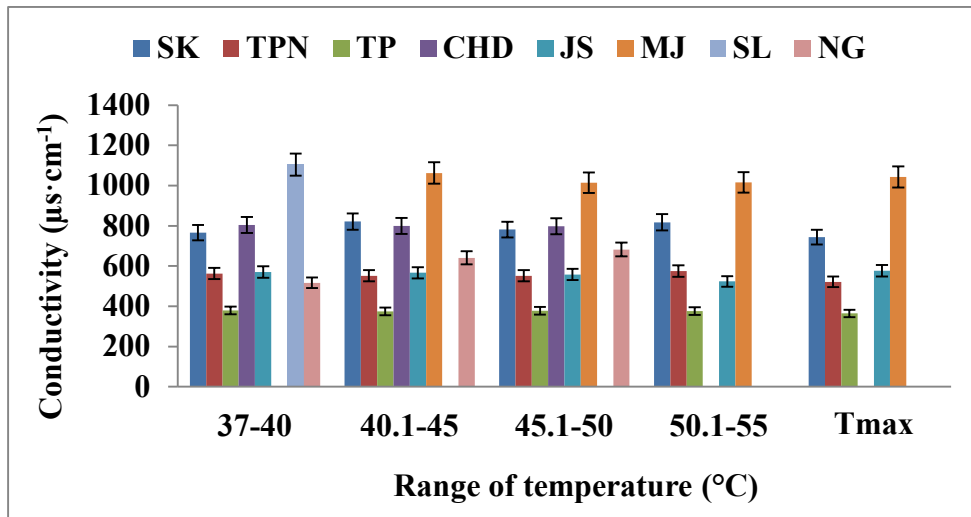


Figure 3.19 Conductivity of 8 hot springs sampling sites in 4 temperature ranges and Tmax (T>55°C)

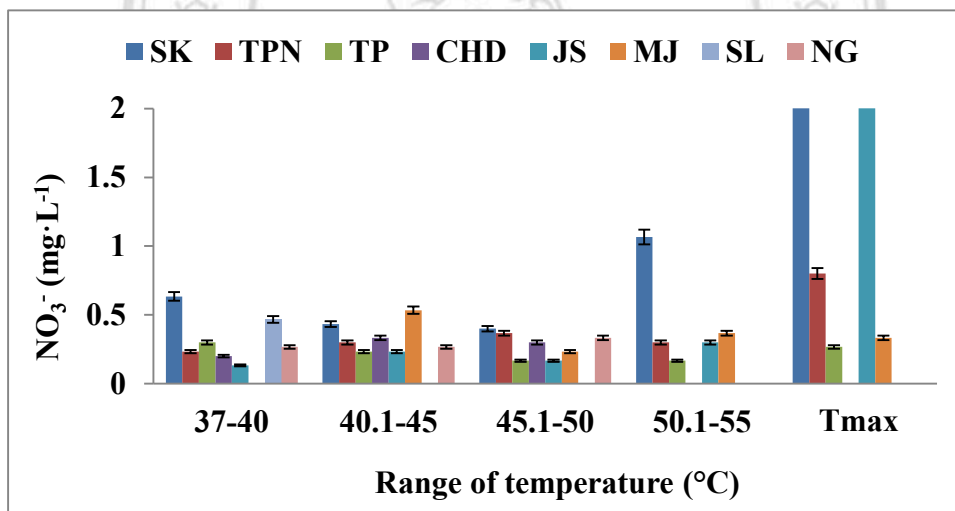


Figure 3.20 Nitrate-nitrogen of 8 hot springs sampling sites in 4 temperature ranges and Tmax (T>55°C)

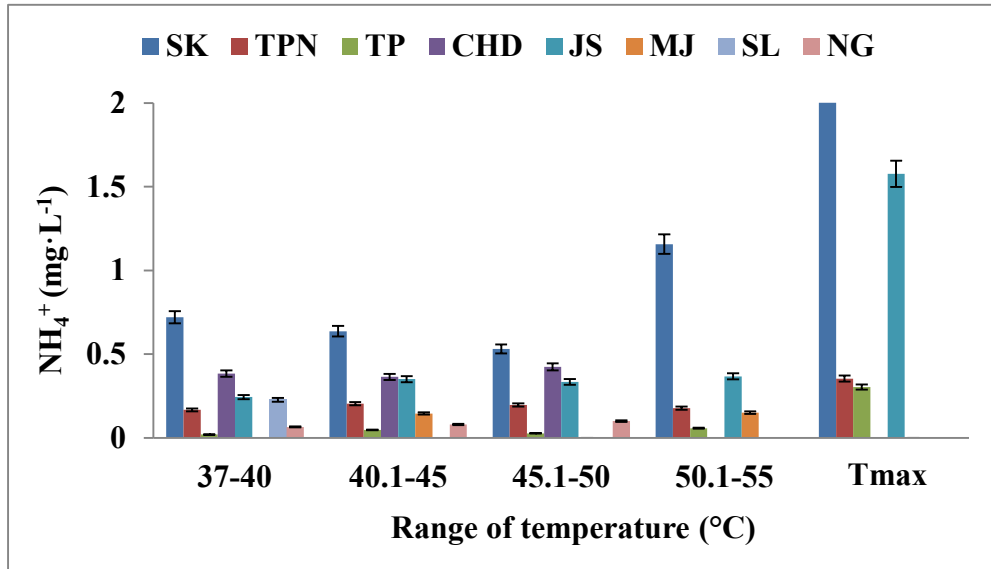


Figure 3.21 Ammonium–nitrogen of 8 hot springs sampling sites in 4 temperature ranges and Tmax (T>55°C)

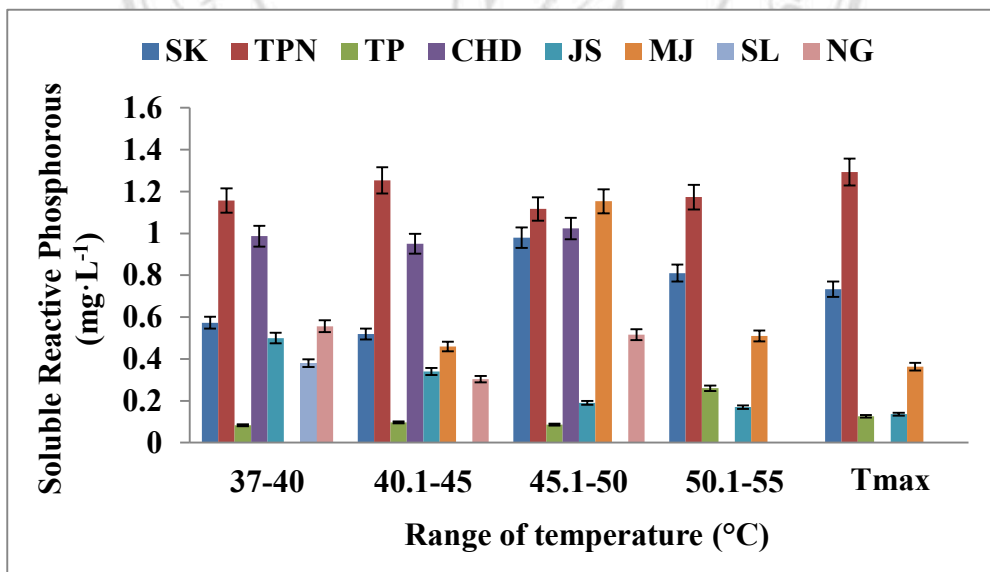


Figure 3.22 Soluble reactive phosphorus (SRP) of 8 hot springs sampling sites in 4 temperature ranges and Tmax (T>55°C)

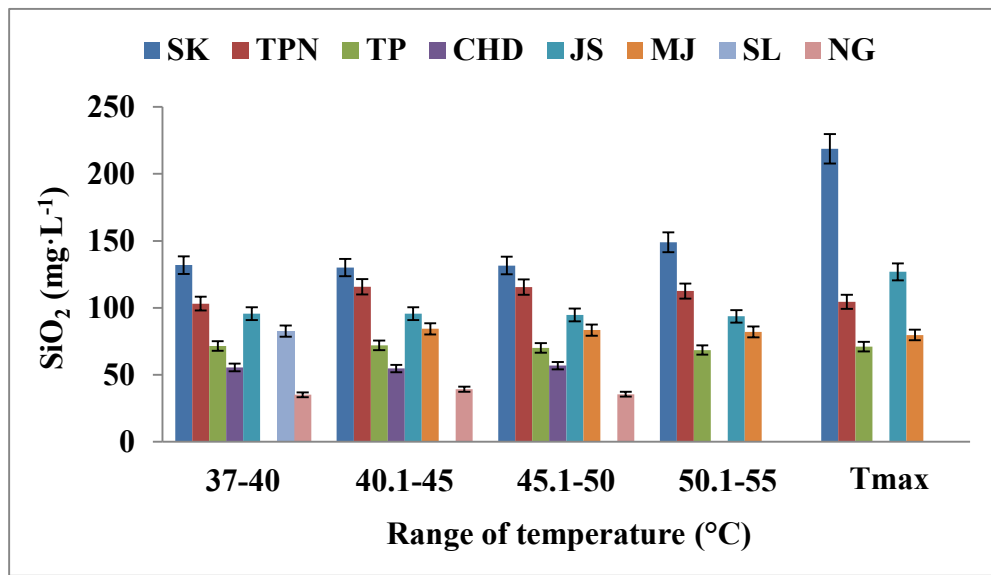


Figure 3.23 Silicon dioxide of 8 hot springs sampling sites in 4 temperature ranges and Tmax (T>55°C)

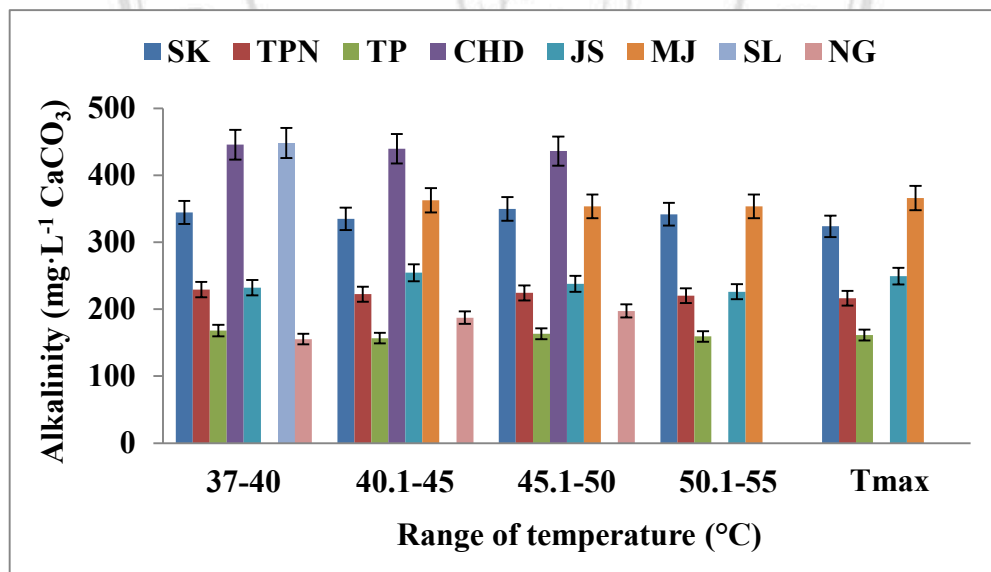


Figure 3.24 Alkalinity of 8 hot springs sampling sites in 4 temperature ranges and Tmax (T>55°C)

#### 3.5.1.10 Sulfide

Sulfide is an inorganic anion of sulfur. Sulfide compounds are fairly soluble. Sulfide-rich hot springs with neutral or alkaline pH values are relatively rare in most geothermal areas in the world. Microorganisms that thrive in such springs often form long streamers or mats, but the appearance of the mats and the types of microorganisms in them seem to vary depending on the sulfide concentration, pH, temperature, as well as other chemical and physical factors. The ranges of sulfide in the SK, TPN, TP, CHD, JS, MJ, SL and NG sites were 0.011–5.687, 0–0.055, 0–0.033, 0.001–0.002, 0.003–0.730, 0–0.006, 0.003 and 0.001–0.002 mg·L<sup>-1</sup>, respectively. The range of sulfide at all sampling sites was 0–5.69 mg·L<sup>-1</sup>. The highest level was recorded at SK5 and the lowest at TPN3, TP1, TP2, TP3 and MJ3. (Figure 3.26, Appendix C).

#### 3.5.2 Water temperature investigation in 24-hour

Water temperatures in eight hot spring sampling sites fluctuated by less than 10°C (2.3–9.7°C) over a 24-hour period (Figure 3.27–3.35, Appendix E). The effects of heat loss by conductive cooling, mixing, and boiling is quantified for the springs which are the major source of hot water discharge. The range of temperature tolerance is different during different periods for the same species. The hot water component is assumed to be influenced by the geothermal reservoir at differing depths and involves chemical characteristics and temperatures that are distinctly different from the colder, fresher water that mixes with it. The highest fluctuation was recorded at NG1 at 9.7°C (Figure 3.34) and the lowest temperature gradients were recorded at TP4 min at 2.3°C (Figure 3.29). For all sampling sites, the highest average fluctuated temperature was noted at NG at 6.9°C and the lowest was noted at CHD at 3.2°C (Figure 3.30). At SK, the variation in water temperature is caused by human disturbance that the water pressure pump was built and turned on and off in day period. This may affect the distribution of diatoms.

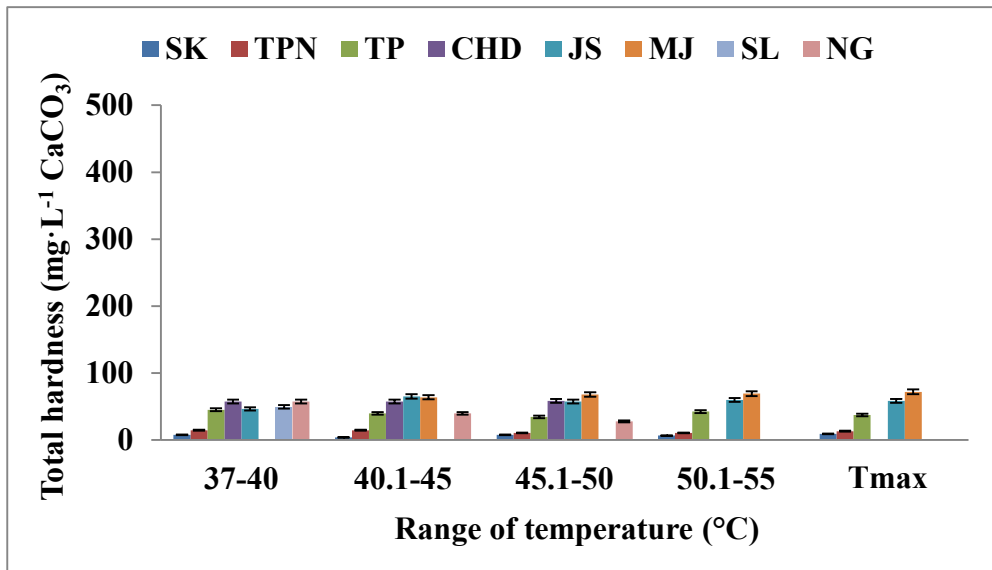


Figure 3.25 Total hardness of 8 hot springs sampling sites in 4 temperature ranges and Tmax (T>55°C)

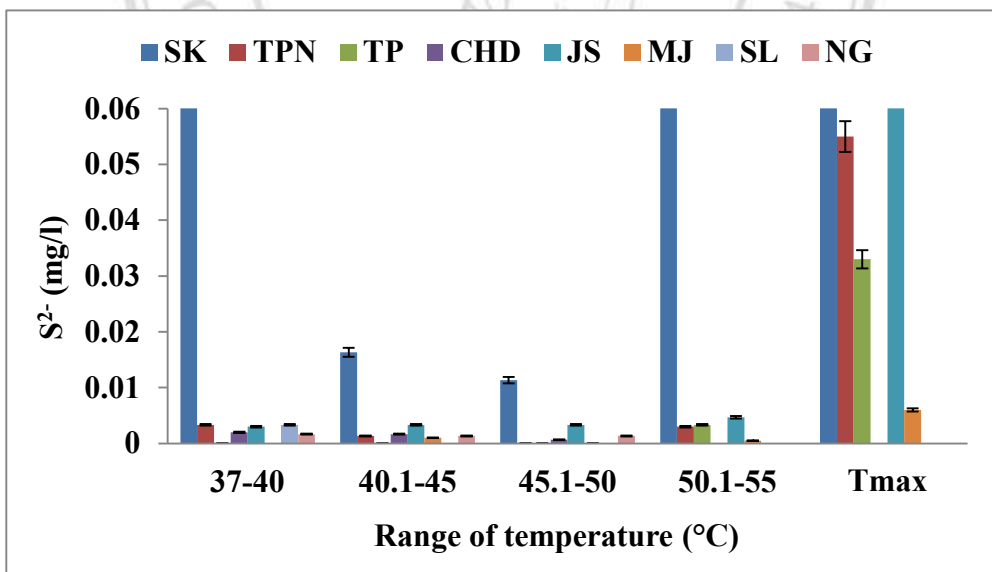


Figure 3.26 Sulfide of 8 hot springs sampling sites in 4 temperature ranges and Tmax (T>55°C)

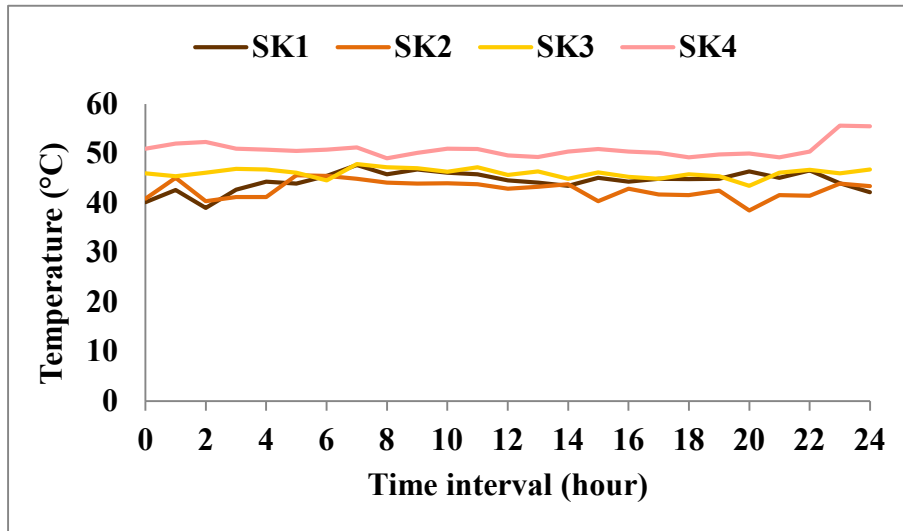


Figure 3.27 Water temperature fluctuations of each sampling sites at San Kamphaeng hot springs in 24 hours.

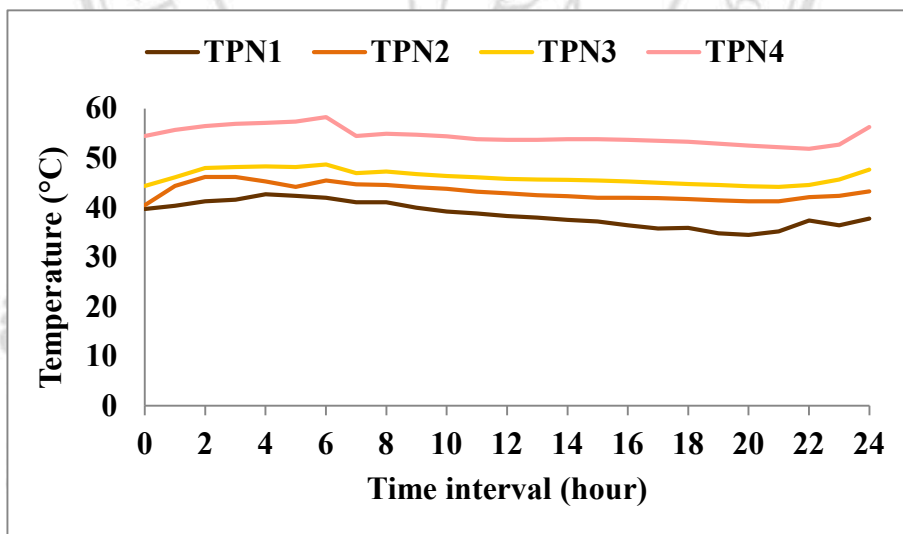


Figure 3.28 Water temperature fluctuations of each sampling sites at Theppanom hot springs in 24 hours.

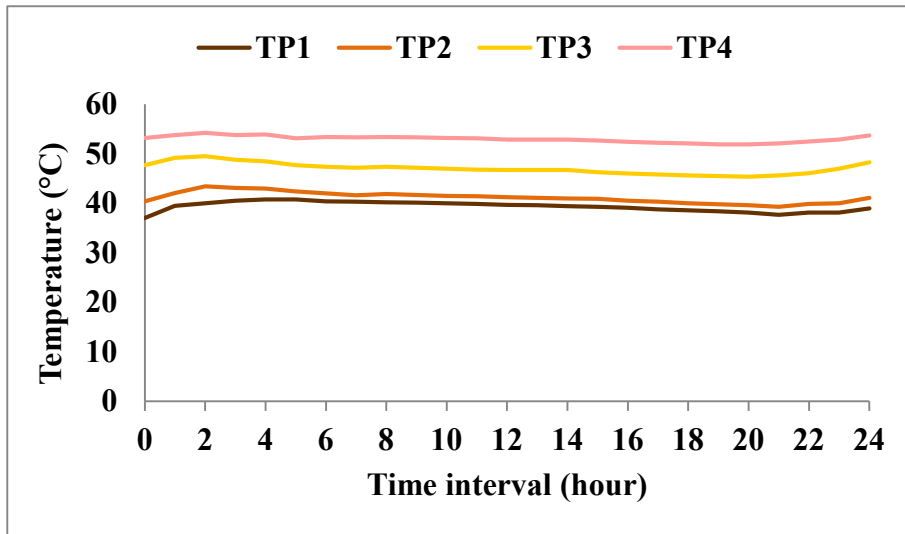


Figure 3.29 Water temperature fluctuations of each sampling sites at Ta Pai hot springs in 24 hours.

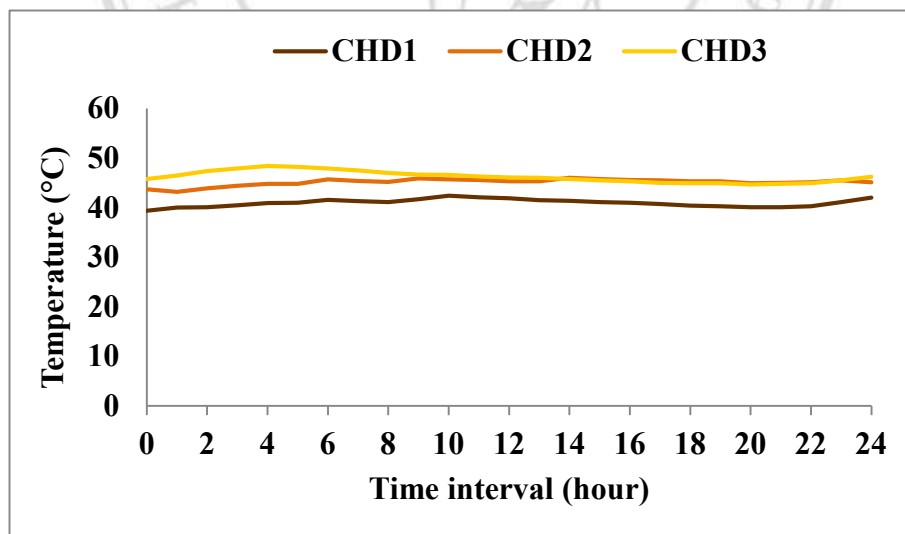


Figure 3.30 Water temperature fluctuations of each sampling sites at Pong Ang hot springs in 24 hours.

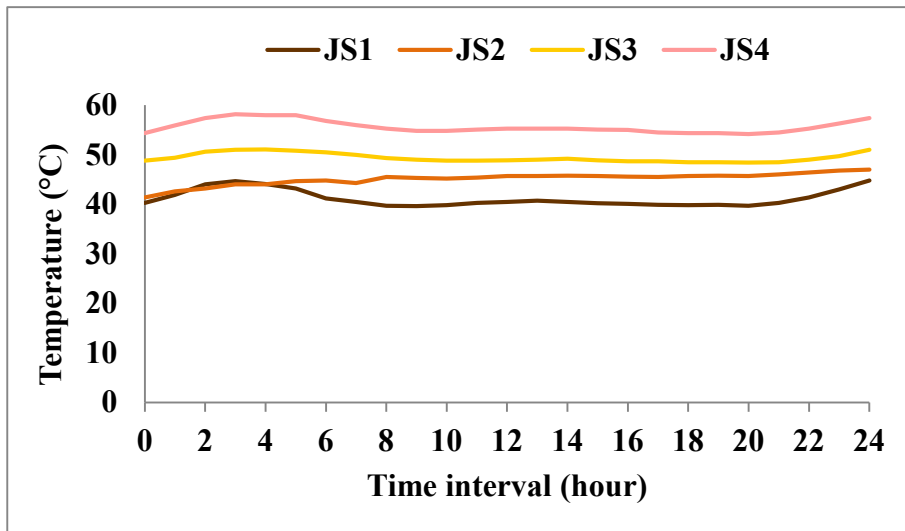


Figure 3.31 Water temperature fluctuations of each sampling sites at Chae Sorn hot springs in 24 hours.

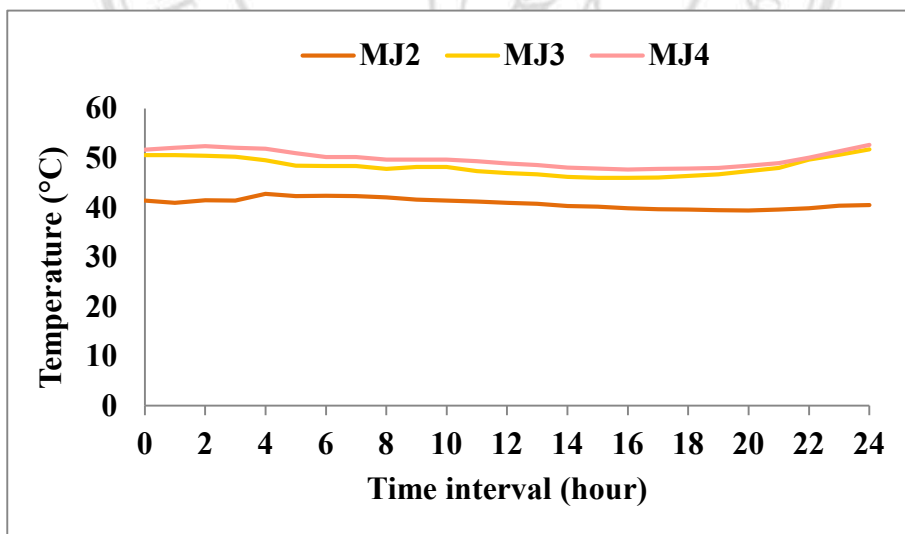


Figure 3.32 Water temperature fluctuations of each sampling sites at Mae Chok hot springs in 24 hours.

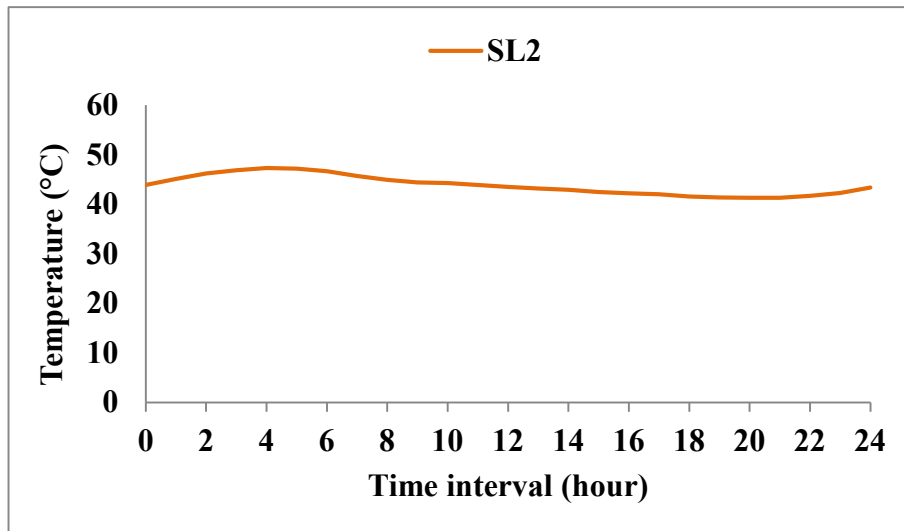


Figure 3.33 Water temperature fluctuations of sampling sites at Wat Salaeng hot springs in 24 hours.

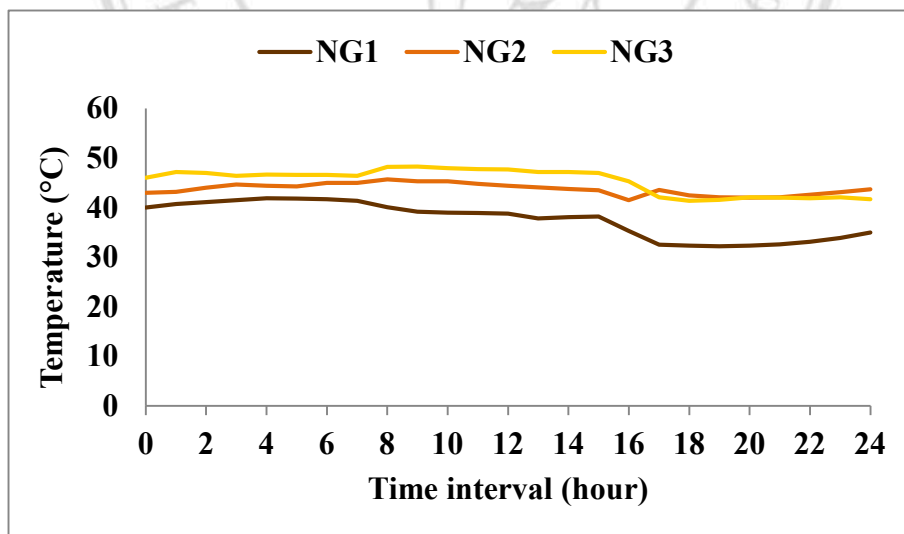


Figure 3.34 Water temperature fluctuations of each sampling sites at Pong Gi hot springs in 24 hours.

### 3.5.3 Hot spring diatoms

Forty-six species of hot spring diatoms were investigated in this study, and they belong to 2 Classes (Class Coscinodiscophyceae and Bacillariophyceae), 14 Orders (Order Aulacoseirales, Melosirales, Mastogloiales, Cocconeidales, Thalassiophysales, Cymbellales, Naviculales, Cocconeidales, Cymbellales, Rhopalodiales, Fragilariales, Bacillariales, Rhopalodiales and Surirellales) 18 Families (Family Aulacoseiraceae, Melosiraceae, Achnanthaceae, Achnanthidiaceae, Catenulaceae, Anomoeoneidaceae, Gomphonemataceae, Naviculaceae, Stauroneidaceae, Diadesmidaceae, Diploneidaceae, Amphipleuraceae, Sellaphoraceae, Cocconeidaceae, Rhopalodiaceae, Fragilariaceae, Bacillariaceae, Surirellaceae) and 27 Genera. The dominant genera according to high relative abundance (more than 1%) were *Diatomella* (41.7%), *Achnanthidium* (20.9%), *Anomoeoneis* (11.2%), *Rhopalodia* (6.4%), *Sellaphora* (5.7%), *Navicula* (2.9%), *Nitzschia* (2.4%) and *Craticula* (2.1%) (Figure 3.35).

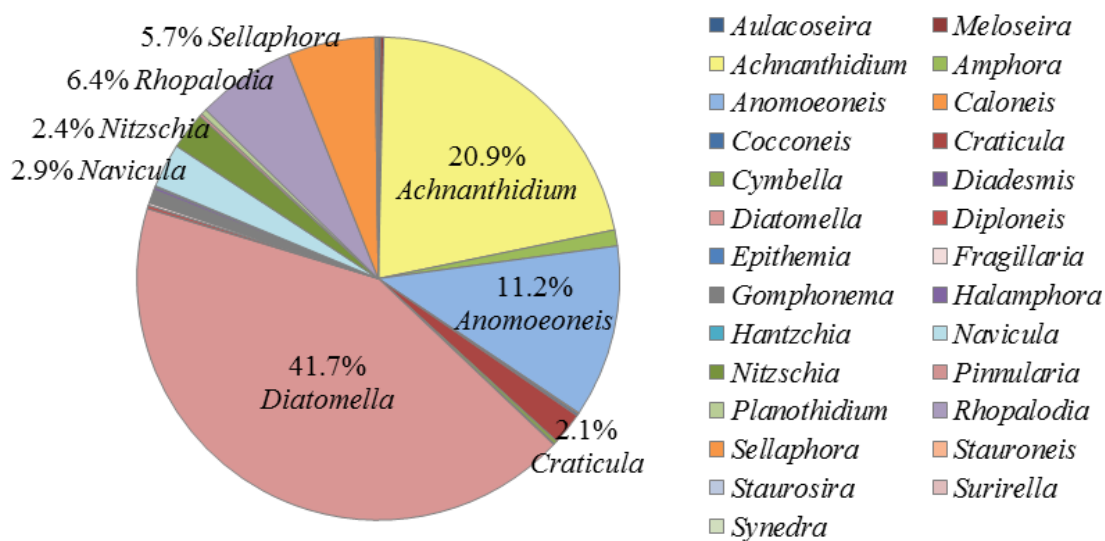


Figure 3.35 Relative abundance percentage of total diatom genera in hot springs sampling sites

Furthermore, *Caloneis molaris* (Grunow) Krammer, *Craticula acidoclinata* Lange-Bertalot & Metzeltin, *Navicula subrhynchocephala* Hustedt and *Pinnularia saprophila* Lange-Bertalot, Kobayashi and Krammer were identified as new records in Thailand (Figure 3.48, 3.49). They were compared with the freshwater algae checklist in Thailand and other related books (Lewmanomont *et al.* 1995; Pekthong 2002; Pekthong and Peerapornpisal 2001; Kunpradid 2005; Suphan 2004 and 2009; Inthasotti 2006a, b; Leelahakriengkrai 2007a, b; Pruetiworanan 2008; Yana 2010; Suphan and Peerapornpisal 2010; Leelahakriengkrai 2011; Yana 2014; Nakkaew 2015).

#### 3.5.3.1 San Kamphaeng Hot Spring (SK), Chiang Mai Province

Thirty-five species of hot spring diatoms were established at the SK site. The most abundant species found in this sampling site were *Diatomella balfouriana* Greville, *Achnantheidium exiguum* (Grunow) Czarnecki and *Anomoeoneis sphaerophora* (Ehrenberg) Pfitzer. The highest level of abundance was in SK1e (24 species) and the lowest level of abundance was found at SK4p (4 species) (Appendix D).

#### 3.5.3.2 Theppanom Hot Spring (TPN), Chiang Mai Province

Nineteen species of hot spring diatoms were established at the TPN site. The most abundant species found in this sampling site were *Diatomella balfouriana* Greville, *Achnantheidium exiguum* (Grunow) Czarnecki and *Rhopalodia gibberula* (Ehrenberg) O.F. Müller. The highest level of abundance was recorded at TPN2e (16 species) and the lowest level of abundance was found at TPN5 (1 species) (Appendix D).

#### 3.5.3.3 Ta Pai Hot Spring (TP), Mae Hong Son Province

Sixteen species of hot spring diatoms were established at the TP site. The most abundant species found in this sampling site were *Diatomella balfouriana* Greville, *Achnantheidium exiguum* (Grunow) Czarnecki and *Sellaphora lanceolata* D.G. Mann & S. Dropp in Mann *et al.* The highest level of abundance was recorded at TP1e (13 species) and the lowest level of abundance was found at TP4p (1 species) (Appendix D).

#### 3.5.3.4 Pong Ang Hot Spring (CHD), Chiang Mai Province

Fourteen species of hot spring diatoms were established at the CHD site. The most abundant species found in this sampling site were *Achnantheidium exiguum* (Grunow) Czarnecki, *Diatomella balfouriana* Greville, and *Craticula acidoclinata* Lange-Bertalot & Metzeltin. The highest level of abundance was recorded at CHD1e (10 species) and the lowest level of abundance was found at CHD2p (4 species) (Appendix D).

#### 3.5.3.5 Chae Sorn Hot Spring (JS), Lampang Province

Fifteen species of hot spring diatoms were established at the JS site. The most abundant species found in this sampling site were *Diatomella balfouriana* Greville, *Sellaphora lanceolata* D.G. Mann & S. Dropp in Mann *et al.* and *Anomoeoneis sphaerophora* (Ehrenberg) Pfitzer. The highest level of abundance was recorded at JS1e (11 species) and the lowest levels of abundance were found at JS4e and JS4p (1 species) (Appendix D).

#### 3.5.3.6 Mae Chok Hot Spring (MJ), Phrae Province

Eleven species of hot spring diatoms were established at the MJ site. The most abundant species found in this sampling site were *Achnantheidium exiguum* (Grunow) Czarnecki, *Rhopalodia gibberula* (Ehrenberg) O.F. Müller, and *Sellaphora lanceolata* D.G. Mann & S. Dropp in Mann *et al.* The highest level of abundance was recorded at MJ2e (9 species) and the lowest level of abundance was found at MJ4p (1 species) (Appendix D).

#### 3.5.3.7. Wat Salaeng Hot Spring (SL), Phrae Province

Eleven species of hot spring diatoms were established at SL. The most abundant species found at this sampling site were *Anomoeoneis sphaerophora* (Ehrenberg) Pfitzer, *Navicula grimmei* Krasske in Hustedt and *Anomoeoneis* sp. The highest level of abundance was found at SL1e (11 species) and the lowest level of abundance was recorded at SL2p (8 species) (Appendix D).

### 3.5.3.8 Pong Gi Hot Spring (NG), Nan Province

Nine species of hot spring diatoms were established at SK. The most abundant species found at this sampling site were *Achnantheidium exiguum* (Grunow) Czarnecki, *Navicula grimmei* Krasske in Hustedt, and *Anomoeoneis sphaerophora* (Ehrenberg) Pfitzer. The highest level of abundance was recorded at NG2e (8 species) and the lowest level of abundance was found at NG1p (4 species) (Appendix D).

### 3.5.4 Diversity index

A diversity index is a mathematical measure of species diversity within a community. Diversity indices provide more information about community composition than simply species richness, such as the number of species present. They also take the relative abundances of different species into account. Diversity indices provide important information about the rarity and commonness of species in a given community. The ability to quantify diversity in this way is an important tool for biologists who are trying to understand community structure.

Shannon's diversity index, evenness and the species richness of benthic diatoms in eight hot springs in northern Thailand are presented in Table 3.8. Shannon's diversity index ranged from 0.000 – 2.365 and the evenness ranged from 0.000 – 0.875, whereas the species richness was found to range from 0 – 24. The lowest values of the diversity index and the evenness values were observed at sampling sites TPN5, TP4p, JS4e, JS4p and MJ4p, and the highest values were observed at sampling site SK1e. The highest values of evenness were revealed at sampling site CHD1p. The highest numbers of species were recorded at sampling site SK1e, while the lowest value was recorded at sampling sites TPN5, TP4p, JS4e, JS4p and MJ4p. The number of species in most sampling sites was found to have decreased while the water temperature was higher.

### 3.5.5 Statistics analysis

Water properties and sampling sites were distinguished based on percentage diatoms data, using Hierarchical Cluster Analyses (HCA) carried out with the R package NbClust. HCA was chosen because it does not require the number of cluster

to be specified in advance. However, there is a wide variety of AHC methods, but little consensus on which produces the best results. Different choices could lead to a variety of classifications and cause confusion when comparing study. Clustering is the partitioning of an arrangement of articles into gatherings (groups) so protests inside a gathering are more similar to every others than objects in various groups. The vast majority of the clustering calculations depend on a few suppositions in order to characterize the subgroups display in an informational index. As a NbClust, the subsequent grouping plan requires a type of assessment as respects its validity. The evaluation procedure has to grab difficult problems such as the quality of clusters, the degree with which a clustering scheme fits a specific data set and the optimal number of clusters in a partitioning.

The comparison of cluster dendrogram and optimal number of cluster were analyzed by 7 methods (ward.D, single, complete, average, mcquitty, median and ward.D2) carried out with the R package NbClust. Based on the results, the cluster size can be divided into groups according to the 6 methods except the median method. The optimum cluster number of ward.D, single, complete, average, mcquitty and ward.D2 were 4, 8, 3, 2, 3 and 4 respectively (Figure3.36). Then the data from six methods were analyzed by using a heat map dendrogram to improve and reduce error of the results (Figure 3.37). All results of ward.D2 were consistent and the result showed that the CA dendrogram and heat map illustrated in 4 groups (group 1-group 4). Group 1 included MJ2-MJ5, CHD1-CHD3 and SL2 sampling sites. Group 2 included NG1-NG3, TP1-TP5 and JS1-JS4 sampling sites. Group 3 was made up of only JS5 samples. Group 4 was composed of SK1-SK4 and TPN1-TPN5 sampling sites (Figure3.38).

Copyright© by Chiang Mai University  
All rights reserved

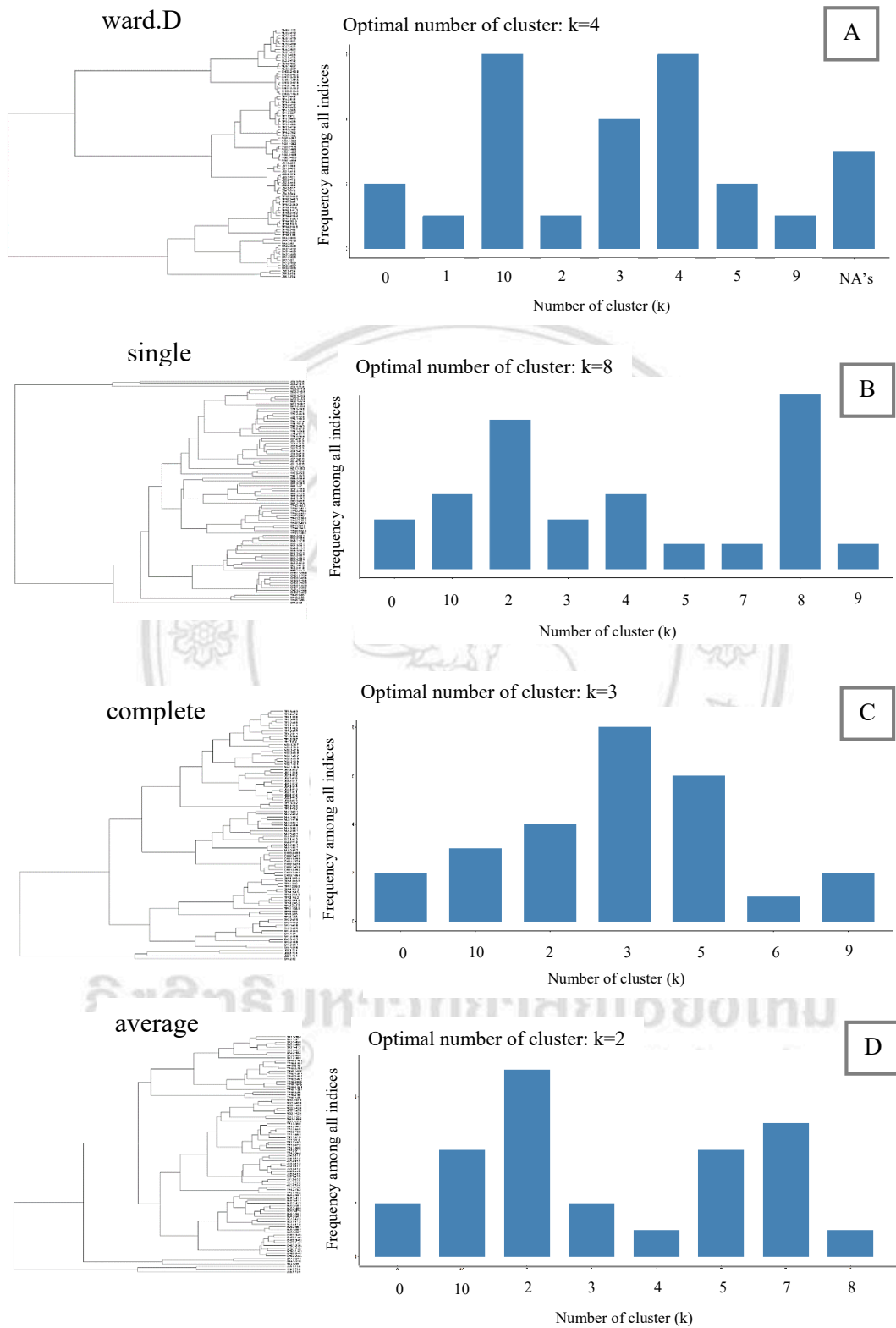


Figure 3.36 The comparison of cluster dendrogram and number of cluster analyzed by 7 methods carried out with the R package NbClust

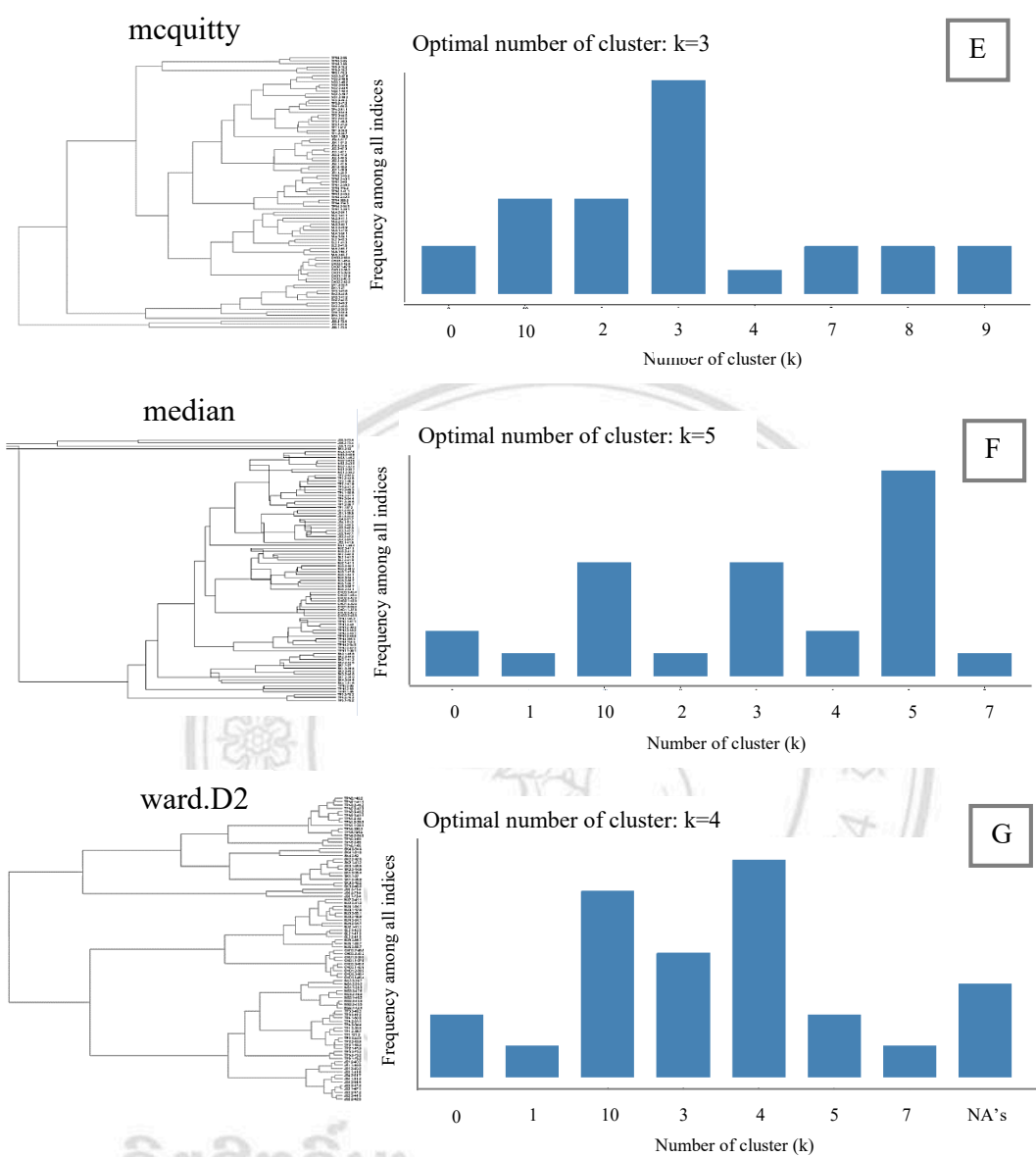


Figure 3.36 The comparison of cluster dendrogram and number of cluster analyzed by 7 methods carried out with the R package NbClust (continued)

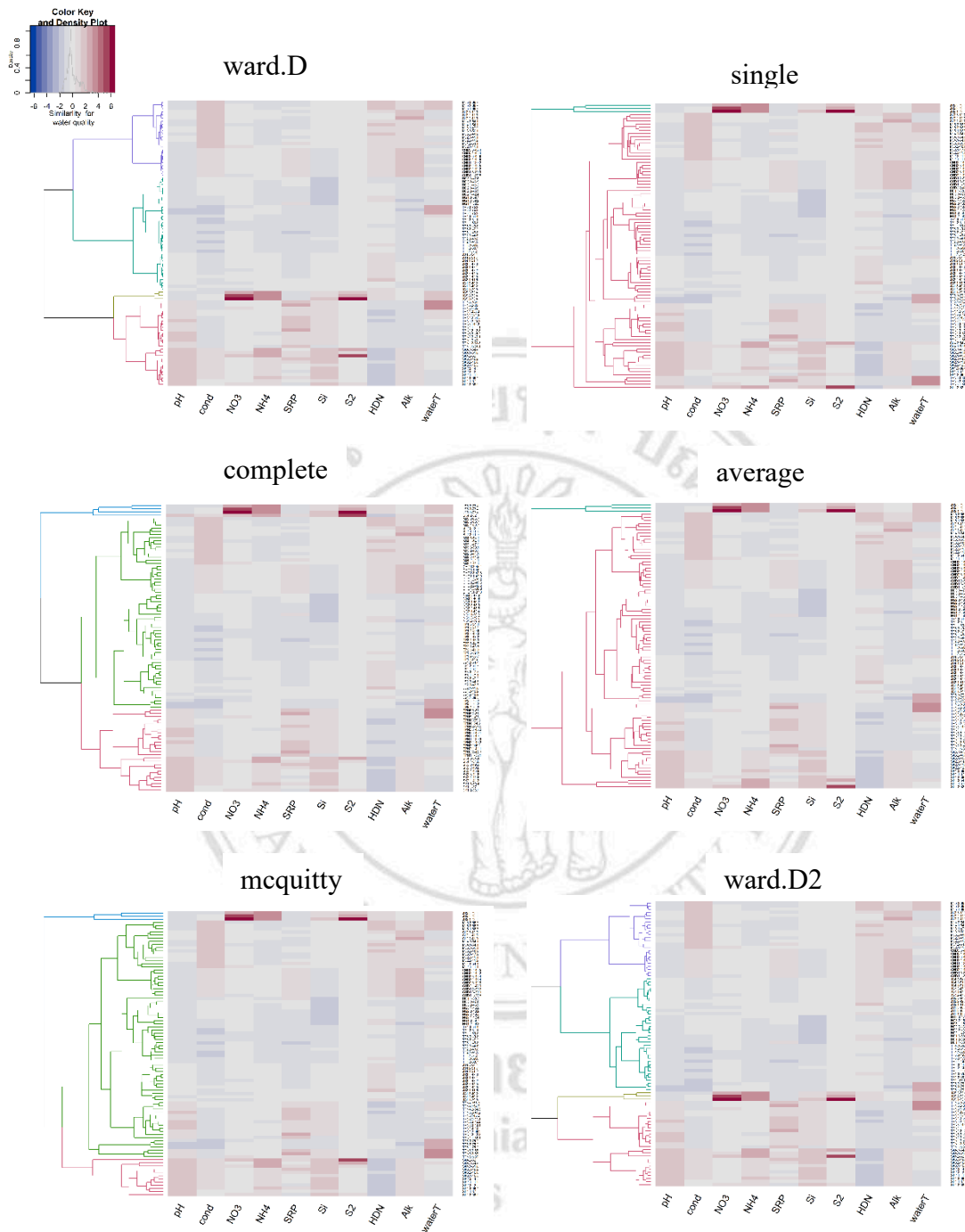


Figure 3.37 Cluster dendrogram and heat map of sampling sites according to the physico-chemical factors in 8 hot spring sampling sites analyzed by 6 methods carried out with the R package NbClust

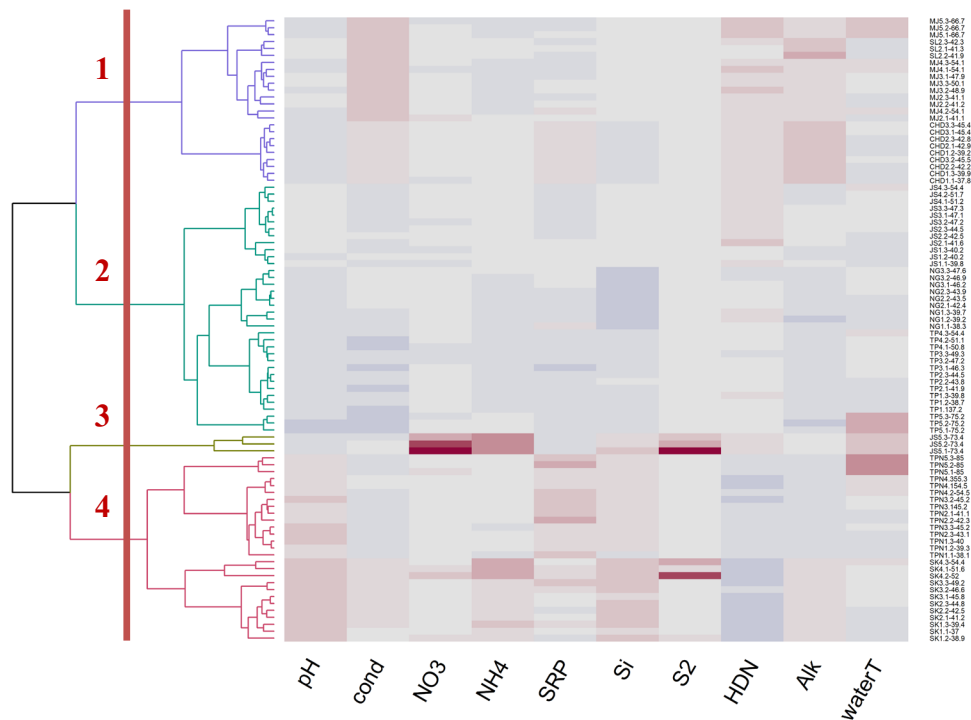


Figure 3.38 Cluster dendrogram and heat map of sampling sites according to the physico-chemical factors in 8 hot spring sampling sites analyzed by ward.D2

### 3.5.6 Principal component analysis (PCA)

PCA was done in order to study the relationship between the hot spring sampling sites and the physico-chemical factors from December 2015 to April 2016. The typical PCA results should consist of a set of eigenvalues that provide information of the variability in the data. Figure 3.39 illustrated the eigenvalues that is the variance of all variables for measure the amount of variation retained by each principal component. Eigenvalues can be used to determine the number of principal components to retain after PCA (Kaiser 1961). Unfortunately, there is no well-accepted objective way to decide how many principal components are enough. This will depend on the specific field of application and the specific data set. In this analysis, the first four principal components explain 85% of the variation as an acceptably percentage. The relationship between water properties and sampling sites was related to the CA results by which the sampling sites

were separated into 4 groups. A positive correlation between alkalinity, conductivity and total hardness and CHD1-CHD3, SL2 and MJ2-MJ5 sampling sites was revealed in the first group. The second group included JS1-JS4, NG1-NG3 and TP1-TP5 did not present a relationship between the water properties and the sampling sites. The third group was made up of the JS5 sampling sites that had a positive correlation with nitrate-nitrogen, ammonium-nitrogen and sulfide. The last group, SK1-SK4 and TPN1-TPN5 sampling sites had a positive correlation with pH, SRP and SiO<sub>2</sub> (Figure 3.40).

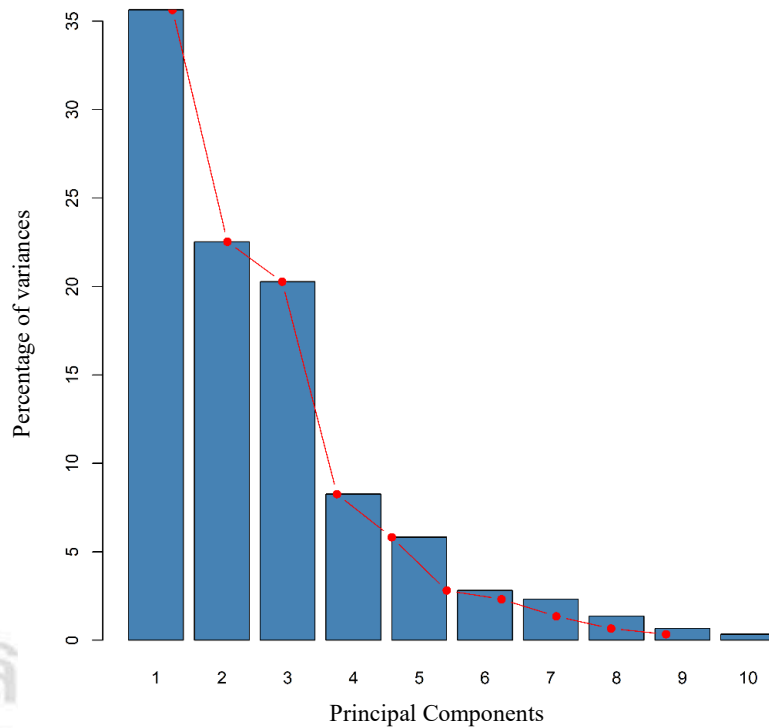


Figure 3.39 The plot of explained variance by different principal components

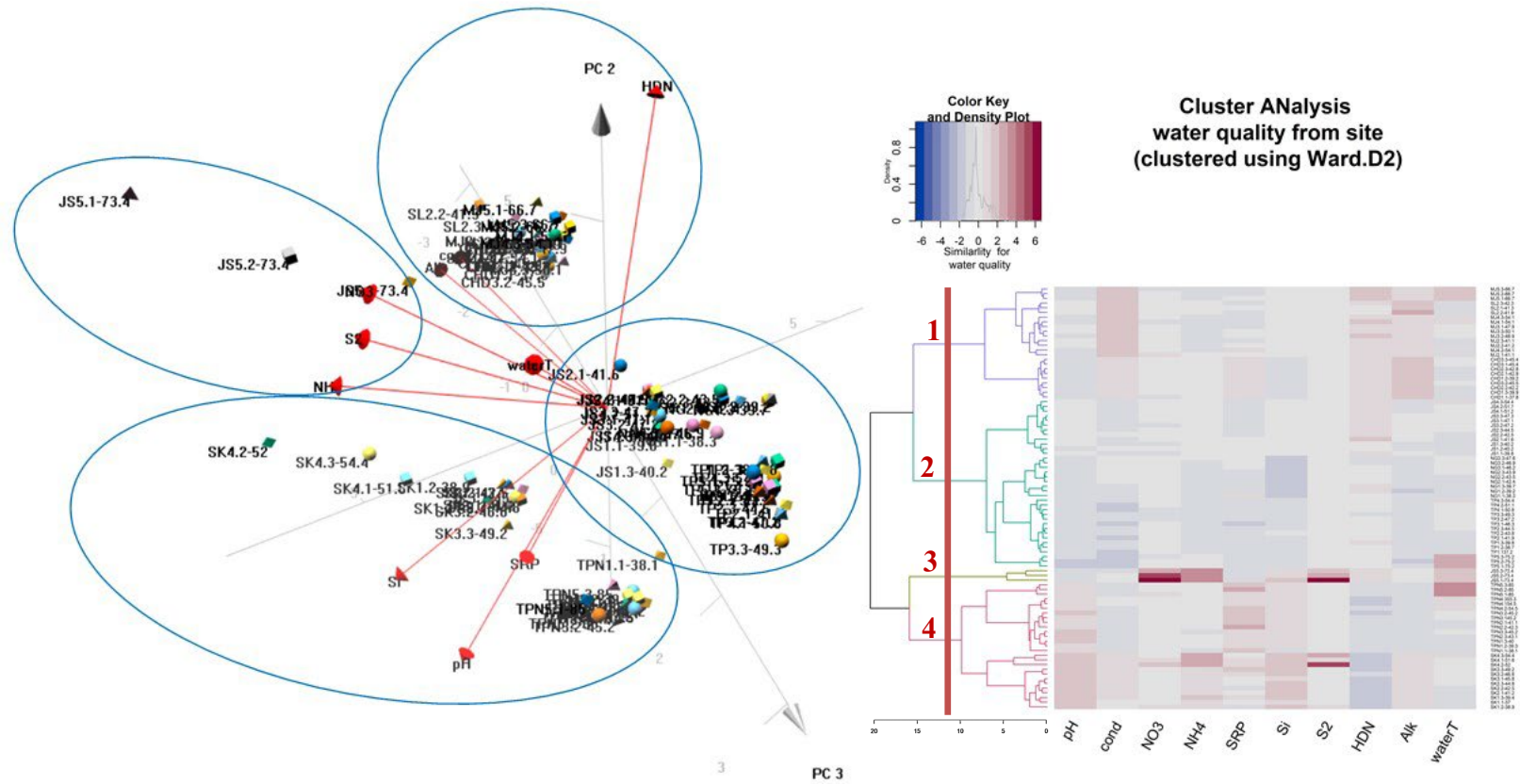


Figure 3.40 PCA 3D plot graph, cluster dendrogram and heat map showing relationship between of sampling sites according to the physico-chemical factors in 8 hot spring sampling sites analyzed by ward.D2 carried out with the R package NbClust



Table 3.7. Relationships between the species ordination scores (NMDS) and the influenced environmental factors.

	NMDS1	NMDS2	$R^2$	$p$
pH	0.20429	-0.97891	0.3840	0.002 **
Cond. ( $\mu\text{S cm}^{-1}$ )	-0.94098	0.33847	0.3720	0.007**
$\text{NO}_3^-$ ( $\text{mg L}^{-1}$ )	0.60151	-0.79887	0.0285	0.699
$\text{NH}_4^+$ ( $\text{mg L}^{-1}$ )	0.61863	-0.78568	0.1907	0.084
SRP ( $\text{mg L}^{-1}$ )	0.21071	0.97755	0.0099	0.895
$\text{SiO}_2$ ( $\text{mg L}^{-1}$ )	0.30347	-0.95284	0.4242	0.001***
$\text{S}_2$ ( $\text{mg L}^{-1}$ )	0.90644	-0.42234	0.0556	0.507
HDN ( $\text{mg L}^{-1} \text{CaCO}_3$ )	-0.24303	0.97002	0.3426	0.012*
Alk. ( $\text{mg.L}^{-1} \text{CaCO}_3$ )	-0.86020	0.50995	0.1614	0.121
Water Temp. ( $^\circ\text{C}$ )	0.87696	0.48056	0.3590	0.001***

Significant codes: (\*\*\*):  $p < 0.001$ , (\*\*):  $p < 0.01$ , (\*):  $p < 0.05$

Permutation: free, Number of permutations: 999

Table 3.8 Shannon's diversity index, evenness and the species richness of benthic diatoms in 8 hot springs in northern Thailand during December 2015 – April 2016.

Sampling site	Diversity Index	Species Evenness	Species Richness
SK1e	2.365	0.744	24
SK1p	2.064	0.689	20
SK2e	2.153	0.719	20
SK2p	1.782	0.675	14
SK3e	1.464	0.610	11
SK3p	1.464	0.571	13
SK4e	0.782	0.436	6
SK4p	0.947	0.683	4
SK5	Not found	Not found	Not found
TPN1e	1.708	0.647	14
TPN1p	1.412	0.589	11
TPN2e	1.763	0.636	16
TPN2p	1.303	0.566	10
TPN3e	0.957	0.492	7
TPN3p	0.919	0.513	6
TPN4e	0.561	0.510	3
TPN4p	0.534	0.332	5
TPN5	0.000	0.000	1
TP1e	1.339	0.522	13
TP1p	1.255	0.545	10
TP2e	1.347	0.692	7
TP2p	1.051	0.540	7
TP3e	1.178	0.536	9
TP3p	0.875	0.421	8
TP4e	0.203	0.185	3
TP4p	0.000	0.000	1
TP5	Not found	Not found	Not found

Table 3.8 (continued)

Sampling site	Diversity Index	Species Evenness	Species Richness
CHD1e	1.755	0.762	10
CHD1p	1.703	0.875	7
CHD2e	0.831	0.464	6
CHD2p	1.002	0.723	4
CHD3e	1.430	0.798	6
CHD3p	1.176	0.656	6
JS1e	1.327	0.553	11
JS1p	1.256	0.604	8
JS2e	0.809	0.451	6
JS2p	0.701	0.506	4
JS3e	0.682	0.424	5
JS3p	0.466	0.290	5
JS4e	0.000	0.000	1
JS4p	0.000	0.000	1
JS5	Not found	Not found	Not found
MJ2e	1.765	0.803	9
MJ2p	1.598	0.768	8
MJ3e	1.006	0.562	6
MJ3p	1.140	0.822	4
MJ4e	1.205	0.749	5
MJ4p	0.000	0.000	1
MJ5	Not found	Not found	Not found
SL1e	1.152	0.480	11
SL1p	0.800	0.385	8
NG1e	1.279	0.657	7
NG1p	1.041	0.751	4
NG2e	1.534	0.738	8
NG2p	1.217	0.756	5
NG3e	1.155	0.594	7
NG3p	1.560	0.871	6

### 3.6 Discussion for Investigation of Diatom Diversity

#### 3.6.1 Diversity of hot spring diatoms and relationship of benthic diatoms with physical and chemical properties

A total of forty–six species of hot spring diatoms were identified in this study. These belonged to 2 classes, 14 orders, 18 families and 27 genera. The dominant genera according to high relative abundance (more than 1%) were *Diatomella* (41.7%) followed by *Achnantheidium* (20.9%), *Anomoeneis* (11.2%), *Rhopalodia* (6.4%), *Sellaphora* (5.7%), *Navicula* (2.9%), *Nitzschia* (2.4%) and *Craticula* (2.1%). These genera included 16 species i.e., *Achnantheidium exiguum* (Grunow) Czarnecki, *Anomoeneis sphaerophora* (Ehrenberg) Pfitzer, *Anomoeneis* sp.3, *Craticula acidoclinata* Lange-Bertalot & Metzeltin, *Craticula ambigua* (Ehrenberg) Mann in Round, Crawford & Mann, *Craticula cuspidate* (Kützing) Man, *Diatomella balfouriana* Greville, *Navicula grimmei* Krasske in Hustedt, *Navicula rostellata* (Kützing) Cleve, *Navicula subrhynchocephala* Hustedt, *Nitzschia amphibia* Grunow, *Nitzschia clausii* Hantzsch, *Nitzschia ignorata* Krasske 1929, *Nitzschia palea* (Kützing) W. Smith, *Rhopalodia gibberula* (Ehrenberg) O.F. Müller and *Sellaphora lanceolata* D.G. Mann & S. Dropp in Mann *et al.* Furthermore, *Caloneis molaris* (Grunow) Krammer, *Craticula acidoclinata* Lange-Bertalot & Metzeltin, *Navicula subrhynchocephala* Hustedt and *Pinnularia saprophila* Lange–Bertalot, Kobayashi and Krammer were determined to be new records in Thailand. They were compared with the freshwater algae checklist published in Thailand and other related books (Lewmanomont *et al.*, 1995; Pekthong, 1998 and 2002; Pekthong and Peerapornpisal, 2001; Kunpradid, 2005; Suphan, 2004 and 2009; Inthasotti 2006a, b; Leelahakriengkrai, 2007a, b; Pruetiworanan, 2008; Yana 2010; Suphan and Peerapornpisal, 2010; Leelahakriengkrai, 2011; Yana, 2014; Nakkaew 2015). The newly recorded species of hot spring diatoms for Thailand in this study were found in fewer numbers than the earlier reports that had been published in Thailand. This occurred because the study collected samples from the specific environments that microbes were able to survive under harsh conditions such as those of high temperatures, pH and alkalinity that cause the type and number of diatom species to react according to conditions of the ecosystem which they inhabit. The hot springs in northern Thailand indicate surface temperatures of between 40-100°C. The range of water temperatures in

this study were between 38.4-85°C. This is attributable to the mixing of geothermal water with groundwater during the course of circulation and at the time it flows to the surface (Ramingwong *et al.* 1979; Geothermica Italiana Slr 1984; Raksaskulwong 2002). Moreover, most of the hot springs in Thailand are alkaline hot springs found in territories where the pH is over 7 and can be as high as 11 or 12. During the course of this research, the range of pH values was from 6.8-8.8, which correlated with the expected hot spring type conditions. Additionally, hot springs in this region were typically discovered close to areas with a lot of limestone or dolostone (Kruse 1997) where a broad measure of silica material causes that can be the host for the algal mats. Silicon is thus essential to diatoms as an insufficient supply of Si in the environment will prevent diatoms from flourishing or can result in teratological specimens (Seckbach 2007). From this point of view, the positive correlation between silicon oxide concentrations and diatom assemblages was found at all sampling sites investigated in this study.

*A. exiguum* (Grunow) Czarnecki, *D. balfouriana* Greville and *A. sphaerophora* (Ehrenberg) Pfitzer were the dominant genera in almost all sampling sites, and this finding was similar to that which was reported by (Owen *et al.* 2008) who stated that the most common taxa included: *A. exiguum* v. *heterovalvum* (Kras.) Czarn., *A. sphaerophora* (Ehrenb.) Pfitz in Kenyan springs. Also, *A. exiguum*, *G. parvulum*, *A. ovalis* have been previously reported as thermophiles existing at 40–58°C (Mannino 2007; Stavreva 2010; Nikulina and Kociolek 2011; Quintela *et al.* 2013; Covarrubias *et al.* 2016). Moreover, *A. exiguum* was recorded in all samples collected from limnocrene springs of Bunica situated in the south of Bosnia and Herzegovina and has been frequently found in alkaline hot springs (Dedić *et al.* 2015). Sompong (2001) reported that *D. balfouriana* Greville was a dominant species at temperatures between 30 to 59°C, whereas a small number of the publications in the world have identified this species as a dominant species in hot springs. Hot springs also offer the opportunity to test hypotheses regarding the biogeography of microbial organisms. Kociolek (2000) detailed some families, genera, and species that appear to be localized with regard to their distribution. Hot springs offer the possibility to examine habitats that may have similar temperatures and water chemistries, but occur in very different geographic locales and see if they harbor and support similar or different species of diatoms (Vyverman *et al.* 2007).

Villeneuve and Pienitz (1998) compared the floras of hot springs from Canada, Iceland, and Japan, and found that although they had similar environmental conditions, the structure of the diatom communities was entirely different, especially in relation to species. Likewise, Owen *et al.* (2008) compared hot springs in Iceland, New Zealand, and Kenya, and the dominant taxa that was present in these systems were all quite regarding the significant groups represented. However, Hobbs *et al.* (2009) reported the presence of *Pinnularia acoricola* Hustedt and *Eunotia exigua* (de Brébisson ex Kützing) Rabenhorst in the hot springs of an acid habitat and noted that these taxa had also been reported from similar environments around the world (e.g., (Denicola 2000)). With regard to certain diatoms found in South Africa (*Synedra*, *Aulacoseira*, *Nitzschia*, *Cyclotella*, *Gyrosigma*, *Craticula*), these occurred exclusively at temperatures less than 45°C and pH values less than 8 (Jonker *et al.* 2013b). Additionally, sediments are living spaces for benthic organisms, where they offer a place for resting stage and refugia. Organisms can be enlisted or re-suspended from sediments in the water body (Dobson and Frid 2008). Further, residue provides a source of chemical compounds that exist in the catchment area. All the hot spring sampling sites are approachable to the public, while some are attractive as tourist destinations. Thus, human activities may have led to disturbance or disruption to the fluctuations of the physicochemical features and diatom distribution. Nevertheless, the sampling intention did not recognize the scope to which human activities changed the natural ecosystem and impacted the diversity of the diatom community.

### **3.6.2 Investigation of water temperature in 24-hour**

Temperature is one of the essential parameters gathered with water-quality information since, for example, conductivity, pH, and dissolved oxygen fixations are reliant upon water temperature. Temperature likewise assumes a vital part of biology by deciding the rate of biochemical responses. Aquatic creatures have an optimal range of water temperatures which have higher and poorer temperature tolerances that are incompatible with life outside this range and where creatures also could not grow (Weber *et al.* 2007). Resource fluctuations can have an imperative role in structuring ecological communities (Litchman and Klausmeier 2001). Although, water depth typically impacts water temperature because vitality from the sun can penetrate and warm the entire water

column, the water temperature in hot springs may actually display little difference between the top and bottom layers. The overall of water temperature in this study fluctuated between 2.3°C and 9.7°C. The highest fluctuated range was reported at the NG sampling sites which were located near the small river that passed through the village. The same weekly temperature measurements at the discharge point were observed at Berkeley Springs and varied from 36.8°C to 41.7°C. Notably, the temperature fluctuations here were caused by the river water moving into the spring house during times of high flow in the river and which consequently reduced the temperature of the spring (Hobba 1979). Rainfall, air and water temperatures were continuously monitored at 15-min intervals in a previously published study (Cox *et al.* 2015). The spring fluctuated at background values from 56 to 58°C with minor diurnal variety; however, temperature fell drastically to around 40°C amid overwhelming precipitation when deep upwelling liquids were diluted close to the surface by cool meteoric water. Recuperation to background temperatures commonly took 3–5 h after the rain stopped falling, contingent upon the magnitude of the rainstorm. Less frequent but more extreme temperature decreases happened because of shaking from distal earthquakes. With regard to the estimation and demonstration of water temperature, anthropogenic components adjusted water temperature values. The impacts of temperature changes can be observed on the physical and relevant attributes of the water and on the aquatic organisms and ecosystems (Dallas 2008). Furthermore, Jonker *et al.* (2013b) reported that while trying to assess the impact of temperature and pH on algal distribution, pH and temperature areas in which the algal genera happen were superimposed to optimize the optimal conditions. At that point, it was observed to be in the temperature and pH ranges of 40– 50°C and 7.5– 8.4, respectively, and also at 60+°C and pH >9. Macan and Maudsley (1966) studied a continuous temperature record of the water at a depth of 15-20 cm for seven years and the results indicated the effect of air temperature, wind and sunshine on the water temperature.

### **3.6.3 Diversity index and statistics analysis**

Results from the statistical tests indicated a higher taxonomic richness in SK sampling site in comparison to others. Furthermore, there were not differences in species richness or the diversity index values between epilithic and epiphytic

assemblages, but temperature changes were the main environmental factors influencing diatom assemblages. This finding was in accordance with the findings of Nikulina and Kociolek (2011) who observed that the diversity of diatom taxa present in hot springs decreased significantly when water temperatures exceeded 70°C. These findings are in agreement with Mogna *et al.* (2015) and Cantonati *et al.* (2006) who reported no significant differences in numbers between epilithic and epiphytic diatom communities. Additionally, pH, temperature, conductivity, altitude, and shading were the core factors impacting diatom communities. Besides, the temperature independence of diatoms growing in hot springs does not mean that other climatic variables cannot be assumed from their changing abundance. Other factors are important in determining the growth of diatoms, most remarkably, instability and thermal stratification (Anderson 2000). Positive correlations between alkalinity, conductivity, total hardness and sampling sites were presented at the CHD, SL and MJ sampling sites. High alkalinity, conductivity and total hardness values occurred because this site was situated in a mountainous limestone area and was affected by the presence of carbonate and bicarbonate ions from the limestone. If waters flow through limestone regions or bedrock areas that contain carbonates, they have high alkalinity values, which lead to high conductivity levels (Cravotta 2003). Moreover, a positive correlation between sampling sites and water properties for instants pH, SRP and SiO<sub>2</sub> were reported at the SK1-SK4 and TPN1-TPN5 sampling sites, which revealed the highest diatom assemblages in this study. Similar results were obtained by other authors, e.g. Gesierich and Kofler (2010), who studied springs situated in the central Alps in Austria and found that conductivity and nitrates were the most relevant differentiating variables of diatom assemblage composition. Except for three genera, *Diatomella*, *Rhopalodia* and *Achnantheidium*, diatoms seem to prefer lower temperatures. However, water temperature does not appear to be the only limiting factor in the distribution of diatoms. Jonker *et al.* (2013a) said that most diatoms (e.g., *Synedra*, *Aulacoseira*, *Nitzschia*, *Cyclotella*, *Gyrosigma* and *Craticula*) are restrained to pH neutral water (pH 7–8). This is because the essential source of supplements for algal growth in thermal waters would be as dissolved cations and anions. The event can be subject to the geochemical mineral substance of the thermal water.

The diatom taxa in the NMDS ordination diagram indicated that the increase of silicon showed a positive correlation to the diversity of the diatoms. Silicon is thus essential to diatoms, as an insufficient supply of Si in the environment will prevent diatoms from flourishing or can result in teratological specimens (Seckbach 2007). From this point of view, a positive correlation between silicon oxide concentrations and diatom assemblages was found at all sampling sites that were investigated in this study.

However, silicon concentration does not appear to be the only limiting factor in the distribution of diatoms. Jonker *et al.* (2013a) said that most hot spring diatoms are restrained to pH values in a range of 7–8. This is because the essential source of supplements for algal growth in thermal waters would be as dissolved cations and anions. This event can be subject to the geochemical mineral substances of the thermal water. Our data specify that pH and silicon concentrations seem to be an imperative factor in hot spring diatom distribution in the same way they do in many alkaline springs found elsewhere in Europe (Kollár *et al.* 2015), on Majorca (Delgado *et al.* 2013) and the distributed in springs in the Alps (Cantonati & Lange-Bertalot 2010 and Mogna *et al.* 2015). The species that were associated with higher pH and SiO<sub>2</sub> values in this study were *Caloneis aequatorialis* Hustedt, *Cocconeis placentula* Ehrenberg, *Craticula cuspidate* (Kützing) Man, *Diploneis elliptica* (Kützing) Cleve 1894, *Gomphonema affine* Kützing, *Gomphonema augur* Ehrenberg 1841, *Halamphora fontinalis* (Hustedt) Z. Levkov, *Planothidium lanceolatum* (Breb.) Round & Bukhtiyarova and *Stauroneis anceps* Ehrenberg. These conditions were relevant to the SK1 and SK2 samples. Consistent with Leira *et al.* (2017), who found *Planothidium lanceolatum* (Breb.) Round & Bukhtiyarova in water bodies of slightly alkaline pH conditions in the thermo-mineral springs of Galicia (NW Spain).

Another factor which affected diatom diversity was conductivity. From this study, *Achnanthydium exiguum* (Grunow) Czarnecki, *Sellaphora lanceolata* D.G. Mann & S. Dropp in Mann *et al.* and *Pinnularia abaujensis* (Pantoscek) Ross had a positive relationship with conductivity that occurred in the MJ2 and MJ3 samples. Mangadze (2017) revealed that diatom assemblages are proper indicators of ionic composition/conductivity and stream size in lotic ecosystems. Also, it is well known that conductivity and ionic composition have an impact on diatom distribution (Bere and

Tundisi 2011). Conductivity is highly correlated with variables that directly affect diatom assemblage composition and individual species responses along the gradient (Ryves *et al.*, 2002).

Water temperature showed a negative influence on the diversity of diatoms. Only one species of *Amphora montana* Krasske was allocated near the temperature arrow, which indicates that the abundance of this species was found to be higher at the higher temperature sampling sites. This finding was in accordance with the findings of Nikulina and Kociolek (2011) who observed that the diversity of diatom taxa present in hot springs decreased significantly when water temperatures exceeded 70°C. These findings are also in agreement with Mogna *et al.* (2015). However, temperature independent diatoms were observed in many hot springs. It means that other climatic variables are assumed from their changing abundance.

Total hardness showed a positive relationship with *Amphora ovalis* (Kützing) Kützing, *Craticula acidoclinata* Lange-Bertalot & Metzeltin, *Craticula ambigua* (Ehrenberg) Mann in Round, Crawford & Mann, *Navicula grimmei* Krasske in Hustedt and *Surirella elegans* Ehrenberg. High conductivity and total hardness values occurred because these sites were situated in a mountainous limestone area and were affected by the presence of carbonate and bicarbonate ions from limestone. Naturally, limestone areas contain three carbonate species ( $\text{H}_2\text{CO}_3^*$ ,  $\text{HCO}_3^-$  and  $\text{CO}_3^{2-}$ ) that can affect the alkalinity of a water body in a given area. If waters flow through limestone regions or bedrock areas that contain carbonates, they tend to have high alkalinity values, which can lead to high conductivity levels (Cravotta 2003). Similar results were obtained by other authors, e.g. Gesierich and Kofler (2010), who studied springs situated in the central Alps in Austria and found that conductivity and nitrates were the most relevant differentiating variables of diatom assemblage composition.

### **3.7 Conclusion**

Corresponding to the preliminary results, some of the diatoms distribution and physicochemical parameters at each station were not substantially inconstant with the changing seasons except alkalinity. *Diatomella balfouriana*, *Rhopalodia gibberula* and *Sellaphora lanceolata* were the most abundant and most common species found in nine

thermal samplings. This case study showed that in these environments, fewer changes occurred in terms of the number of species present and with the substitution of some species by others, according to their limits of tolerance and the seasonal variations. The community diversity of hot spring diatoms in eight hot spring sampling sites were established in forty-six species. These belonged to 2 classes, 14 orders, 18 families and 27 genera. Of these, four species; *Caloneis molaris* (Grunow) Krammer, *Craticula acidoclinata* Lange-Bertalot & Metzeltin, *Navicula subrhynchocephala* Hustedt and *Pinnularia saprophila* Lange-Bertalot, Kobayashi and Krammer were determined to be new records for Thailand. The dominant genera according to high relative abundance (more than 1%) were *Diatomella* (41.7%) followed by *Achnantheidium* (20.9%), *Anomoeoneis* (11.2%), *Rhopalodia* (6.4%), *Sellaphora* (5.7%), *Navicula* (2.9%), *Nitzschia* (2.4%) and *Craticula* (2.1%). Nonetheless, there are some species that could grow within a wide range of water properties such as *A. exiguum* (Grunow) Czarnecki. The fluctuation of water temperature occurred in all sampling sites over 24 hours. The benthic diatoms in this study were able to adapt to changing temperatures over a single-day period. Insignificant differences were found in terms of species richness or the diversity index values between epilithic and epiphytic assemblages, but temperature changes were the main environmental factor that influenced diatom assemblages.

## HOT SPRING DIATOM DESCRIPTIONS

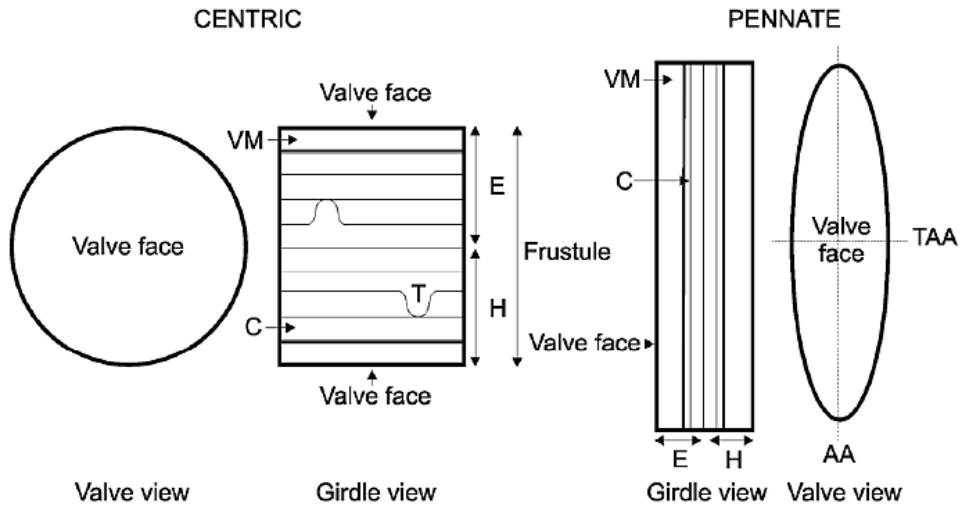


Figure 3.42 Diagram of diatom cells.

E = epivalve + epicingulum; H = hypovalve + hypocingulum; C = copulae or girdle bands; VM = valve mantle. Copulae (girdle bands) may have a tongue-like extension (T) which inserts into any space between the ends of the adjacent split copula. AA = apical axis, TAA = transapical axis

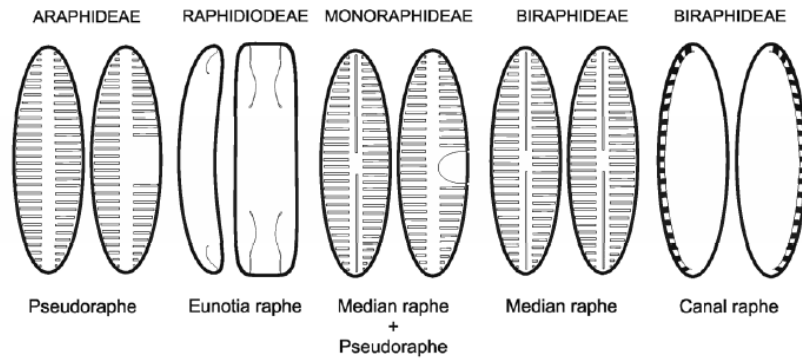


Figure 3.43 Suborders of pennate diatoms with associated raphe types

### Valve outlines

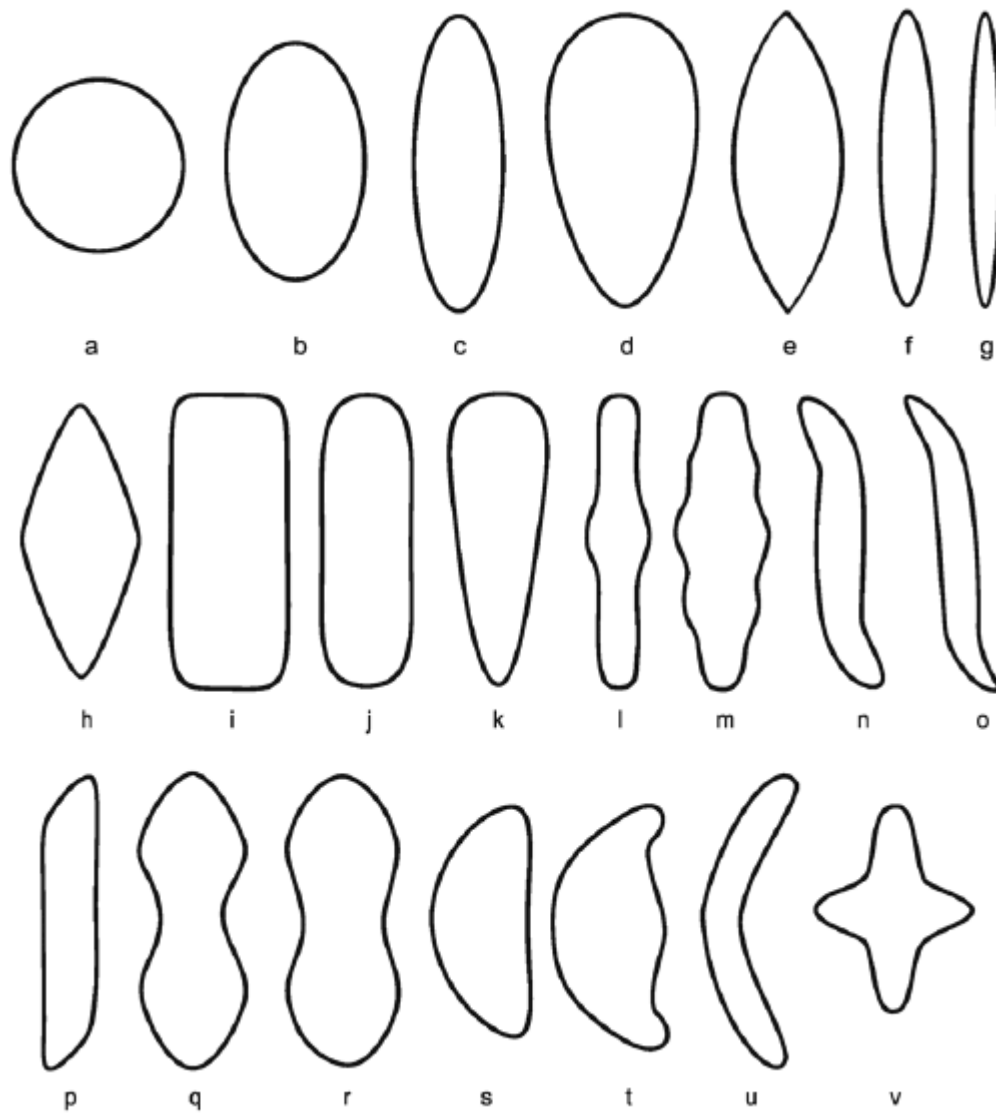


Figure 3.44 Diagrams to show valve and girdle shapes. All isopolar except **d** and **k** which are heteropolar and **s–u** which are dorsiventral. **a**, circular ; **b**, elliptical; **c**, narrow elliptical; **d**, ovate; **e** broadly lanceolate; **f**, lanceolate; **g**, narrowly lanceolate (fusiform); **h**, rhomboidal ; **i**, rectangular; **j**, linear; **k**, clavate; **l**, linear with swollen or expanded mid-region; **m**, triundulate (3:2); **n**, sigmoid; **o**, sigmoid lanceolate; **p**, sigmoid linear; **q**, paduriform; **r**, panduriform, slightly constricted; **s**, semi-circular; **t**, semi-circular with ventral edge swollen (tumid); **u**, lunate or arcuate; **v**, cruciform.

Apex shapes

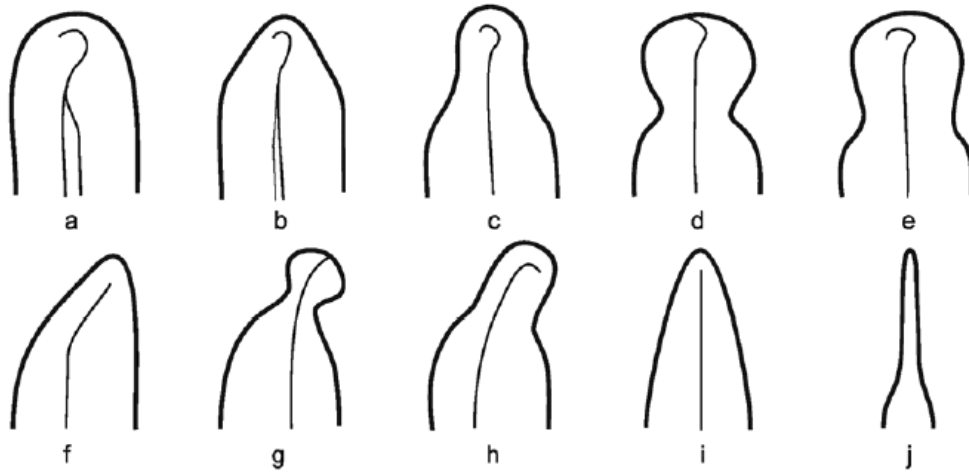


Figure 3.45 Diagrams to show valve apices. **a**, obtusely or broadly rounded; **b**, cuneate; **c**, rostrate; **d**, capitate; **e**, subcapitate; **f**, sigmoidly cuneate; **g**, capitate; **h**, rostrate; **i**, acutely or sharply rounded; **j**, elongate.

ลิขสิทธิ์มหาวิทยาลัยเชียงใหม่  
Copyright© by Chiang Mai University  
All rights reserved

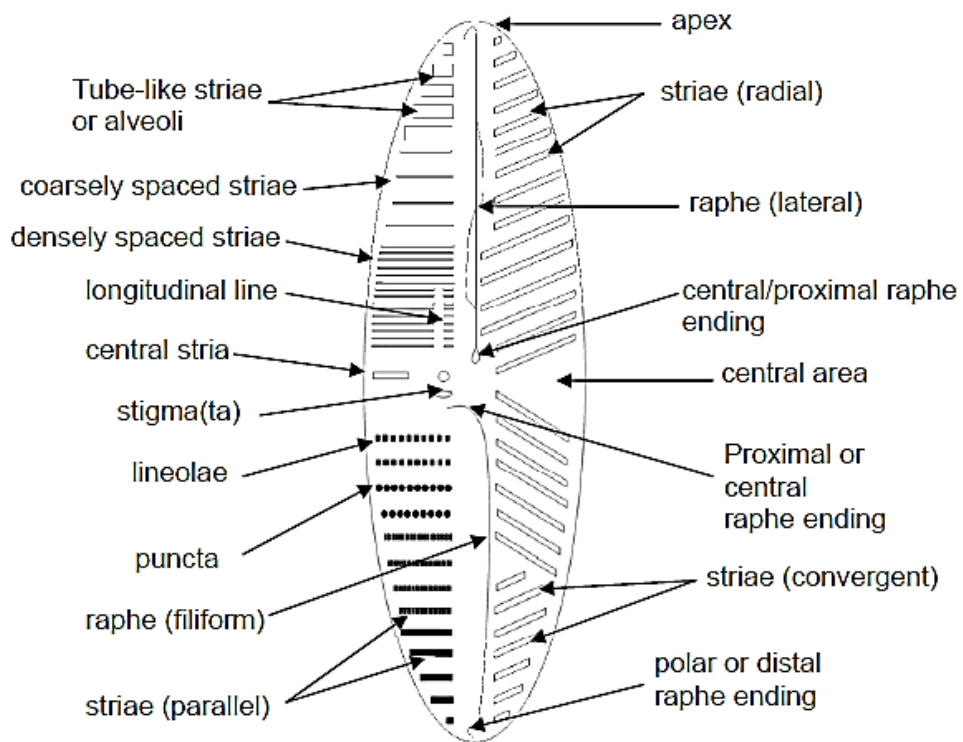


Figure 3.46 Some general features of pennate diatoms (composite diagram)

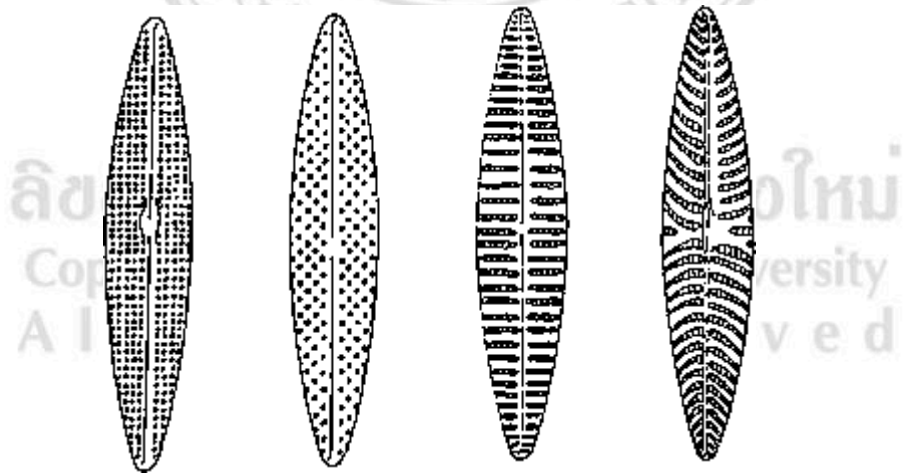


Figure 3.47 Valve striation in pennate diatoms, (a) Parallel striae; (b) radiate striae; (c) lineate, parallel striae; and (d) lineate, radiate striae.

***Aulacoseira ambigua* (Grunow) Simonsen**

**Valves in diameter:** 3 – 12  $\mu\text{m}$  with a mantle height of 5 – 15  $\mu\text{m}$

**Rows of areolae in 10  $\mu\text{m}$ :** 17 – 22

The proportion of the mantle height to valve diameter is more than 1. The mantle areolae spiral rows are curved to the right. The separation valves, rows of areolae coalesce near the valve face, giving the appearance of spines originating from two perivalvar costae. Spines are situated toward the end of each perivalvar costa. Linking spines are short, triangular or bifurcated. Separation spines are small and pointed. The ringleiste is empty, portrayed by a few authors as a 'U-formed sulcus'.

***Aulacoseira granulata* Ehrenberg**

**Valves in diameter:** 4 – 17  $\mu\text{m}$  with a mantle height of 4 – 20  $\mu\text{m}$

**Rows of areolae in 10  $\mu\text{m}$ :** 8 – 18

The proportion of the mantle height to valve diameter is usually greater than 0.8 but lower than 5. The mantle areolae are square, and the rows of areolae on the mantle are curved to the right. Some are almost straight and parallel to perivalvar axis in separation valves. The short linking spines are positioned at the end of each perivalvar costa. Division spines start from two perivalvar costae. Most separation spines are 2 – 6  $\mu\text{m}$  long, yet a couple, normally 1 – 2 spines for each valve, are long, practically measure up to long to the valve mantle. The ringleiste is strong and moderately shallow. Coiled rimoportulae are typically situated along a stria at the separation of 1 – 3 areolae from the collum.

***Meloseira varians* Agardh**

**Frustules in diameter:** 6 – 30  $\mu\text{m}$  with a mantle height of 5 – 15  $\mu\text{m}$

**Rows of areolae in 10  $\mu\text{m}$ :** 8 – 18

Cells are cylindrical, forming chains. The valve face is slightly curved, covered with little spines. Small granules cover the mantle. The frustule has a loculate structure. Various

rimoportulae are scattered over valve face and mantle, and one row of rimoportulae happens on the mantle edge.

***Achnantheidium minutissimum* (Kützing) Czarnecki**

**Frustules in diameter:** 6 – 30  $\mu\text{m}$  with a mantle height of 5 – 15  $\mu\text{m}$

**Length range:** 5.6 – 20.8  $\mu\text{m}$

**Width range:** 1.5 – 3.3  $\mu\text{m}$

**Striae in 10  $\mu\text{m}$ :** 25 – 35

Valves are linear-lanceolate with marginally drawn-out or somewhat capitate ends. Frustules with a concave raphe valve and convex rapheless valve are monoraphid. Central external raphe ends are straightforward; terminal raphe fissures are short, straight, or absent. Inside, the central raphe ends are handed over inverse direction. Striae are radiate all through the two valves. Striae comprise one row of areolae. The striae are regularly hindered in the central part of raphe valve to frame a symmetrical or asymmetrical fascia. One row of the extended areolae is available on the valve mantle. Outer areolae openings of areolae differ fit as a fiddle from round to transapically elongated slits. Inward openings of the areolae are elliptical, blocked by hymens punctured by little pores. Girdle bands are plain, open.

***Achnantheidium exiguum* (Grunow) Czarnecki**

**Frustules in diameter:** 6 – 30  $\mu\text{m}$  with a mantle height of 5 – 15  $\mu\text{m}$

**Length range:** 5.6 – 20.8  $\mu\text{m}$

**Width range:** 1.5 – 3.3  $\mu\text{m}$

**Striae in 10  $\mu\text{m}$ :** The raphe valve has 24 – 34 in mid-valve, up to 40 – 45 at the apices. The raphless valve has 20 – 25 at mid-valve and up to 35 – 40 at the apices.

Valves are linear-elliptical to elliptical-lanceolate and narrowly capitate to subrostrate apices. The raphe valve has a distinct fascia. The small rapheless valve has a transapically rectangular central area. The raphe is straight but deflected to opposite sides near the

apices with terminal raphe fissures strongly curved to opposite sides. The inner external raphe ends appear to be expanded. The striae are radiate on both valves but almost parallel at the apices. Areolae are transapically elongated externally, round, or apically elongated internally. A few very small areolae may be present on the mantle of both valves.

***Amphora montana* Krasske**

**Length range:** 9 – 15  $\mu\text{m}$

**Width range:** 4 – 6  $\mu\text{m}$

**Striae in 10  $\mu\text{m}$ :** 36

Valves are semi-lanceolate. Valve ends are extended, barely rostrate and bent ventrally. The raphe is situated close to the center of the valve, tenderly angled, with proximal raphe ends with slight dorsal diversion. Axial area limit. The central area on dorsal side structures a thickened semi-stauros reaching out to valve edge. Dorsal and ventral striae hard to determine in LM.

***Amphora ovalis* (Kützing) Kützing**

**Length range:** 32 – 95  $\mu\text{m}$

**Width range:** 8 – 17  $\mu\text{m}$

**Striae in 10  $\mu\text{m}$ :** 10 – 12

Valves semi-elliptical with an easily angled dorsal edge and marginally concave ventral edge. A continuous raphe edge is available. The raphe edge is noticeable broadening the length of the cell, covering the dorsal and ventral striae close to the axial area. Raphe angled with proximal and distal ends dorsally redirected. Striae interfered with dorsally by intercostal ribs, made ventrally out of a single row of areolae. Dorsal fascia absent, ventral fascia present and reaching out to the valve edge.

***Anomoeoneis sphaerophora* (Ehrenberg) Pfitzer**

**Length range:** 32 – 95  $\mu\text{m}$

**Width range:** 8 – 17  $\mu\text{m}$

**Striae in 10  $\mu\text{m}$ :** 10 – 12

Valves lanceolate to elliptical-lanceolate with rostrate to subcapitate ends. Striae are particularly punctate. Hyaline areas are on either side of the axial area. Distal raphe ends redirected to the other side.

***Caloneis bacillum* (Grunow) Mereschkowsky**

**Length range:** 8 – 20  $\mu\text{m}$

**Width range:** 3  $\mu\text{m}$

**Striae in 10  $\mu\text{m}$ :** 25 – 29

Valves are linear to linear-lanceolate with adjusted apices. The valve edges are straight to slightly convex in small specimens. The axial area is linear and extended at the central valve to form a deep transverse fascia. The fascia is regularly asymmetric from one side of the axial area to the other. The raphe is straight and filiform, with widened proximal outside ends. The striae are parallel to radiate. Longitudinal lines are visible in bigger specimens.

***Caloneis molaris* (Grunow) Krammer**

**Length range:** 33 – 50  $\mu\text{m}$

**Width range:** 5 – 8  $\mu\text{m}$

**Striae in 10  $\mu\text{m}$ :** 15 – 17

Valves linear, slender and gradually rejuvenated from the middle wedge. Ends rounded. The raphe finely, narrowly or almost missing in the middle to wide breadth extending to the shell margin broadened. Strips in the center light-emitting, parallel, converging at the ends. Middle nodes are strong.

***Cocconeis placentula* Ehrenberg**

**Length range:** 9.5 – 68.0  $\mu\text{m}$

**Width range:** 7.0 – 32.0  $\mu\text{m}$

**Striae in 10  $\mu\text{m}$ :** 15 – 25 on rapheless valve, 20–24 on raphe valve

Valves are elliptic to linear-elliptic and flat. The raphe valve has a limited axial area and a small round or oval central area. The raphe is filiform and straight. Striae in both raphe and rapheless valves are radiate. The striae on the raphe valve are hindered by a hyaline ring situated near valve edge. Areolae are typically well recognized under LM. The valvocopula appended to the raphe valve has obvious fimbriae. The rapheless valve has a linear to a linear-lanceolate axial area.

***Craticula acidoclinata* Lange–Bertalot & Metzeltin**

**Length Range:** 94 – 168  $\mu\text{m}$

**Width Range:** 22 – 29  $\mu\text{m}$

**Striae in 10  $\mu\text{m}$ :** 12 – 14

Valves are lanceolate with feebly extended (subrostrate) and broadly rounded apices. The axial area is thin and broadens gradually into the central area, which is longitudinally prolonged with convex sides. The raphe is feebly lateral with proximal ends that are modestly distant, somewhat inflated and hooked to a similar side. Striae are feebly radiate but convergent very close to the apices. Areolae are effortlessly recognized in LM and number 23 – 24 out of 10  $\mu\text{m}$ .

***Craticula ambigua* (Ehrenberg) Mann in Round, Crawford & Mann**

**Length Range:** 38 – 75  $\mu\text{m}$

**Width Range:** 12 – 19  $\mu\text{m}$

**Striae in 10  $\mu\text{m}$ :** 13 – 21 in the valve center, 17 – 21 at the ends

Valves are lanceolate, with extended rostrate ends. The axial area is tight and linear. The central area is just somewhat amplified around the center. The raphe is filiform. The proximal raphe ends are marginally extended. Striae are marginally radiate, getting to convergent at the ends. Striae might be somewhat denser on one side of the valve when contrasted with the opposite side. Stria density increments as the size range decrease in this taxon.

***Craticula cuspidata* (Kützing) Man**

**Length Range:** 95 – 157  $\mu\text{m}$

**Width Range:** 24 – 36  $\mu\text{m}$

**Striae in 10  $\mu\text{m}$ :** 12 – 14 transverse, 24 – 26 longitudinal

Valves are rhombic-lanceolate and most stretched out at the center of the valve before decreasing to narrow apices. Striae are made out of small, elliptic areolae. Striae are parallel and equidistant all through the whole valve, with thin transapical costae crossing opposite to the longitudinal striae developing an orthostichous pattern. The axial area is restricted to a slightly augmented central area with marginally concave edges. The raphe is filiform. The proximal raphe ends are extended and either straight or marginally hooked a similar direction. The distal raphe ends form hooks, redirected in a similar direction.

***Cymbella tumida* (Brébisson) Van Heurck**

**Length Range:** 35 – 95  $\mu\text{m}$

**Width Range:** 16 – 22  $\mu\text{m}$

**Striae in 10  $\mu\text{m}$ :** 8 – 11

Valves asymmetrical around an apical axis and symmetrical to the transapical axis. Cells are showing slight to pronounced dorsiventrality. Ends rounded to sub-capitate. Raphe central or slightly ventral. Stigmata lack or on the ventral side of the central area. Terminal raphe ends straight or redirected dorsally.

***Diadesmis confervacea* Kützing**

**Length Range:** 14 – 18  $\mu\text{m}$

**Width Range:** 6.5 – 7.5  $\mu\text{m}$

**Striae in 10  $\mu\text{m}$ :** 18 – 21

Valves are elliptical with apices extended in larger specimens. Central area wide and rounded, proceeding into the axial area, which decreases toward the ends. There is an adjusted central nodule visible when concentrating on the inside of the valve. The striae are punctate, radiate, crossed by longitudinal wavy rows, and of variable length. The raphe is straight and filiform and might be lost because of secondary filling amid silicification.

***Diatomella balfouriana* Greville**

**Length Range:** 12 – 40  $\mu\text{m}$

**Width Range:** 3.5 – 6.0  $\mu\text{m}$

**Striae in 10  $\mu\text{m}$ :** 18 – 22

Valves are linear with rounded apices. The axial area is wide. The raphe is filiform, arcuate, with expanded outside proximal raphe ends that terminate distant from each other. The striae are short and parallel to transmit, not distinctly punctate. A septum is available on each valvocopula. The septum broadens the whole length of the valve and has three expansive openings, the biggest in the center and two smaller at the ends.

***Diploneis elliptica* (Kützing) Cleve 1894**

**Length Range:** 30 – 65  $\mu\text{m}$

**Width Range:** 17 – 36  $\mu\text{m}$

**Striae in 10  $\mu\text{m}$ :** 9 – 10

Valves are elliptic, with convex edges and adjusted apices. The axial area is narrow lanceolate, expanding slightly from the apices to the central area. The central area is vast

and round. Longitudinal canals are available on the two sides of the axial and central areas. These are vastest close to the central area and restricted towards the valve apices. The raphe is straight with extended proximal raphe ends. Terminal raphe fissures avoid singularly, ending short of the valve edge. Striae are radiate mid-valve, ending up strongly radiate towards the apices. Striae made out of complex, round to rectangular areolae. Striae are uniseriate. Areolae number 11 – 14 out of 10  $\mu\text{m}$ . One row of areolae is situated along the longitudinal canal, but in a few specimens, two lines may happen.

***Diploneis subovalis* Cleve, 1894**

**Length Range:** 10 – 50  $\mu\text{m}$

**Width Range:** 9 – 18  $\mu\text{m}$

**Striae in 10  $\mu\text{m}$ :** 10 – 12

Valves are elliptic to linear-elliptical, with ends rounded. The axial area is narrow at the ends, becoming broader towards the center. Broadly lateral raphe enclosed in a rib that is thin, narrow and straight. A rounded central area is present. Proximal raphe ends range into the central area. Longitudinal canals narrow. Striae are composed of two rows of puncta. Puncta are distinct.

***Epithemia zebra* (Ehrenberg) Kützing 1844**

**Length Range:** 32 – 70  $\mu\text{m}$

**Width Range:** 7.5 – 9.7  $\mu\text{m}$

**Striae in 10  $\mu\text{m}$ :** 12 – 14

Valves are dorsiventral, with rounding to rostrate ends. Costae are 3 – 4 in 10  $\mu\text{m}$  with 3 – 7 striae between costae. The dorsal margin is strongly convex, and the ventral margin is moderately concave. Raphe canal lies alongside the ventral margin at distal ends of the valve arching toward the dorsal margin in valve center. The central curve of the canal is around 3 – 6  $\mu\text{m}$  over the ventral edge achieving less than a large portion of the separation to the dorsal edge.

***Fragilaria crotonensis* Kitton**

**Length Range:** 60 – 72  $\mu\text{m}$

**Width Range:** 2 – 3  $\mu\text{m}$

**Striae in 10  $\mu\text{m}$ :** 17 – 18

Valves are lanceolate, with a swelled inside edge. Valve apices are rounded to capitate. Spines are situated on edge, a spine display toward the end of a stria. Frustules participate in ribbon-like colonies.

***Gomphonema affine* Kützing**

**Length Range:** 26 – 77  $\mu\text{m}$

**Width Range:** 9.5 – 13  $\mu\text{m}$

**Striae in 10  $\mu\text{m}$ :** 8 – 10

Valves have a rhomboid–lanceolate shape consistent in individuals of varying lengths, a feature that differs from that of the nominate. The characteristic small circular depressions in the area–system appearing as grayish spots in LM are lacking. The position of the stigmata is distinguished being likewise distant from the center of the central nodule and the next stria instead of close–standing to the proximal areola of stria.

***Gomphonema augur* var. *sphaerophorum* Lange–Bertalot**

**Length Range:** 37 – 56  $\mu\text{m}$

**Width Range:** 12.8 – 13.2  $\mu\text{m}$

**Striae in 10  $\mu\text{m}$ :** 12 – 16

Valves are clavate, with a particularly capitate head pole and a restricted foot pole. A stigma is available opposite a single shortened stria. Striae are almost parallel mid–valve, getting to be plainly radiate at the apices. Areolae are distinctly punctate and obvious in LM, measuring 25–27 of every 10  $\mu\text{m}$ .

***Gomphonema gracile* Ehrenberg 1838**

**Length Range:** 20 – 100  $\mu\text{m}$

**Width Range:** 4 – 11  $\mu\text{m}$

**Striae in 10  $\mu\text{m}$ :** 9 – 17

Valves slightly asymmetrical to the transapical axis (heteropolar), symmetrical to apical axis. Valves appear lanceolate in outline. Cells wedge-molded in girdle view with pseudo-septa visible. Apices narrowly rounded to narrowly sub-rostrate. The raphe is regularly slightly sinuous. A single stigma is available on one side of the central area. Striae are coarse and punctate, regularly with one shorter stria in the central area.

***Gomphonema parvulum* (Kützing) Van Heurck**

**Length Range:** 10 – 46  $\mu\text{m}$

**Width Range:** 4 – 8  $\mu\text{m}$

**Striae in 10  $\mu\text{m}$ :** 7 – 20

Valves only slightly asymmetrical to the transapical axis (heteropolar), symmetrical to apical axis. Cells box-shaped in girdle view with pseudosepta visible. Apices rounded, sub-rostrate or rostrate (occasionally sub-capitate). The raphe is often marginally sinuous. A single stigma is existent on one side of the central area. Striae coarse and often visibly punctate – one short stria opposite the central stigma. Striae often almost parallel. Very variable species.

***Halumphora fontinalis* (Hustedt) Z. Levkov**

**Length Range:** 23.5 – 29.0  $\mu\text{m}$

**Width Range:** 5.2 – 5.5  $\mu\text{m}$

**Striae in 10  $\mu\text{m}$ :** 20 – 22 on the dorsal side, 22 – 23 on the ventral side.

Valves are dorsiventral, with a curved dorsal edge and a linear to the weakly convex ventral edge. Apices are extended, capitate, and diverted ventrally. Dorsal striae are

coarse, particularly at mid-valve and toward the dorsal edge; areolae measure 18 – 20 of every 10  $\mu\text{m}$ . Ventral striae are interfered with, short, most so at mid-valve. The axial area is insignificant on the dorsal side and extended ventrally. The raphe is straight, with dorsally avoided proximal ends. Central dorsal striae have a darker quality in LM because of a basic siliceous plate. Under SEM, striae are biseriate closest the raphe.

***Hantzchia amphioxys* (Ehrenberg) Grunow in cleve et Grunow**

**Length Range:** 20 – 100  $\mu\text{m}$

**Width Range:** 5 – 10  $\mu\text{m}$

**Striae in 10  $\mu\text{m}$ :** 14 – 20

Valves bi-laterally asymmetrical (dorsiventral), with a slight bowl-shaped ventral margin and a convex dorsal margin. The valve faces are flat and parallel. Poles rostrate or capitate, rarely simply rounded. Transverse striae visible, regularly spaced, occasionally visibly uniseriate. The raphe system keeps running along the ventral edge of the valve face and is subtended by substantial square or rectangular fibulae, which can sometimes be seen to be composite, comprising of fused extensions of a few of the transapical ribs (virgae). The central pair of fibulae is often slightly further apart. The raphe systems of both valves occur on the same side ('hantzschoid symmetry').

***Navicula grimmei* Krasske in Hustedt**

**Length Range:** 12.5 – 26.5  $\mu\text{m}$

**Width Range:** 5 – 7  $\mu\text{m}$

**Striae in 10  $\mu\text{m}$ :** 18 – 22

Valves distinctly capitate poles and linear with central parallel margins. Striae are radiate, flatterer nearly parallel at the apices. Bowtie-shaped with irregularly placed shortened striae at the central area. The axial area is linear and narrow. Areolae are coarse and visible in LM. The filiform raphe with unilaterally deflected distal ends.

***Navicula rostellata* (Kützing) Cleve**

**Length Range:** 32 – 41  $\mu\text{m}$

**Width Range:** 8 – 9.1  $\mu\text{m}$

**Striae in 10  $\mu\text{m}$ :** 12 – 14

Valves are linear to linear-lanceolate with slightly curved to straight edges and sub-rostrate apices. The axial area is tight and straight. The central area is elliptic and marginally asymmetric. The raphe is straight, with external proximal raphe ends that are marginally expanded and twisted toward the primary side of the valve. The central nodule is unevenly developed the interior valve surface to the primary side. Terminal raphe fissures are hooked to the secondary valve side. Striae are bowed and radiate around the inside. The striae are more inaccessible from each other close to the center of the valve. The striae wind up plainly parallel, then convergent at the apices. The areolae are obvious under LM and number around 30 in 10  $\mu\text{m}$ .

***Navicula subrhynchocephala* Hustedt**

**Length Range:** 29 – 42  $\mu\text{m}$

**Width Range:** 7.5 – 8.9  $\mu\text{m}$

**Striae in 10  $\mu\text{m}$ :** 12 – 14

Valves are linear-lanceolate with sub-rostrate to capitate apices. The central area is adjusted and marginally asymmetrical. The raphe is straight. The external proximal raphe ends hooked towards the optional side of the valve. Striae are radiate, getting to be noticeably parallel, at that point merged at the apices. The central striae are transmitted and are straight or twisted. The areolae are visible under LM, approximately 24 – 25 in 10  $\mu\text{m}$ .

***Nitzschia amphibia* Grunow**

**Length Range:** 14 – 37  $\mu\text{m}$

**Width Range:** 4.0 – 4.5  $\mu\text{m}$

**Striae in 10  $\mu\text{m}$ :** 14 – 18

Valves are linear to lanceolate. The valves reduction to rounded apices bluntly. The central nodule is obvious. Striae are distinctively noticeable and distinctly punctate, but not consistently separated. Fibulae are distinct and number 7 – 9 in 10  $\mu\text{m}$ .

***Nitzschia clausii* Hantzsch**

**Length Range:** 20 – 68  $\mu\text{m}$

**Width Range:** 3.0 – 5.0  $\mu\text{m}$

Valves are linear and marginally inward at the center. Frustules a are distinctly sigmoid in girdle view. The apices are distinctly adjusted, capitate or rostrate and twisted to frame a sigmoid valve shape. The striae are fine. The keeled raphe is particular, with robust fibulae. Fibula density is 10 – 13 of every 10  $\mu\text{m}$ .

***Nitzschia ignorata* Krasske 1929**

**Length Range:** 40 – 55  $\mu\text{m}$

**Width Range:** 4.5 – 5.0  $\mu\text{m}$

**Striae in 10  $\mu\text{m}$ :** 33

The shell surface is an elongated lanceolate shape bent in an S shape, thin at the end. The shell end does not protrude. The central part of the keel side of the shell surface indented. The center two of the keel point are separated. The striations are delicate.

***Nitzschia palea* (Kützing) W. Smith**

**Length Range:** 12 – 42  $\mu\text{m}$

**Width Range:** 3 – 4  $\mu\text{m}$

**Striae in 10  $\mu\text{m}$ :** 36 – 38

Valves are lanceolate with sides parallel and decreasing rapidly at the poles, ending with sub-capitate apices. Striae are barely visible in LM. Fibulae are distinct, with a separate central nodule and number 11 – 13 in 10  $\mu\text{m}$ .

***Pinnularia abaujensis* (Pantoscek) Ross**

**Length Range:** 55 – 90  $\mu\text{m}$

**Width Range:** 8 – 12  $\mu\text{m}$

**Striae in 10  $\mu\text{m}$ :** 9 – 12

Valves linear to linear-lanceolate with broad, sub-capitate apices. Striae radiate at center becoming convergent over the apices, sometimes lacking at the center of the valve. The axial area is expanding progressively from a point close to the basis of the polar raphe fissure fork to the central area, that might achieve the valve edges. Polar raphe fissures hooked, central fissures marginally extended and avoided a similar way (essential side of valve).

***Pinnularia saprophila* Lange–Bertalot, Kobayashi and Krammer 2000**

**Length Range:** 22 – 45  $\mu\text{m}$

**Width Range:** 5.2 – 6.7  $\mu\text{m}$

**Striae in 10  $\mu\text{m}$ :** 10 – 12

Valves are linear with apices that are capitate in larger specimens to slightly protracted in smaller specimens. The axial area is lanceolate reaching the valve margins and widening into a large central area. Striae are regularly slightly bent, radiate near the valve center

and become extremely convergent at the apices. The raphe is practically straight, with proximal ends deflected to one side.

***Pinnularia borealis* Ehrenberg 1843**

**Length Range:** 27 – 48  $\mu\text{m}$

**Width Range:** 8.0 – 10.2  $\mu\text{m}$

**Striae in 10  $\mu\text{m}$ :** 5 – 6

Valves are linear to linear-elliptic, with parallel to temperately convex edges. Apices are not protracted and broadly rounded. A large transverse central area is shaped by 1 or 2 shorter striae on each side. The axial area is narrow. The raphe is straight and filiform to weakly lateral. Distal raphe ends are sickle-shaped. Proximal raphe ends are bent to one side and tipped with expanded pores. Striae are broad and widely separated, uncertainty radiate near the valve center and becoming convergent toward the apices.

***Pinnularia mesolepta* (Ehrenberg) Smith**

**Length Range:** 30 – 65  $\mu\text{m}$

**Width Range:** 9 – 12  $\mu\text{m}$

**Striae in 10  $\mu\text{m}$ :** 10 – 14

Valve straight with triangulating edges, the central inflation smaller than the other two. Striae firmly transmit at the center of the valve, concurrent at the ends.

***Planothidium lanceolatum* (Breb.) Round & Bukhtiyarova**

**Length Range:** 7 – 24  $\mu\text{m}$

**Width Range:** 4.5 – 8.0  $\mu\text{m}$

**Striae in 10  $\mu\text{m}$ :** 12 – 15

Valves are lanceolate to circular lanceolate with somewhat drawn-out apices. The asymmetrical central range on rapheless valve contains a rimmed sorrow on the interior valve surface. The striae are multiseriate, emanate all through the two valves.

***Rhopalodia gibberula* (Ehrenberg) O.F. Müller**

**Length Range:** 27 – 43  $\mu\text{m}$

**Width Range:** 5 – 9.5  $\mu\text{m}$

**Striae in 10  $\mu\text{m}$ :** 12 – 23

Valves are lunate, with emphatically curved dorsal edges that are frequently marginally indented in the center. The ventral margin is considerably concave to straight. In girdle view, frustules are widely lanceolate to elliptic. The apices can be marginally bowed ventrally or might be protracted and rounded. The raphe is situated on the dorsal edge. The transapical costa thickness ranges from 4 – 7 of every 10  $\mu\text{m}$  on the ventral edge, with 2 – 6 striae between each costa. Costae are parallel at the valve focus to slightly transmitting toward the apices.

***Sellaphora lanceolata* D.G. Mann & S. Dropp in Mann *et al.***

**Length Range:** 24 – 30  $\mu\text{m}$

**Width Range:** 7.1 – 8.1  $\mu\text{m}$

**Striae in 10  $\mu\text{m}$ :** 18 – 22

Valves narrowly elliptical with rostrate ends. Radiate over the vast majority of the valve, however, merged at poles, with sudden change typically set apart by geniculate striae and shorter striae beginning close to the raphe. Narrow linear, straight. Elliptical or transversely oval but irregular of the nearness of rough interchange long and short striae; the nearness of 'ghost striae' (internal expansions of the regular striae that lack poroids: they are more slender segments of silica, showing up as sections inside and sometimes remotely, SEM). Simple filiform, straight; external proximal raphe endings expanded and scarcely deflected towards the primary side, terminal fissures curve smoothly towards the secondary side. Polar bars seem calculated towards the central area.

***Stauroneis anceps* Ehrenberg**

**Length Range:** 48 – 76  $\mu\text{m}$

**Width Range:** 12 – 15  $\mu\text{m}$

**Striae in 10  $\mu\text{m}$ :** 19 – 21

Valves are lanceolate to linear-lanceolate. The apices are narrowly rostrate and protracted. The axial area is temperately broad and linear, expanding marginally near the central area. The narrow rectangular stauros central area is hardly expanded toward valve margins and sometimes with shortened striae. Striae are radiate throughout. The raphe is lateral and proximal raphe ends are weakly expanded, weakly deflected, and widely spaced and not extend into the central area.

***Staurosira elliptica* (Schumann) D.M.Williams & Round**

**Length Range:** 6 – 14  $\mu\text{m}$

**Width Range:** 3 – 3.5  $\mu\text{m}$

**Striae in 10  $\mu\text{m}$ :** 14 – 16

Valves are elliptical to lanceolate with cuneate to rounded ends. Striae are short and usually composed of one round areola on the valve face and another on the valve mantle.

***Surirella biseriata f. amphioxys* (W. Smith) Hustedt**

**Length Range:** 28 – 48  $\mu\text{m}$

**Width Range:** 13.5 – 17  $\mu\text{m}$

**Striae in 10  $\mu\text{m}$ :** 16 – 20

Valves ratio of length to width is 2 and 3. Valves are isopolar with cuneate apices and straight, parallel sides. The valve face is strongly undulate that the structures termed “porcae” these appeared as rectangular structures in the LM. Porca is 4 – 5  $\mu\text{m}$  long and 2 – 3  $\mu\text{m}$  wide and is traversed by 3 – 4 costae, with 1 – 2 costae between each porca. Costae is extending from the margin to the apical axis. Between the costae occur 4 – 5

rows of round areolae that visible only in the SEM. Around the valve, the margin is what appear to be large areolae in the LM, but in the SEM these “areolae” are indentations in the valve face corresponding to fibulae in the interior of the valve. Indentations or portulae are on the mantle face, matching to those on the valve face. Areolae on the surface of the indentations directly beneath the keel penetrate to the mantle. A flat, distinct central area occurs about the axial line.

***Surirella elegans* Ehrenberg**

**Length Range:** 110 – 400  $\mu\text{m}$

**Width Range:** 35 – 90  $\mu\text{m}$

**Striae in 10  $\mu\text{m}$ :** 16 – 20

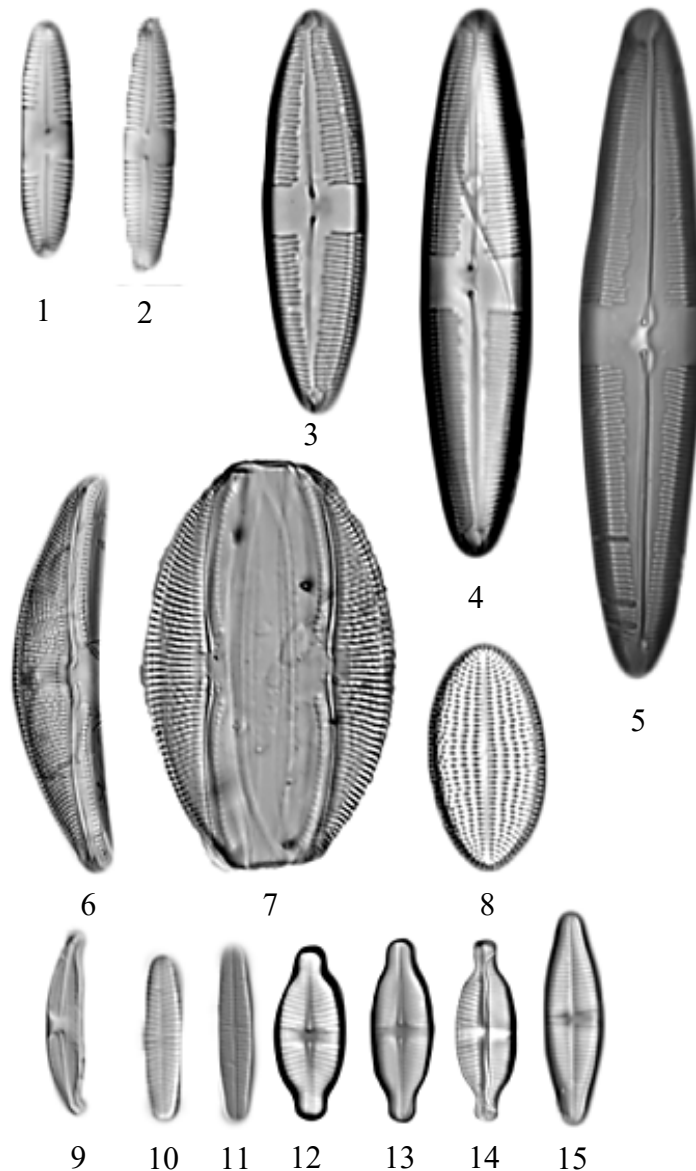
The ends are cuneate from the girdle view and heteropolar from the valve view. The valve view is an ellipsoid, narrow or wide with bluntly rounded poles. Sometimes in longer individuals, the ends are cuneate narrowed. The wing is narrow with a somewhat vague projection.

***Synedra ulna* (Nitzsch) Ehrenberg**

**Length Range:** 50 – 250  $\mu\text{m}$

**Width Range:** 2 – 9  $\mu\text{m}$

Valves are Linear or sometimes linear–lanceolate that narrowing to blunt sub–rostrate or rostrate apices. The Central area is usually reaching the valve margin, and also distinct, roughly square in outline. Ghost striae are regularly visible within the central area. In a few populations, the central area is smaller, circular or elliptical in outline and not reaching the valve edge.

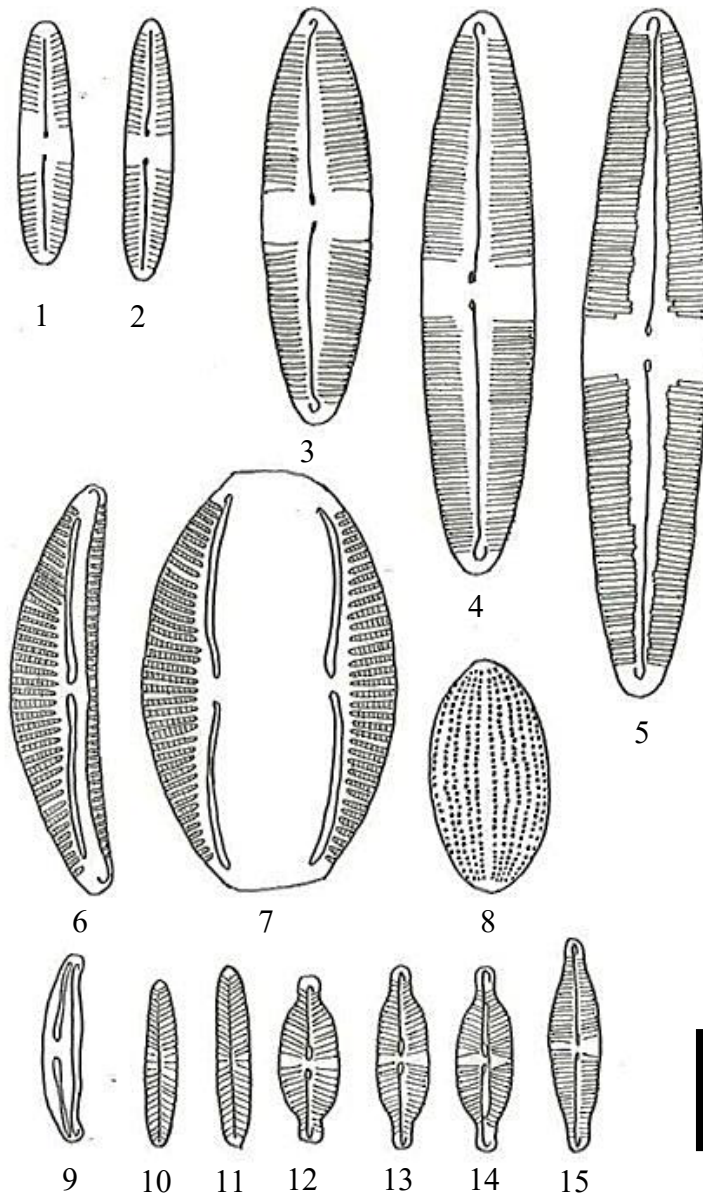


ลิขสิทธิ์มหาวิทยาลัยเชียงใหม่  
 Copyright © by Chiang Mai University

Scale bar = 10  $\mu$ m

Figure 3.48 (plate 1) Light micrograph of benthic diatoms from some hot springs in the northern Thailand during December 2015 to April 2016.

(1-2) *Caloneis bacillum* (Grunov) Mereschkowsky, (3-5) *Caloneis molaris* (Grunow) Krammer, (6-7) *Amphora ovalis* (Kützing) Kützing, (8) *Cocconeis placentula* Ehrenberg, (9) *Amphora montana* Krasske, (10-11) *Achnanthidium minutissimum* (Kützing) Czarnecki, (12-14) *Achnanthidium exiguum* (Grunow) Czarnecki, (15) *Achnanthidium* sp.

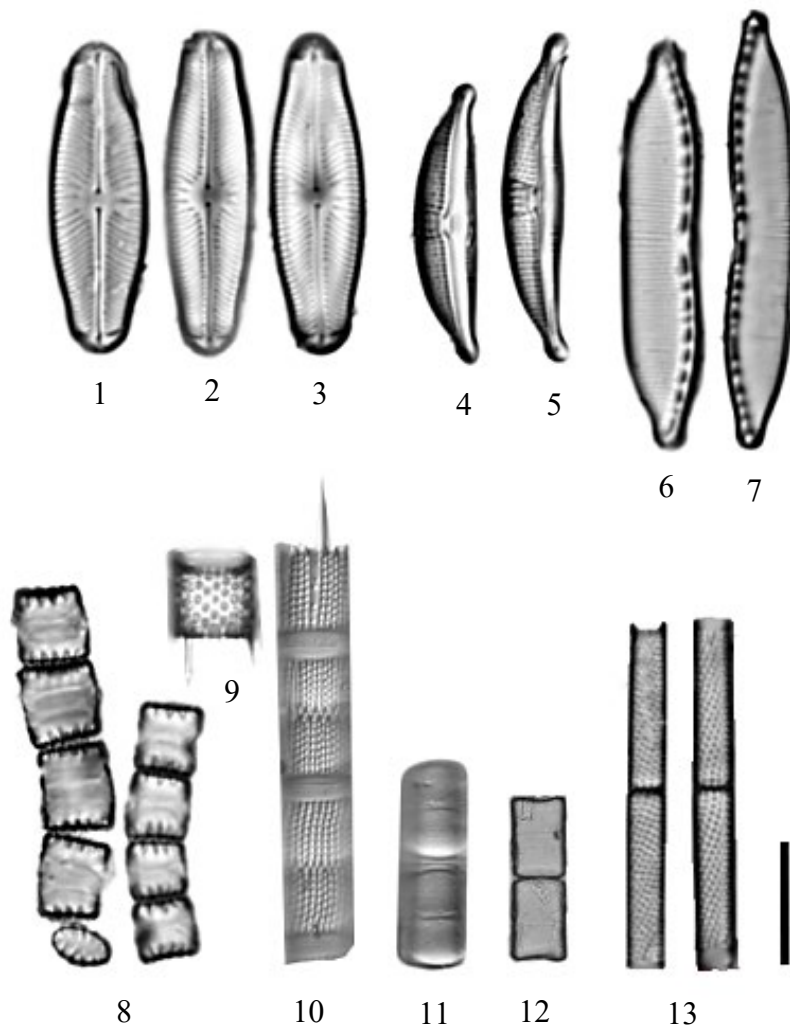


ลิขสิทธิ์มหาวิทยาลัยเชียงใหม่  
 Copyright © by Chiang Mai University

Scale bar = 10  $\mu$ m

Figure 3.49 (plate 1) Drawing of benthic diatoms from some hot springs in the northern Thailand during December 2015 to April 2016.

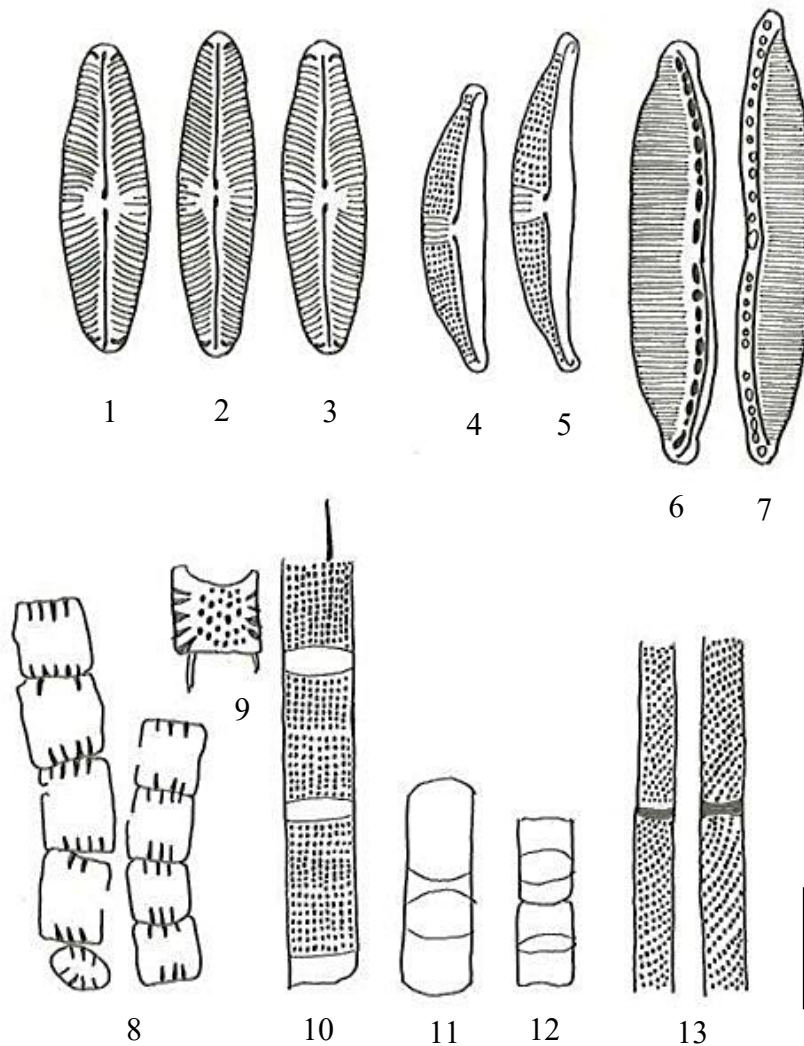
(1-2) *Caloneis bacillum* (Grunov) Mereschkowsky, (3-5) *Caloneis molaris* (Grunow) Krammer, (6-7) *Amphora ovalis* (Kützing) Kützing, (8) *Cocconeis placentula* Ehrenberg, (9) *Amphora montana* Krasske, (10-11) *Achnantheidium minutissimum* (Kützing) Czarnecki, (12-14) *Achnantheidium exiguum* (Grunow) Czarnecki, (15) *Achnantheidium* sp.



Scale bar = 10  $\mu$ m

Figure 3.48 (plate 2) Light micrograph of benthic diatoms from some hot springs in the northern Thailand during December 2015 to April 2016 (continued).

(1-3) *Sellaphora lanceolata* D.G. Mann & S. Dropp in Mann et al., (4-5) *Halamphora fontinalis* (Hustedt) Z. Levkov, (6-7) *Hantzchia amphioxys* (Ehrenberg) Grunow in Cleve et Grunow, (8) *Staurosira elliptica* (Schumann) D.M. Williams & Round, (9-10) *Aulacoseira granulata* Ehrenberg, (11-12) *Meloseira varians* Agardh, (13) *Aulacoseira ambigua* (Grunow) Simonsen

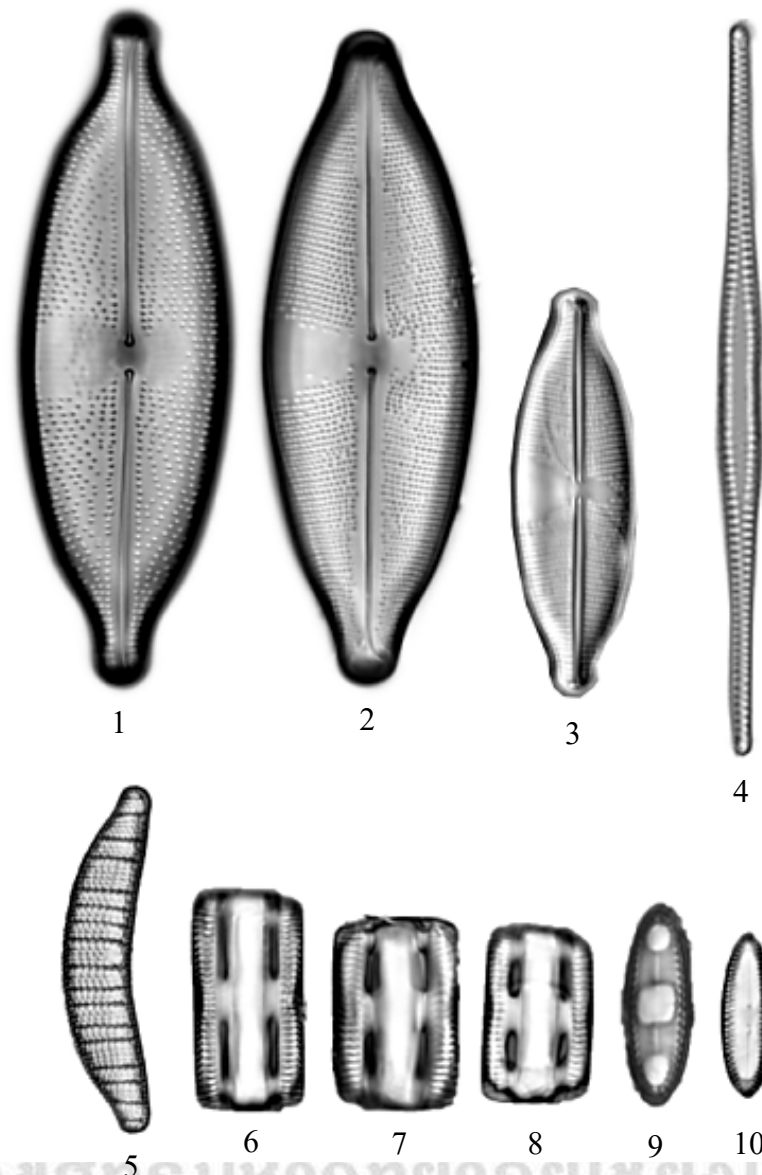


ลิขสิทธิ์มหาวิทยาลัยเชียงใหม่  
 Copyright© by Chiang Mai University

Scale bar = 10  $\mu$ m

Figure 3.49 (plate 2) Drawing of benthic diatoms from some hot springs in the northern Thailand during December 2015 to April 2016 (continued).

(1-3) *Sellaphora lanceolata* D.G. Mann & S. Dropp in Mann et al., (4-5) *Halamphora fontinalis* (Hustedt) Z. Levkov, (6-7) *Hantzchia amphioxys* (Ehrenberg) Grunow in Cleve et Grunow, (8) *Staurosira elliptica* (Schumann) D.M. Williams & Round, (9-10) *Aulacoseira granulata* Ehrenberg, (11-12) *Meloseira varians* Agardh, (13) *Aulacoseira ambigua* (Grunow) Simonsen

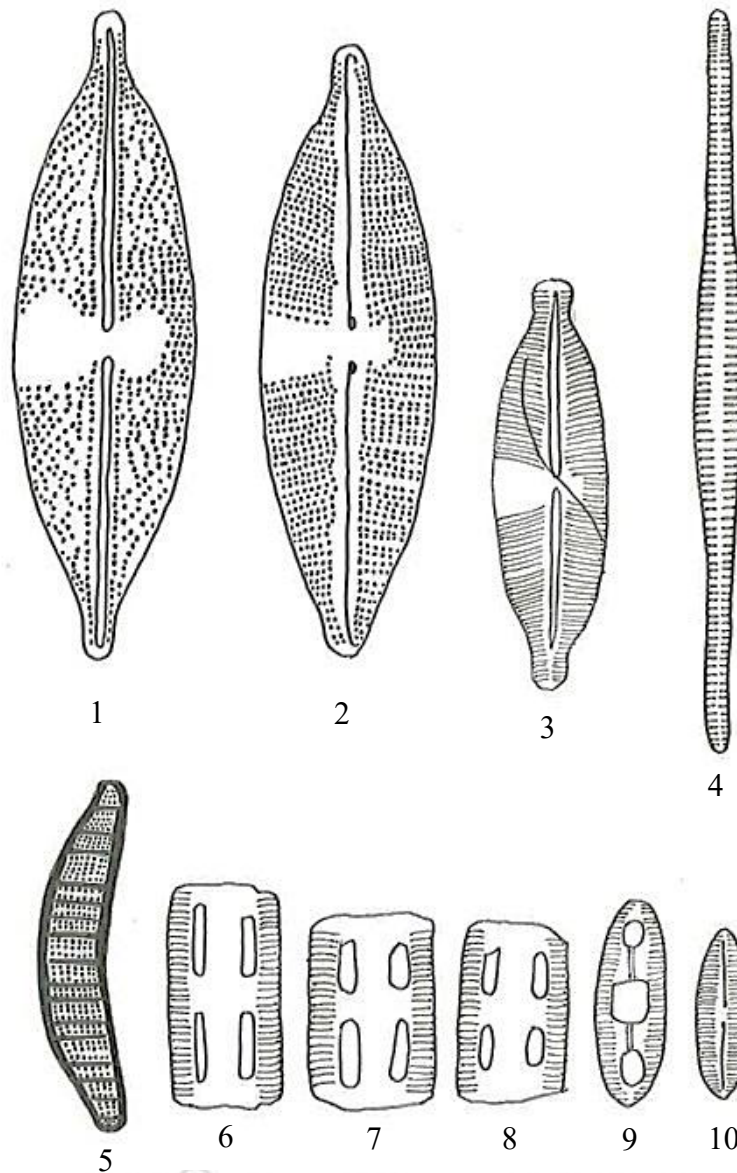


ลิขสิทธิ์มหาวิทยาลัยเชียงใหม่  
 Copyright© by Chiang Mai University  
 All rights reserved

Scale bar = 10  $\mu$ m

Figure 3.48 (plate 3) Light micrograph of benthic diatoms from some hot springs in the northern Thailand during December 2015 to April 2016 (continued).

(1-2) *Anomoeoneis sphaerophora* (Ehrenberg)Pfitzer, (3) *Anomoeneis* sp., (4) *Fragillaria crotonensis* Kitton, (5) *Epithemia zebra* (Ehrenberg) Kützing 1844, (6-10) *Diatomella balfouriana* Greville

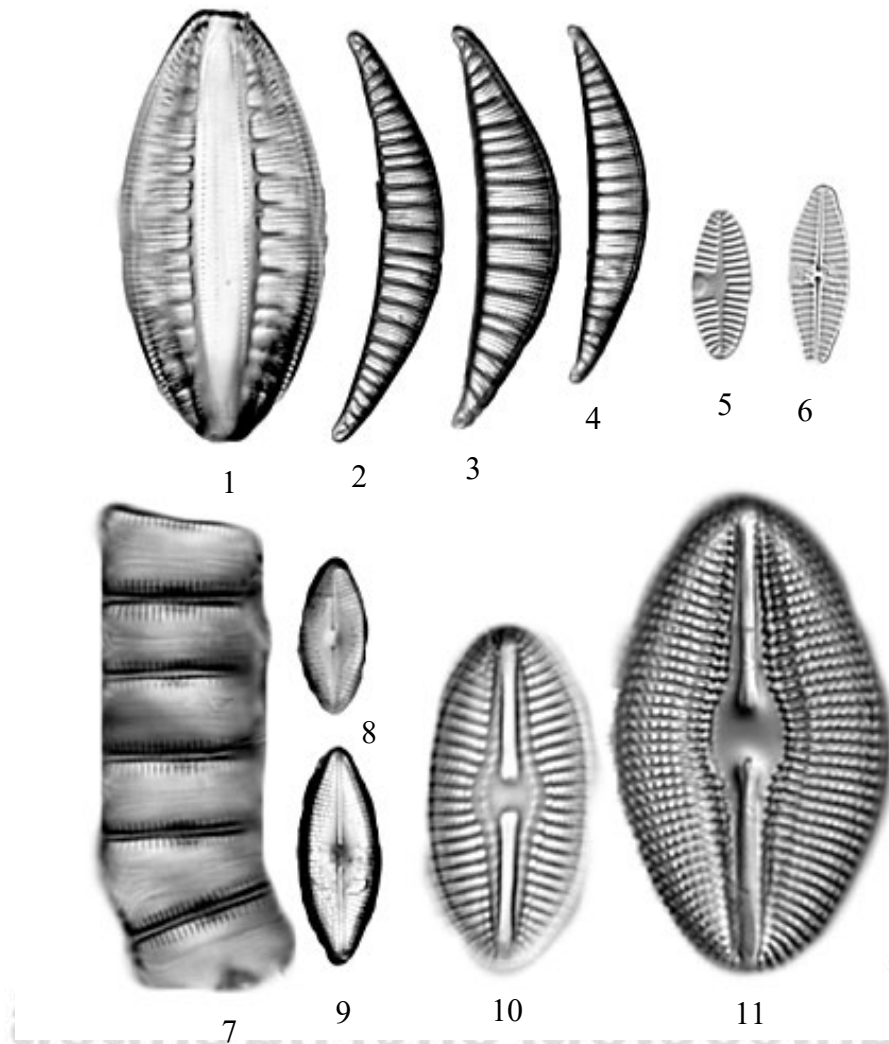


Copyright© by Chiang Mai University  
 All rights reserved

Scale bar = 10  $\mu$ m

Figure 3.49 (plate 3) Drawing of benthic diatoms from some hot springs in the northern Thailand during December 2015 to April 2016 (continued).

(1-2) *Anomoeoneis sphaerophora* (Ehrenberg)Pfitzer, (3) *Anomoeoneis* sp., (4) *Fragillaria crotonensis* Kitton, (5) *Epithemia zebra* (Ehrenberg) Kützing 1844, (6-10) *Diatomella balfouriana* Greville

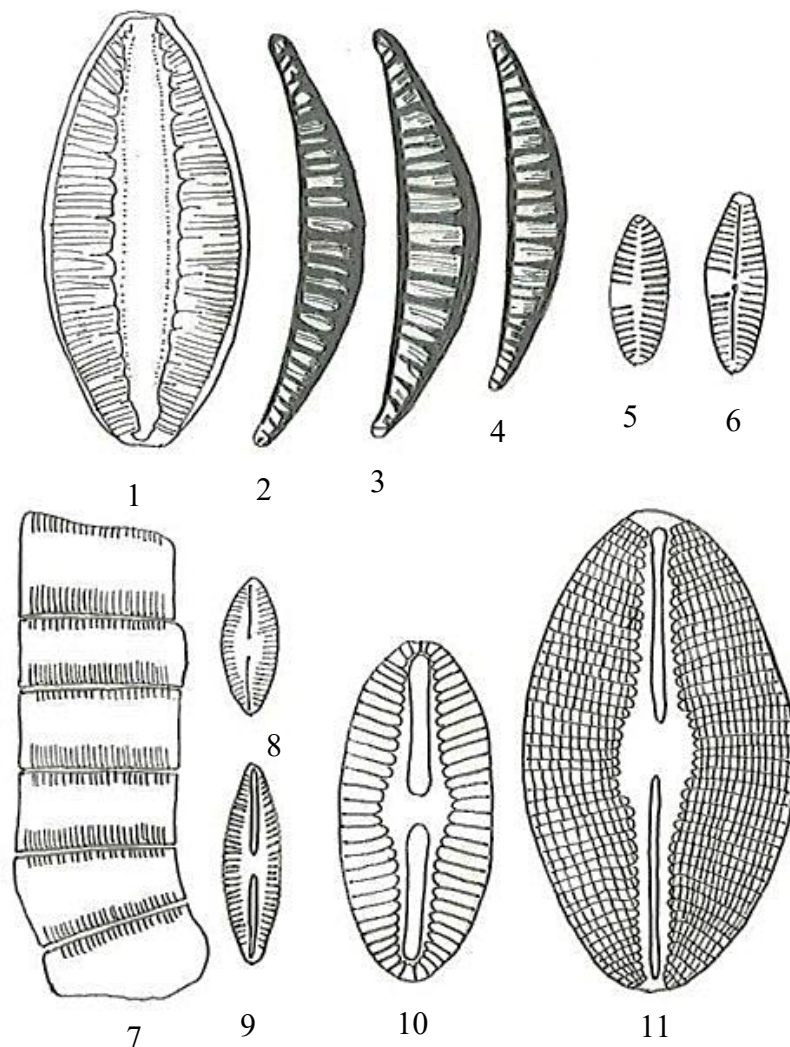


Copyright© by Chiang Mai University  
 All rights reserved

Scale bar = 10 μm

Figure 3.48 (plate 4) Light micrograph of benthic diatoms from some hot springs in the northern Thailand during December 2015 to April 2016 (continued).

(1-4) *Rhopalodia gibberula* (Ehrenberg) O.F. Müller, (5-6) *Planothidium lanceolatum* (Breb.) Round & Bukhtiyarova, (7-9) *Diadesmis confervacea* Kützing (10) *Diploneis subovalis* Cleve, 1894, (11) *Diploneis elliptica* (Kützing) Cleve 1894

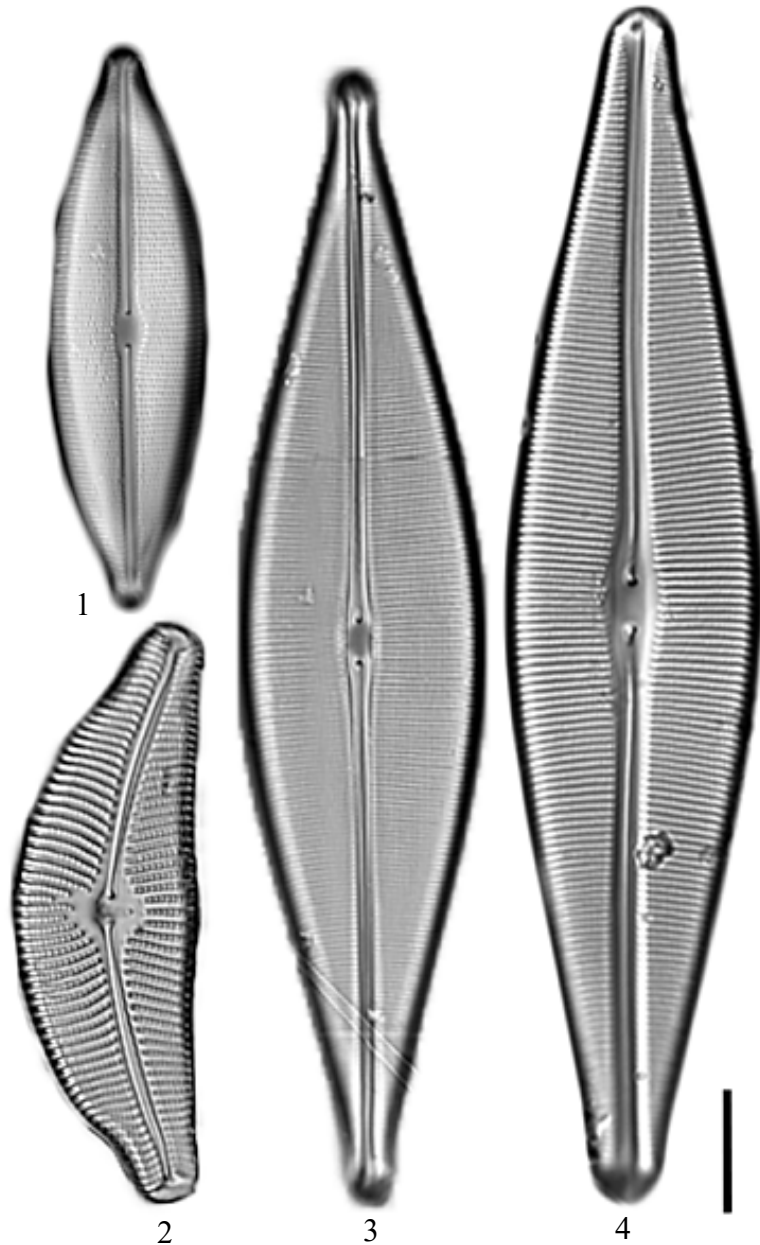


ลิขสิทธิ์มหาวิทยาลัยเชียงใหม่  
 Copyright© by Chiang Mai University  
 All rights reserved

Scale bar = 10  $\mu$ m

Figure 3.49 (plate 4) Drawing of benthic diatoms from some hot springs in the northern Thailand during December 2015 to April 2016 (continued).

(1-4) *Rhopalodia gibberula* (Ehrenberg) O.F. Müller, (5-6) *Planothidium lanceolatum* (Breb.) Round & Bukhtiyarova, (7-9) *Diadesmis confervacea* Kützing (10) *Diploneis subovalis* Cleve, 1894, (11) *Diploneis elliptica* (Kützing) Cleve 1894

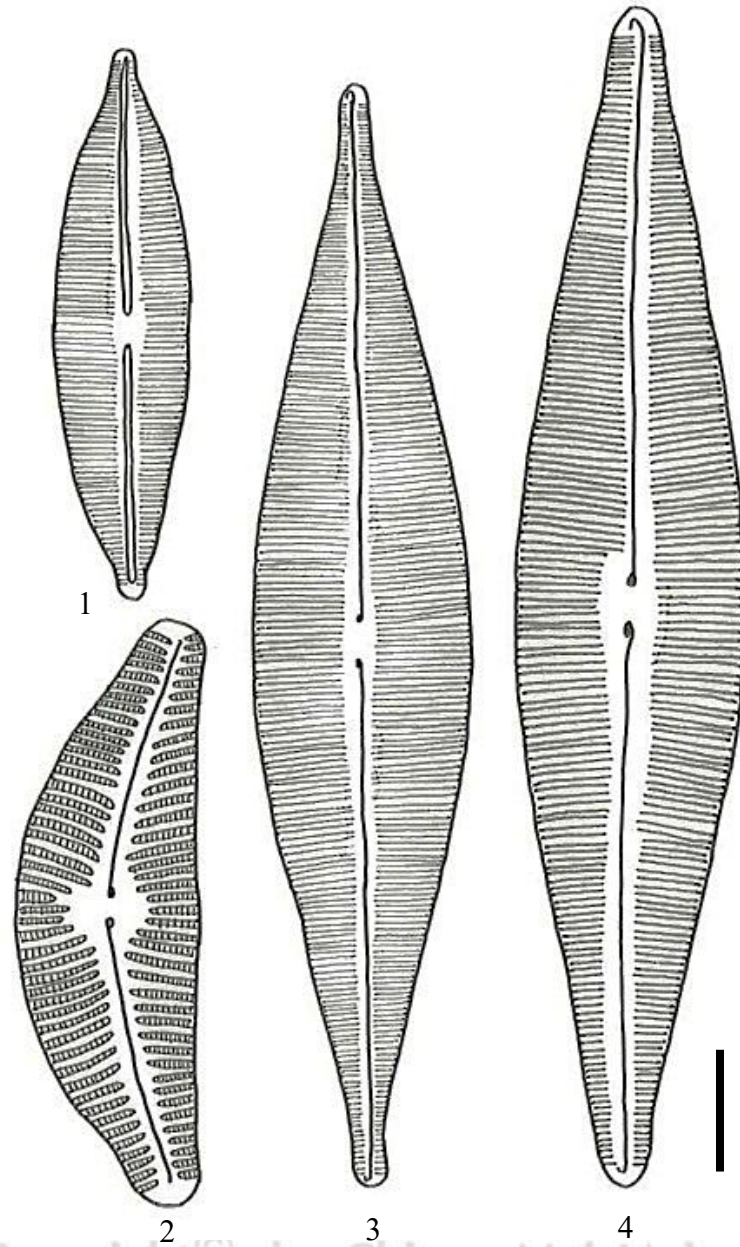


Copyright© by Chiang Mai University  
All rights reserved

Scale bar = 10  $\mu$ m

Figure 3.48 (plate 5) Light micrograph of benthic diatoms from some hot springs in the northern Thailand during December 2015 to April 2016 (continued).

(1) *Craticula ambigua* (Ehrenberg) Mann in Round, Crawford & Mann, (2) *Cymbella tumida* (Brébisson) Van Heurck, (3) *Craticula cuspidata* (Kützing) Man, (4) *Craticula acidoclinata* Lange-Bertalot & Metzeltin

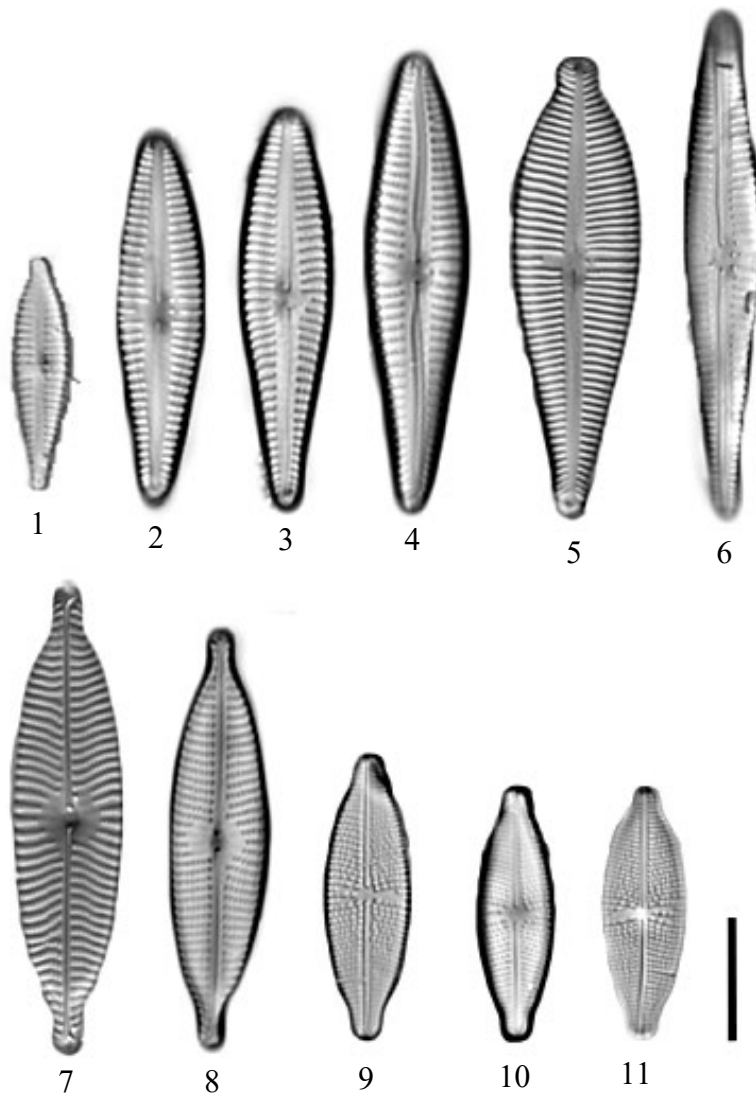


Copyright© by Chiang Mai University  
All rights reserved

Scale bar = 10  $\mu$ m

Figure 3.49 (plate 5) Drawing of benthic diatoms from some hot springs in the northern Thailand during December 2015 to April 2016 (continued).

(1) *Craticula ambigua* (Ehrenberg) Mann in Round, Crawford & Mann, (2) *Cymbella tumida* (Brébisson) Van Heurck, (3) *Craticula cuspidata* (Kützing) Man, (4) *Craticula acidoclinata* Lange-Bertalot & Metzeltin

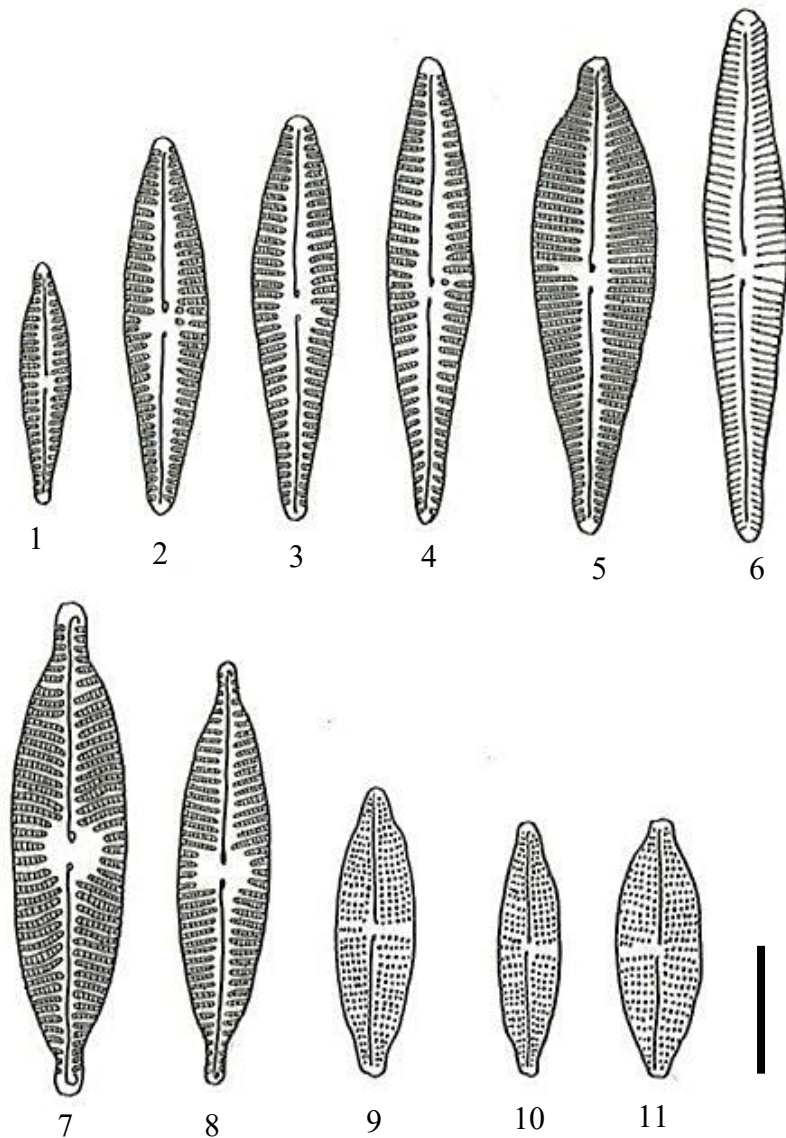


Copyright© by Chiang Mai University  
All rights reserved

Scale bar = 10  $\mu$ m

Figure 3.48 (plate 6) Light micrograph of benthic diatoms from some hot springs in the northern Thailand during December 2015 to April 2016 (continued).

(1) *Gomphonema parvulum* (Kützing) Van Heurck, (2-4) *Gomphonema affine* Kützing, (5) *Gomphonema augur* var. *sphaerophorum* Lange-Bertalot, (6) *Gomphonema gracile* Ehrenberg 1838, (7) *Navicula rostellata* (Kützing) Cleve, (8) *Navicula subrhynchocephala* Hustedt, (9-11) *Navicula grimmei* Krasske in Hustedt



Copyright© by Chiang Mai University  
 All rights reserved

Scale bar = 10  $\mu$ m

Figure 3.49 (plate 6) Drawing of benthic diatoms from some hot springs in the northern Thailand during December 2015 to April 2016 (continued).

- (1) *Gomphonema parvulum* (Kützing) Van Heurck, (2-4) *Gomphonema affine* Kützing, (5) *Gomphonema augur* var. *sphaerophorum* Lange-Bertalot, (6) *Gomphonema gracile* Ehrenberg 1838, (7) *Navicula rostellata* (Kützing) Cleve, (8) *Navicula subrhynchocephala* Hustedt, (9-10) *Navicula grimmei* Krasske in Hustedt

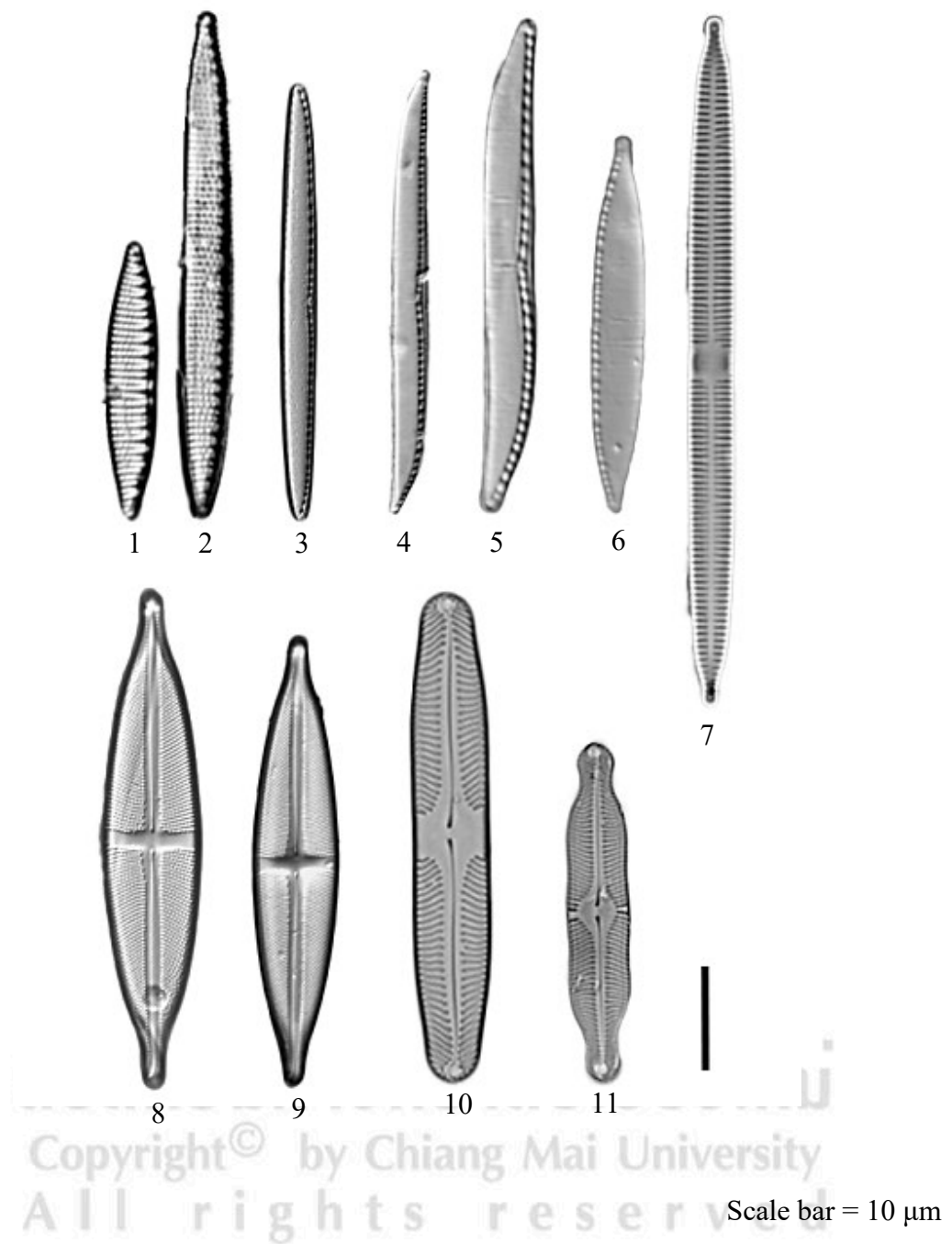


Figure 3.48 (plate 7) Light micrograph of benthic diatoms from some hot springs in the northern Thailand during December 2015 to April 2016 (continued).

(1-2) *Nitzschia amphibia* Grunow, (3) *Nitzschia ignorata* Krasske 1929, (4-5) *Nitzschia clausii* Hantzsch, (6) *Nitzschia palea* (Kützing) W. Smith, (7) *Synedra ulna* (Nitzsch) Ehrenberg, (8-9) *Stauroneis anceps* Ehrenberg, (10) *Pinnularia abaujensis* (Pantoscek) Ross, (11) *Pinnularia mesolepta* (Ehrenberg) Smith

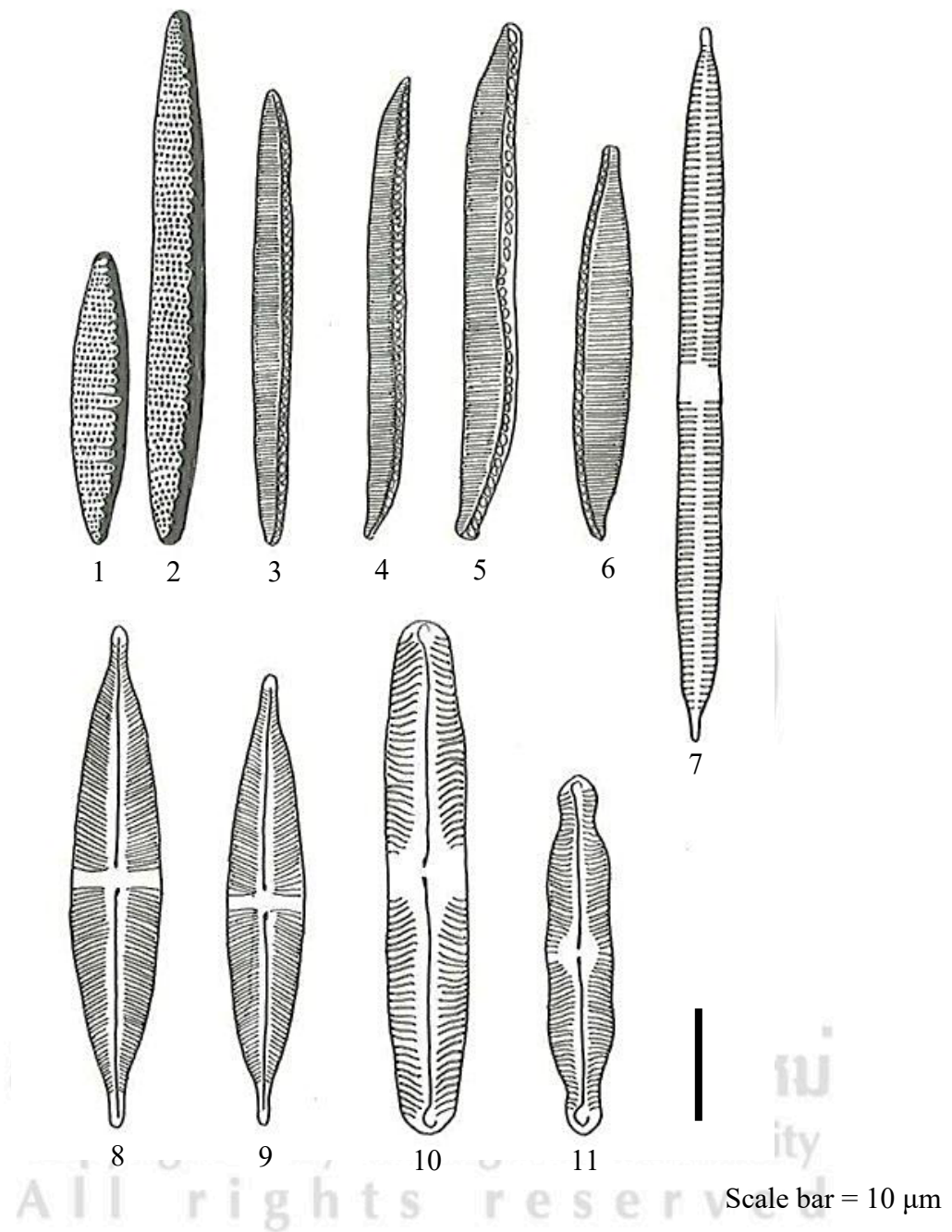
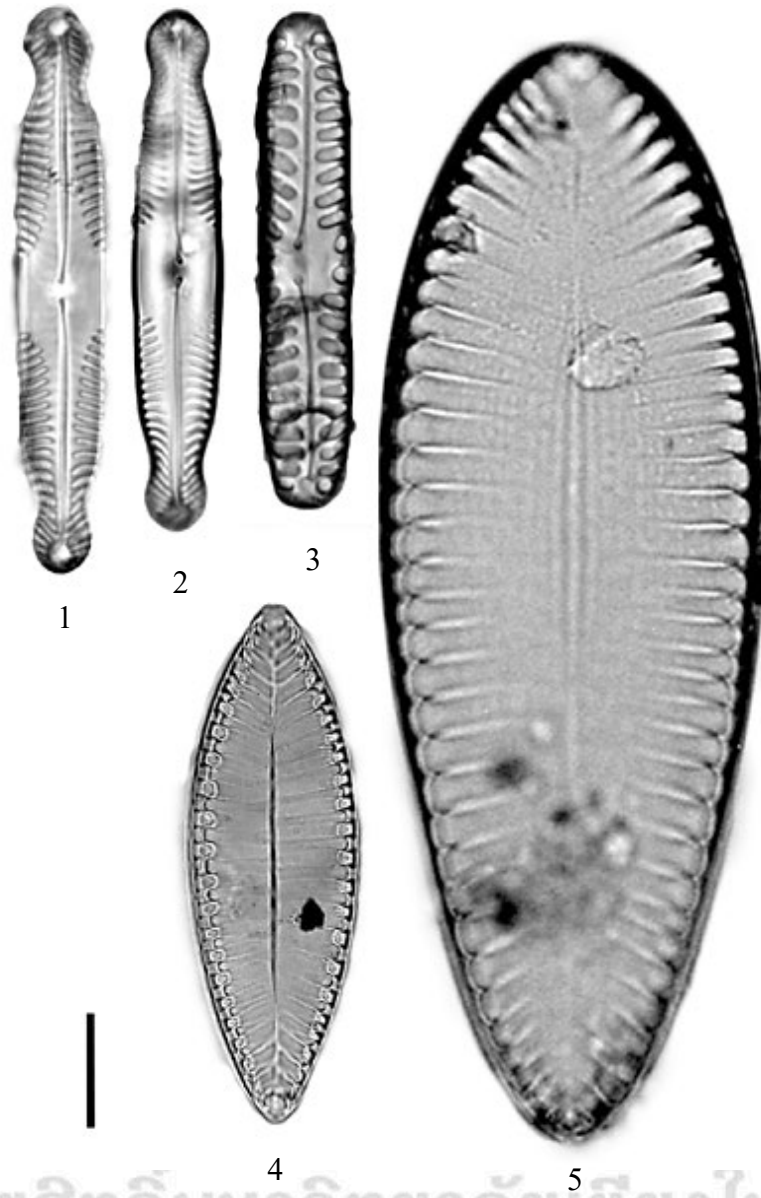


Figure 3.49 (plate 7) Drawing of benthic diatoms from some hot springs in the northern Thailand during December 2015 to April 2016 (continued).

(1-2) *Nitzschia amphibia* Grunow, (3) *Nitzschia ignorata* Krasske 1929, (4-5) *Nitzschia clausii* Hantzsch, (6) *Nitzschia palea* (Kützing) W. Smith, (7) *Synedra ulna* (Nitzsch) Ehrenberg, (8-9) *Stauroneis anceps* Ehrenberg, (10) *Pinnularia abaujensis* (Pantoscek) Ross, (11) *Pinnularia mesolepta* (Ehrenberg) Smith

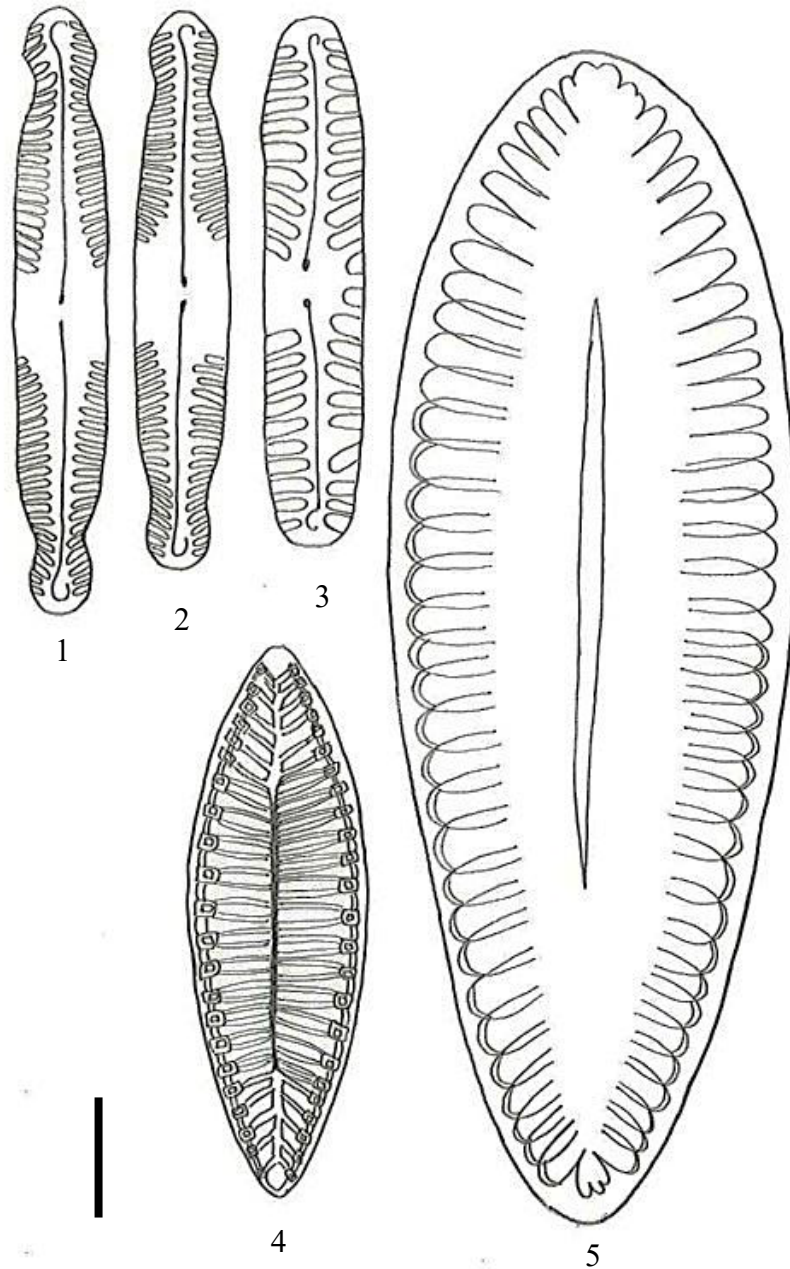


ลิขสิทธิ์มหาวิทยาลัยเชียงใหม่  
 Copyright© by Chiang Mai University  
 All rights reserved

Scale bar = 10  $\mu$ m

Figure 3.48 (plate 8) Light micrograph of benthic diatoms from some hot springs in the northern Thailand during December 2015 to April 2016 (continued).

(1-2) *Pinnularia saphophila* Lange–Bertalot, Kobayashi and Krammer, (3) *Pinnularia borealis* Ehrenberg 1843, (4) *Surirella biseriata* f. *amphioxys* (W. Smith) Hustedt, (5) *Surirella elegans* Ehrenberg



Copyright © by Chiang Mai University  
 All rights reserved

Scale bar = 10 μm

Figure 3.49 (plate 8) Drawing of benthic diatoms from some hot springs in the northern Thailand during December 2015 to April 2016 (continued).

(1-2) *Pinnularia saprophila* Lange–Bertalot, Kobayashi and Krammer, (3) *Pinnularia borealis* Ehrenberg 1843, (4) *Surirella biseriata* f. *amphioxys* (W. Smith) Hustedt, (5) *Surirella elegans* Ehrenberg

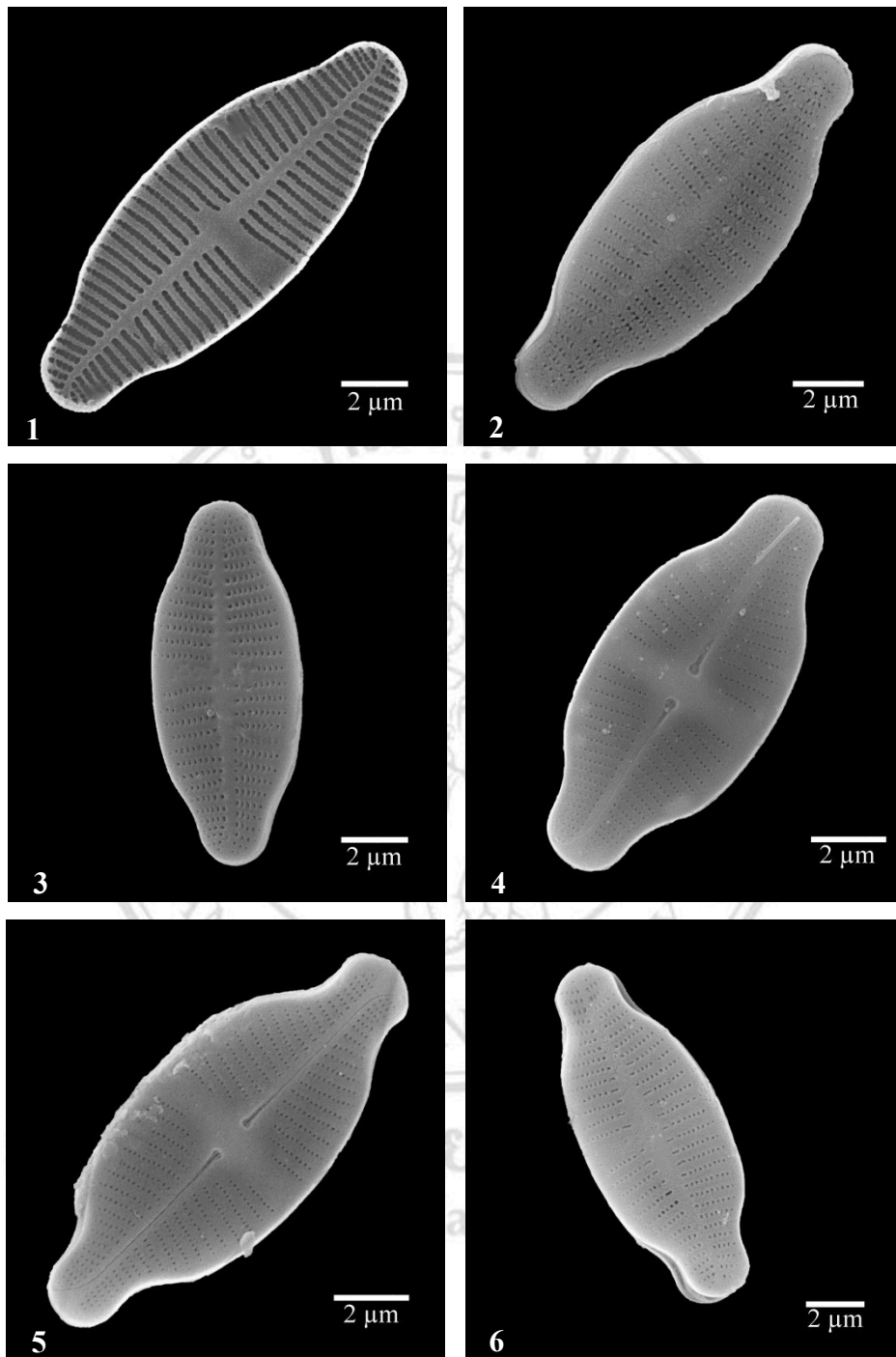


Figure 3.50 Scanning electron microscope photographs of some hot spring diatoms in 8 sampling sites during December 2015 – April 2016

(1-6) *Achnantheidium exiguum* (Grunow) Czarnecki

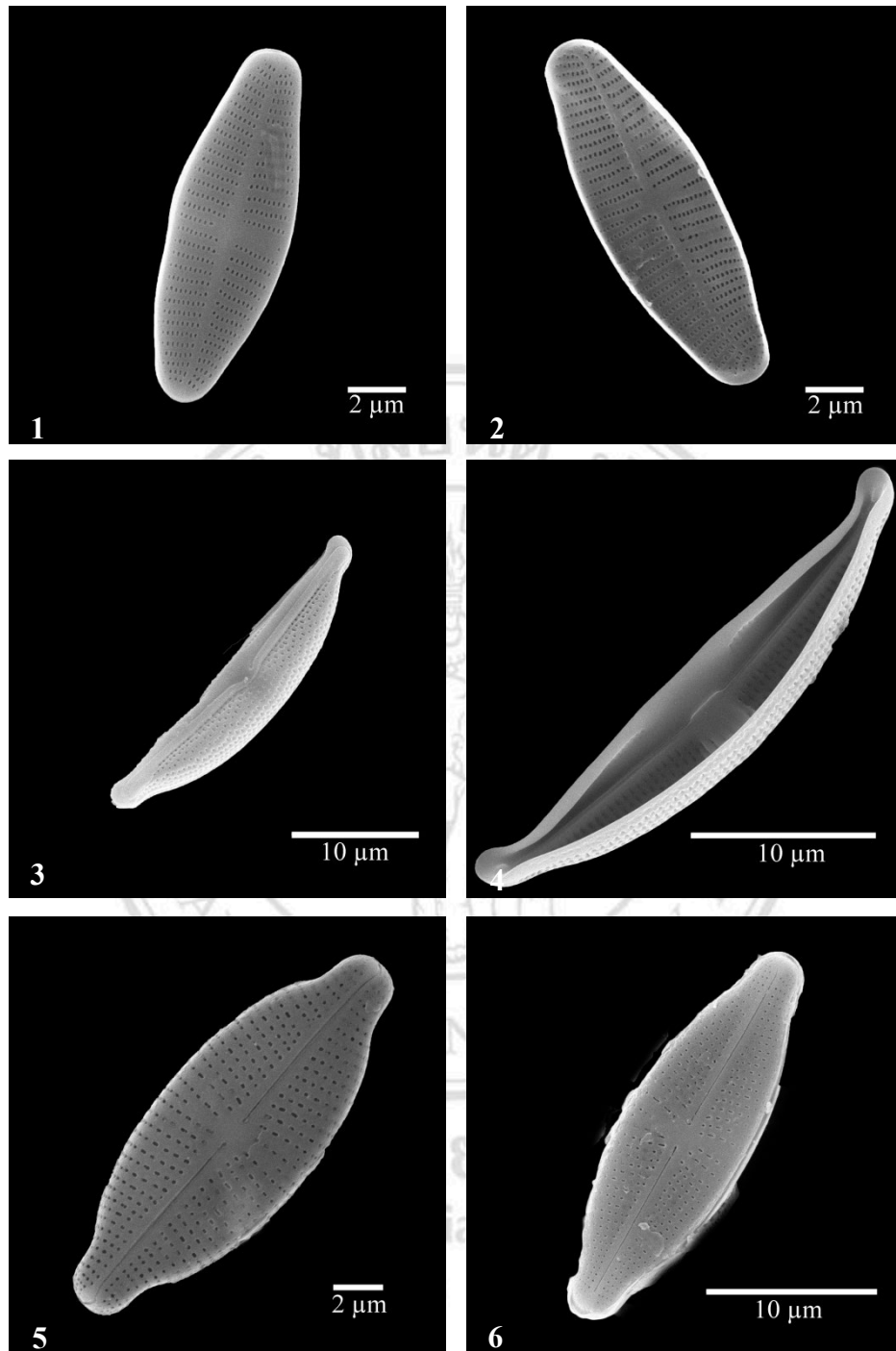


Figure 3.50 Scanning electron microscope photographs of some hot spring diatoms in 8 sampling sites during December 2015 – April 2016 (continued)

(1-2) *Achnantheidium* sp., (3-4) *Halamphora fontinalis* (Hustedt) Z. Levkov,  
 (5-6) *Navicula grimmei* Krasske in Hustedt

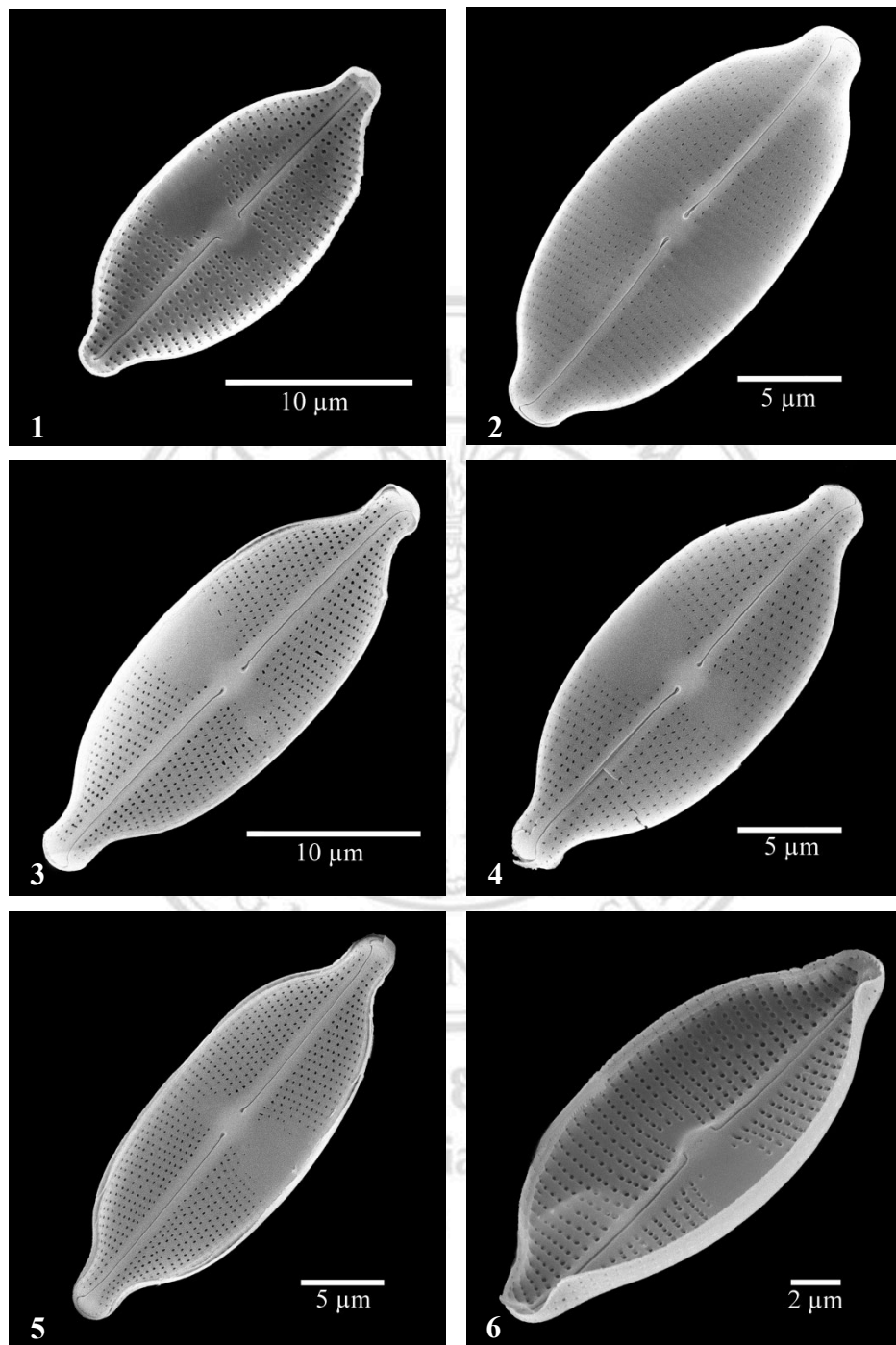


Figure 3.50 Scanning electron microscope photographs of some hot spring diatoms in 8 sampling sites during December 2015 – April 2016 (continued)

(1-2) *Achnantheidium* sp., (3-6) *Anomoeoneis sphaerophora* (Ehrenberg) Pfitzer

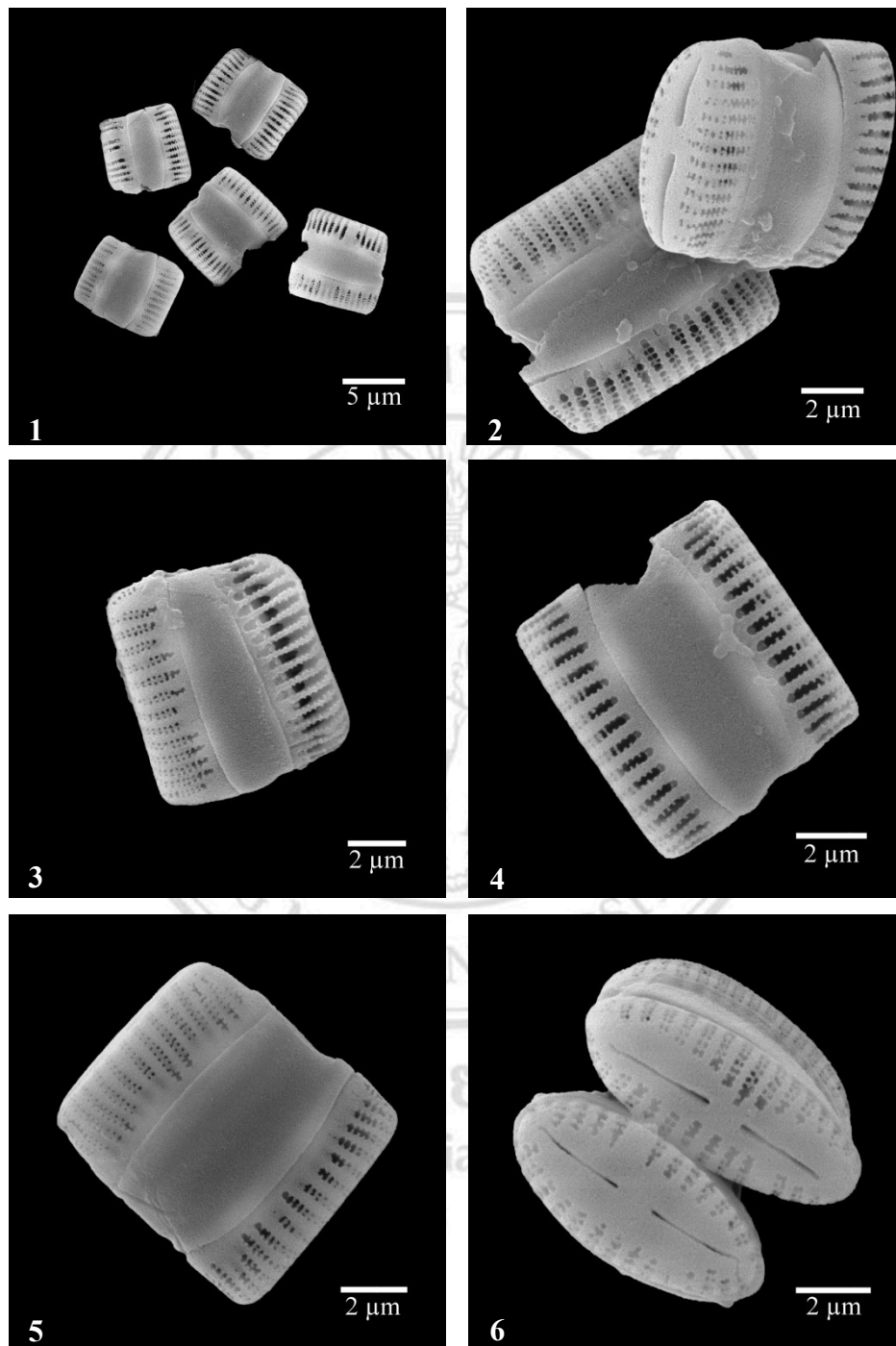


Figure 3.50 Scanning electron microscope photographs of some hot spring diatoms in 8 sampling sites during December 2015 – April 2016 (continued)

(1-6) *Diatomella balfouriana* Greville

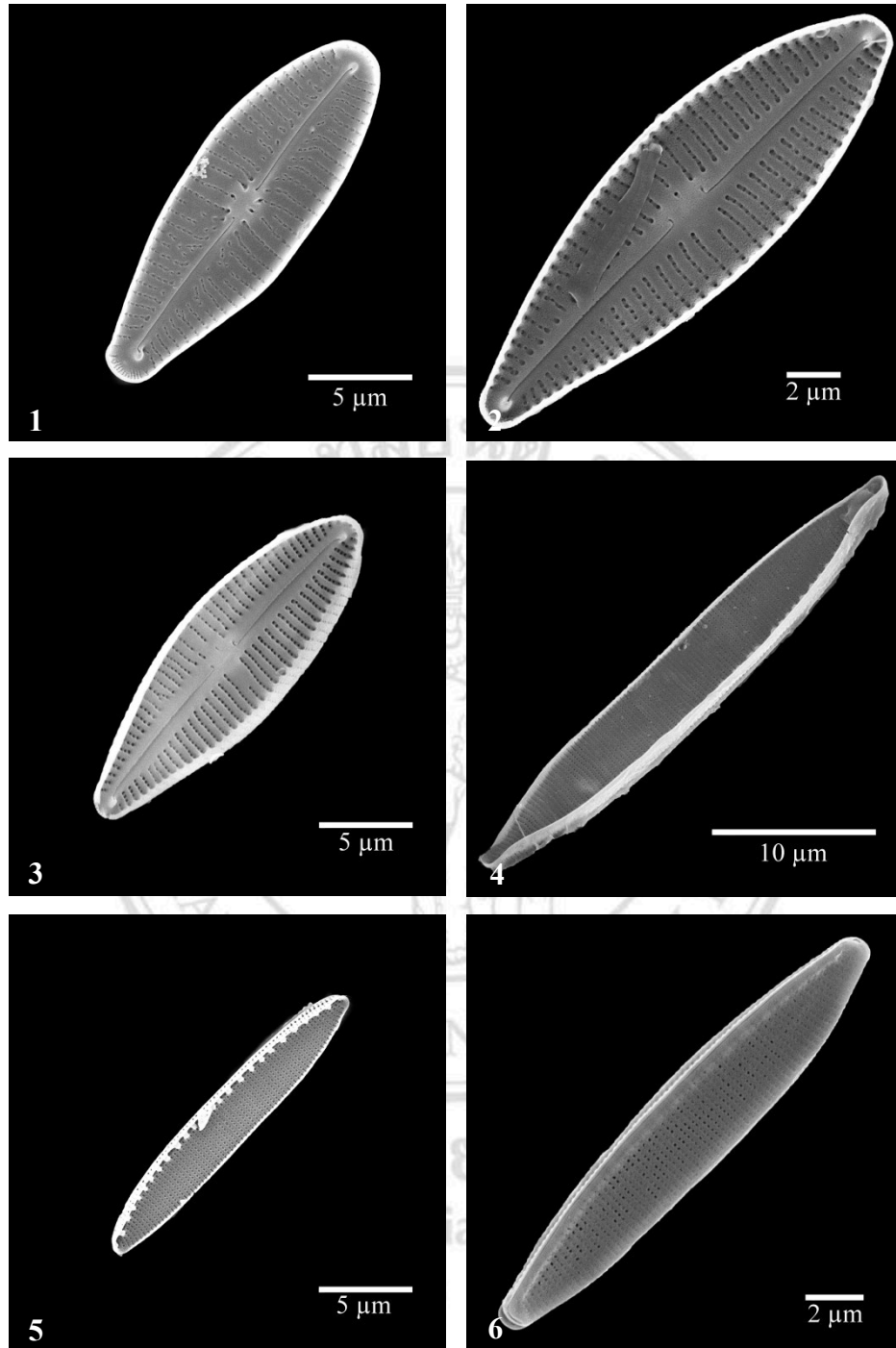


Figure 3.50 Scanning electron microscope photographs of some hot spring diatoms in 8 sampling sites during December 2015 – April 2016 (continued)

(1-3) *Gomphonema affine* Kützing, (4) *Nitzschia amphibia* Grunow,  
 (5) *Nitzschia ignorata* Krasske 1929, (6) *Nitzschia palea* (Kützing) W. Smith

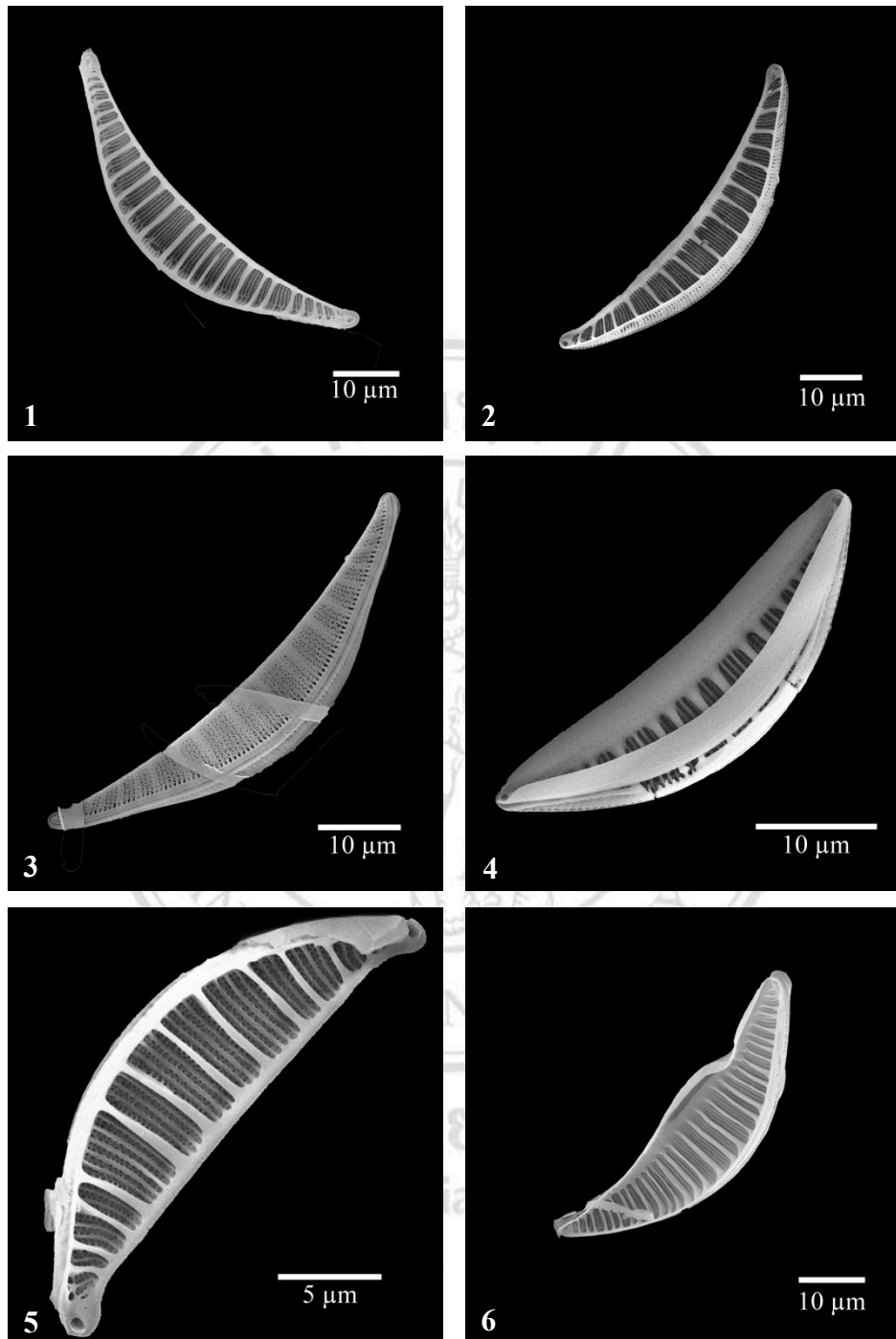


Figure 3.50 Scanning electron microscope photographs of some hot spring diatoms in 8 sampling sites during December 2015 – April 2016 (continued)

(1-6) *Rhopalodia gibberula* (Ehrenberg) O.F. Müller

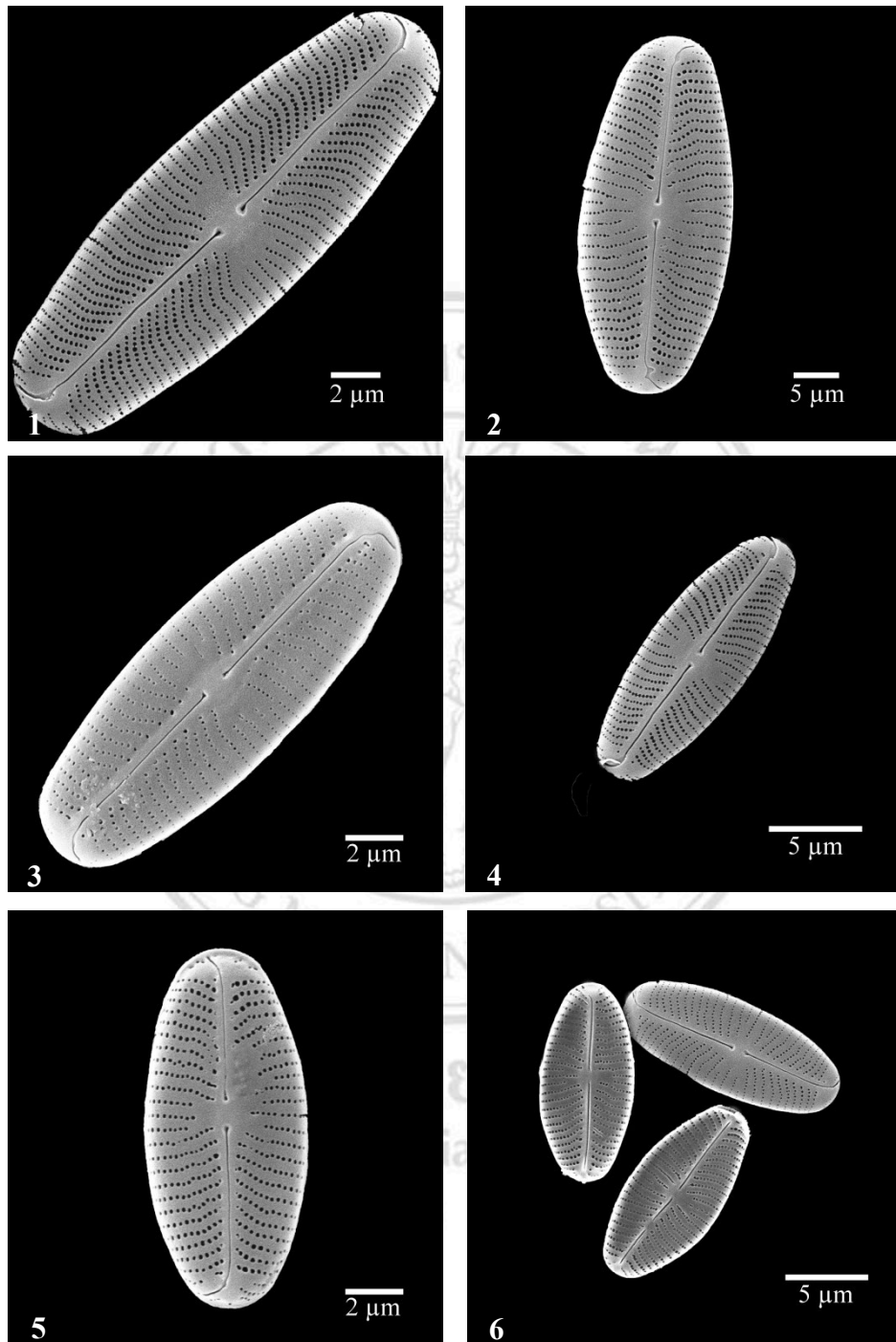


Figure 3.50 Scanning electron microscope photographs of some hot spring diatoms in 8 sampling sites during December 2015 – April 2016 (continued)

(1-6) *Sellaphora lanceolata* D.G. Mann & S. Dropp in Mann *et al.*

Table 3.9 The list of benthic diatoms in 8 hot spring sampling sites during December 2015 - April 2016

Taxa	Synonym
<b>Division</b> Bacillariophyta	
<b>Class</b> Coscinodiscophyceae	
<b>Order</b> Aulacoseirales	
<b>Family</b> Aulacoseiraceae	
<i>Aulacoseira ambigua</i> (Grunow) Simonsen	<i>Melosira ambigua</i> (Grunow in Van Heurck) Otto Müller 1903 <i>Melosira crenulata</i> var. <i>ambigua</i> Grunow in Van Heurck 1882 <i>Melosira granulata</i> var. <i>ambigua</i> (Grunow in Van Heurck) Thum 1889 <i>Melosira italica</i> var. <i>ambigua</i> (Grunow in Van Heurck) A. Cleve-Euler in Backmann & Cleve-Euler 1922 <i>Melosira italica</i> f. <i>ambigua</i> (Grunow in Van Heurck) Balachonzew (Bolochozzew) 1909 <i>Melosira italica</i> subsp. <i>ambigua</i> (Grunow) Cleve-Euler 1938 <i>Melosira italica</i> var. <i>ambigua</i> (Grunow) Cleve-Euler 1951
<i>Aulacoseira granulata</i> Ehrenberg	<i>Gaillonella granulata</i> Ehrenberg 1843 <i>Melosira granulata</i> (Ehrenberg) Ralfs 1861 <i>Melosira punctata</i> var. <i>granulata</i> (Ehrenberg) Cleve & Möller 1879 <i>Lysigonium granulatum</i> (Ehrenberg) Kuntze 1891 <i>Orthoseira granulata</i> (Ehrenberg) Schonfeldt 1907 <i>Melosira polymorpha</i> subsp. <i>granulata</i> (Ehrenberg) H.Bethge 1925
<b>Order</b> Melosirales	
<b>Family</b> Melosiraceae	
<i>Melosira varians</i> Agardh	<i>Lysigonium varians</i> (Agardh) De Toni 1892

Table 3.9 The list of benthic diatoms in 8 hot spring sampling sites during December 2015 - April 2016 (continued)

Taxa	Synonym
<b>Class</b> Bacillariophyceae	
<b>Order</b> Cocconeidales	
<b>Family</b> Achnanthidiaceae	
<i>Achnanthidium exiguum</i> (Grunow) Czarnecki	<i>Achnanthes exigua</i> Grunow in Cleve & Grunow 1880
	<i>Stauroneis exilis</i> Kützing 1844
	<i>Microneis exigua</i> (Grunow) Comber 1901
<i>Achnanthidium minutissimum</i> (Kützing) Czarnecki	<i>Achnanthes minutissima</i> Kützing 1833
	<i>Achnanthidium lanceolatum</i> f. <i>minutissima</i> (Kützing) Tömösvary 1879
	<i>Microneis minutissima</i> (Kützing) Cleve 1895
	<i>Cocconeis minutissima</i> (Kützing) Schönfeldt 1907
	<i>Microneis minutissima</i> (Kützing) Meister 1912
<i>Achnanthidium</i> sp.	
<i>Planothidium lanceolatum</i> (Breb.) Round & Bukhtiyarova	<i>Achnanthes lanceolata</i> (Brébisson ex Kützing) Grunow in Cleve & Grunow 1880
	<i>Achnanthidium lanceolatum</i> Brébisson ex Kützing 1846
	<i>Microneis lanceolata</i> (Brébisson in Kützing) Frenguelli 1923
	<i>Achnantheiopsis lanceolata</i> (Brébisson ex Kützing) Lange-Bertalot 1997
	<i>Planothidium lanceolatum</i> (Brébisson) Round et Bukhtiyarova 1996
	<i>Achnanthes lanceolata</i> (Brébisson ex Kützing) Grunow in Van Heurck 1880
	<i>Planothidium lanceolatum</i> (Brébisson ex Kützing) Bukhtiyarova 1999

Taxa	Synonym
<b>Order</b> Thalassiophysales	
<b>Family</b> Catenulaceae	
<i>Amphora montana</i> Krasske	<i>Halamphora montana</i> (Krasske) Z. Levkov 2009
<i>Amphora ovalis</i> (Kützing) Kützing	<i>Amphora amphora</i> (Ehrenberg) Pantocsek 1902 <i>Amphora ocellata</i> Ehrenberg 1838 <i>Frustulia ovalis</i> Kützing 1833 <i>Navicula amphora</i> Ehrenberg 1832 <i>Clevamphora ovalis</i> (Kützing) Mereschkowsky 1906
<b>Order</b> Cymbellales	
<b>Family</b> Anomoeoneidaceae	
<i>Anomoeoneis sphaerophora</i> (Ehrenberg) Pfitzer	<i>Navicula sphaerophora</i> Kützing 1844 <i>Navicula amphisbaena</i> var. <i>sphaerophora</i> (Kützing) Rabenhorst 1847
<b>Family</b> Gomphonemataceae	
<i>Gomphonema affine</i> Kützing	<i>Gomphonema dichotomum</i> var. <i>affine</i> (Kützing) G.Rabenhorst 1864 <i>Gomphonema lanceolatum</i> var. <i>affine</i> (Kützing) A.Cleve 1932 <i>Gomphonema lanceolatum</i> var. <i>affine</i> (Kützing) Cleve-Euler 1955
<i>Gomphonema augur</i> Ehrenberg 1841	
<i>Gomphonema gracile</i> Ehrenberg 1838	
<i>Gomphonema parvulum</i> (Kützing) Van Heurck 1880	<i>Gomphonella parvula</i> (Kützing) Rabenhorst 1853 <i>Sphenella parvula</i> Kützing 1844 <i>Sphenoneis parvula</i> (Kützing) Trevisan 1848

Table 3.9 The list of benthic diatoms in 8 hot spring sampling sites during December 2015 - April 2016 (continued)



ลิขสิทธิ์มหาวิทยาลัยเชียงใหม่  
Copyright© by Chiang Mai University  
All rights reserved

Table 3.9 The list of benthic diatoms in 8 hot spring sampling sites during December 2015 - April 2016 (continued)

Taxa	Synonym
<b>Order Naviculales</b>	
<b>Family Naviculaceae</b>	
<i>Caloneis bacillum</i> (Grunov) Mereschkowsky	<i>Stauroneis bacillum</i> Grunow 1863
<i>Caloneis molaris</i> (Grunow) Krammer	<i>Navicula molaris</i> Grunow 1863
	<i>Pinnularia molaris</i> (Grunow) Cleve 1895
	<i>Schizonema molare</i> (Grunow) Kuntze 1898
<i>Navicula grimmei</i> Krasske in Hustedt	
<i>Navicula rostellata</i> (Kützing) Cleve	<i>Navicula rhynchocephala</i> ( <i>rhynchocephala</i> ) var. <i>rostellata</i> (Kützing) Cleve & Grunow 1880
	<i>Navicula rostellata</i> var. <i>minor</i> (Grunow in Van Heurck) Cleve-Euler 1953
	<i>Navicula viridula</i> var. <i>rostellata</i> (Kützing) Cleve 1895
	<i>Pinnularia rostellata</i> (Kützing) Rabenhorst 1853
<i>Navicula subrhynchocephala</i> Hustedt	
<b>Family Stauroneidaceae</b>	
<i>Craticula acidoclinata</i> Lange-Bertalot & Metzeltin	
<i>Craticula ambigua</i> (Ehrenberg) Mann in Round, Crawford & Mann	<i>Navicula ambigua</i> Ehrenberg 1843
	<i>Navicula cuspidata</i> var. <i>ambigua</i> (Ehrenberg) Cleve 1894
	<i>Vanheurckia ambigua</i> (Ehrenberg) Brébisson 1869
	<i>Vanheurckia cuspidata</i> var. <i>ambigua</i> (Ehrenberg) Playfair 1914
	<i>Navicula cuspidata</i> var. <i>ambigua</i> (Ehrenberg) Kirchner 1878
<i>Craticula cuspidata</i> (Kützing) Man	<i>Frustulia cuspidata</i> Kützing 1833
	<i>Navicula cuspidata</i> (Kützing) Kützing 1844

Table 3.9 The list of benthic diatoms in 8 hot spring sampling sites during December 2015 - April 2016 (continued)

Taxa	Synonym
<i>Stauroneis anceps</i> Ehrenberg	<i>Schizonema anceps</i> (Ehrenberg) Kuntze 1898 <i>Navicula anceps</i> (Ehrenberg) Mann 1907
<b>Family Diadesmidaceae</b>	
<i>Diadesmis confervacea</i> Kützing	<i>Navicula confervacea</i> (Kützing) Grunow in Van Heurck 1880
<b>Family Pinnulariaceae</b>	
<i>Diatomella balfouriana</i> Greville	<i>Grammatophora balfouriana</i> (Greville) W.Smith 1856
<i>Pinnularia abaujensis</i> (Pantoscek) Ross	<i>Navicula gibba</i> var. <i>abaujensis</i> Pantocsek 1889
<i>Pinnularia saprophila</i> Lange-Bertalot, Kobayasi and Krammer	
<i>Pinnularia borealis</i> Ehrenberg 1843	<i>Navicula borealis</i> (Ehrenberg) Kützing 1844 <i>Schizonema boreale</i> (Ehrenberg) Kuntze 1898
<i>Pinnularia mesolepta</i> (Ehrenberg) Smith	<i>Navicula mesolepta</i> Ehrenberg 1843 <i>Navicula mesolepta</i> Heiberg 1863 <i>Schizonema mesoleptum</i> (Ehrenberg) Kuntze 1898
<b>Family Diploneidaceae</b>	
<i>Diploneis elliptica</i> (Kützing) Cleve 1894	<i>Navicula elliptica</i> Kützing 1844 <i>Schizonema ellipticum</i> (Kützing) Kuntze 1898
<i>Diploneis subovalis</i> (Hilse) Cleve	<i>Schizonema subovale</i> (Cleve) Kuntze 1898 <i>Navicula subovalis</i> (Cleve) Mann 1924

Table 3.9 The list of benthic diatoms in 8 hot spring sampling sites during December 2015 - April 2016 (continued)

Taxa	Synonym
<b>Family</b> Amphipleuraceae	
<i>Halamphora fontinalis</i> (Hustedt) Z. Levkov	<i>Amphora fontinalis</i> Hustedt 1937
<b>Family</b> Sellaphoraceae	
<i>Sellaphora lanceolata</i> D.G. Mann & S. Dropp in Mann et al.	
<b>Order</b> Cocconeidales	
<b>Family</b> Cocconeidaceae	
<i>Cocconeis placentula</i> Ehrenberg	<i>Cocconeis communis</i> f. <i>placentula</i> (Ehrenberg) Chmielewski 1885
	<i>Cocconeis communis</i> var. <i>placentula</i> (Ehrenberg) Gutwinski 1887
	<i>Cocconeis communis</i> var. <i>placentula</i> (Ehrenberg) Kirchner 1878
	<i>Cocconeis pediculus</i> var. <i>placentula</i> (Ehrenberg) Grunow 1867
<b>Order</b> Cymbellales	
<b>Family</b> Cymbellaceae	
<i>Cymbella tumida</i> (Brébisson) Van Heurck	<i>Cocconema tumidum</i> Brébisson ex Kützing 1849
<b>Order</b> Rhopalodiales	
<b>Family</b> Rhopalodiaceae	
<i>Epithemia zebra</i> (Ehrenberg) Kützing 1844	<i>Navicula zebra</i> Ehrenberg 1835
	<i>Cymbella zebra</i> (Ehrenberg) Hassall 1845
	<i>Cystopleura zebra</i> (Ehrenberg) Kuntze 1891
<i>Rhopalodia gibberula</i> (Ehrenberg) O.F. Müller	<i>Eunotia gibberula</i> Ehrenberg 1843
	<i>Epithemia gibberula</i> (Ehrenberg) Kützing 1844
	<i>Cystopleura gibberula</i> (Ehrenberg) Kuntze 1891

Table 3.9 The list of benthic diatoms in 8 hot spring sampling sites during December 2015 - April 2016 (continued)

Taxa	Synonym
<b>Order</b> Fragilariales	
<b>Family</b> Fragilariaceae	
<i>Fragilaria crotonensis</i> Kitton	<i>Synedra crotonensis</i> (Kitton) Cleve & Möller 1878
	<i>Nematoplata crotonensis</i> (Kitton) Kuntze 1898
<i>Staurosira elliptica</i> (Schumann) D.M. Williams & Round	<i>Fragilaria elliptica</i> Schumann 1867
	<i>Fragilaria mutabilis</i> var. <i>elliptica</i> (Schumann) Grunow in Van Heurck 1881
	<i>Fragilaria pinnata</i> var. <i>elliptica</i> (Schumann) Carlson 1913
	<i>Staurosira elliptica</i> (Schumann) Cleve & Möller 1879
	<i>Fragilaria construens</i> var. <i>elliptica</i> (Schumann) Frenguelli 1945
	<i>Pseudostaurosira elliptica</i> (Schumann) Edlund, Morales & Spaulding 2006
<i>Synedra ulna</i> (Nitzsch) Ehrenberg	<i>Bacillaria ulna</i> Nitzsch 1817
	<i>Frustulia ulna</i> (Nitzsch) Agardh 1831
	<i>Fragilaria ulna</i> (Nitzsch) Lange-Bertalot 1980
	<i>Ulnaria ulna</i> (C.L. Nitzsch) Compère 2001
	<i>Exilaria ulna</i> (Harvey) Jenner 1855
	<i>Frustulia ulva</i> (Nitzsch) C.A. Agardh 1829
<b>Order</b> Bacillariales	
<b>Family</b> Bacillariaceae	
<i>Hantzchia amphioxys</i> (Ehrenberg) Grunow in cleve et Grunow	<i>Eunotia amphioxys</i> Ehrenberg 1843
	<i>Nitzschia amphioxys</i> (Ehrenberg) W.Smith 1853
	<i>Homoeocladia amphioxys</i> (Ehrenberg) Kuntze 1898

Taxa	Synonym
<i>Nitzschia amphibia</i> Grunow	<i>Homoeocladia amphibia</i> (Grunow) Kuntze 1898
<i>Nitzschia clausii</i> Hantzsch	<i>Bacillaria amphibia</i> (Grunow) Elmore in Barbour 1895
<i>Nitzschia ignorata</i> Krasske 1929	<i>Nitzschia sigma</i> var. <i>clausii</i> (Hantzsch) Grunow 1878
<i>Nitzschia palea</i> (Kützing) W. Smith	<i>Nitzschia filiformis</i> var. <i>ignorata</i> (Krasske) Cleve-Euler 1952
	<i>Homoeocladia palea</i> (Kützing) Kuntze 1898
	<i>Synedra palea</i> Kützing 1844
<b>Order</b> Surirellales	
<b>Family</b> Surirellaceae	
<i>Surirella biseriata</i> Bräbison	<i>Campylodiscus elegans</i> (Ehrenberg) Ralfs in Pritchard 1861
<i>Surirella elegans</i> Ehrenberg	<i>Suriraya elegans</i> (Ehrenberg) De Toni 1892

Table 3.9 The list of benthic diatoms in 8 hot spring sampling sites during December 2015 - April 2016 (continued)



ลิขสิทธิ์มหาวิทยาลัยเชียงใหม่  
Copyright© by Chiang Mai University  
All rights reserved